An introduction to typical types of dynamics found in complex systems

Henrik Jeldtoft Jensen
Department of Mathematics and Complexity and Networks Group
Imperial College London

Slides [28MB] can be down loaded from

http://www2.imperial.ac.uk/~hjjens/

Physics = the science of the dynamics of lifeless matter

Complexity science = the science of the dynamics of emergent properties

The next essential break through in science:

When statistical mechanics begins to be able to understand the dynamics of the emergent properties of complex systems

- the brain
- cancer
- evolution
- sociology
- . . .

i.e. stat mech of non-equilibrium

Time

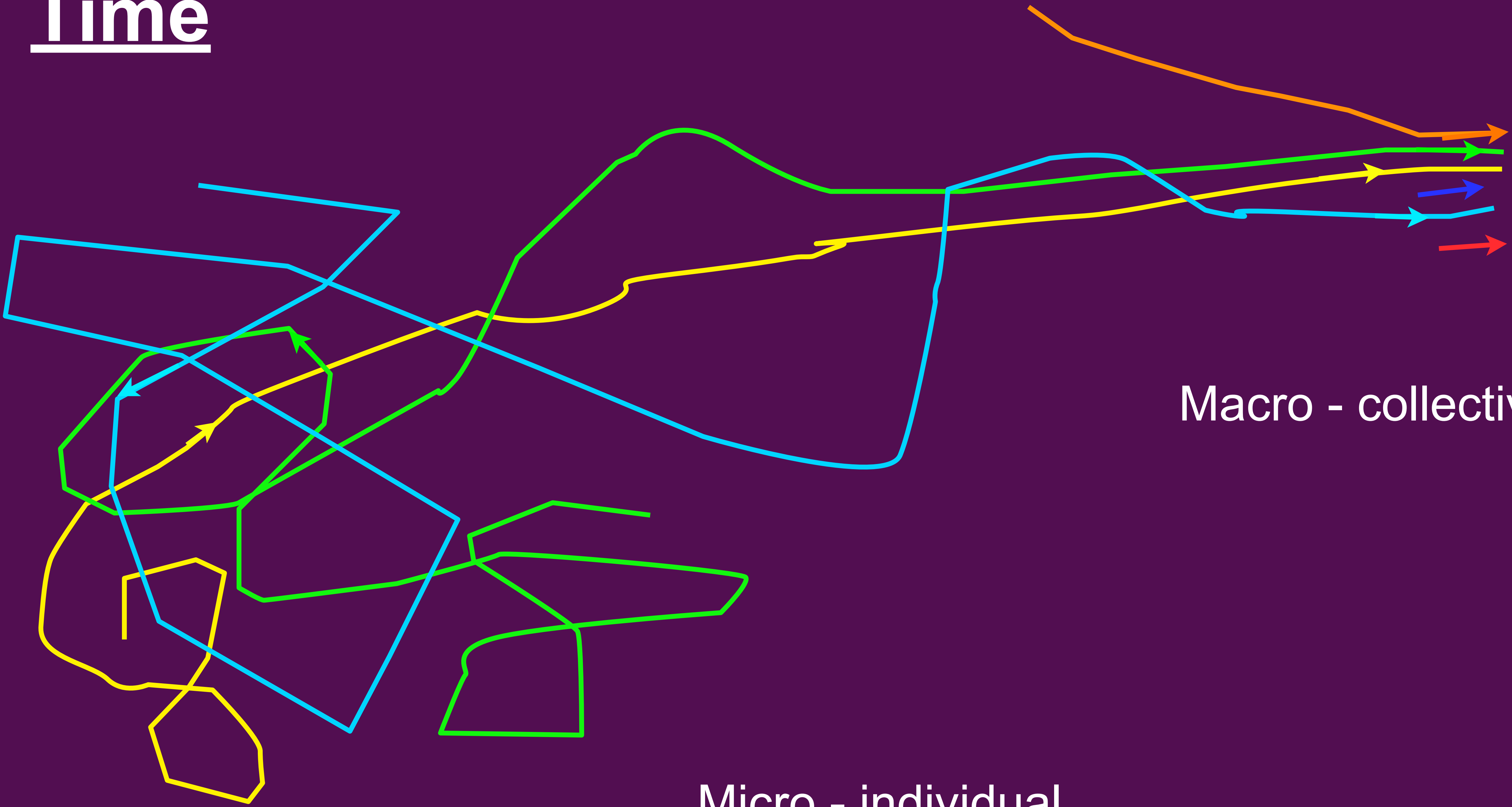

Macro - collective

Micro - individual

Time is in a sense an emergent property

Time

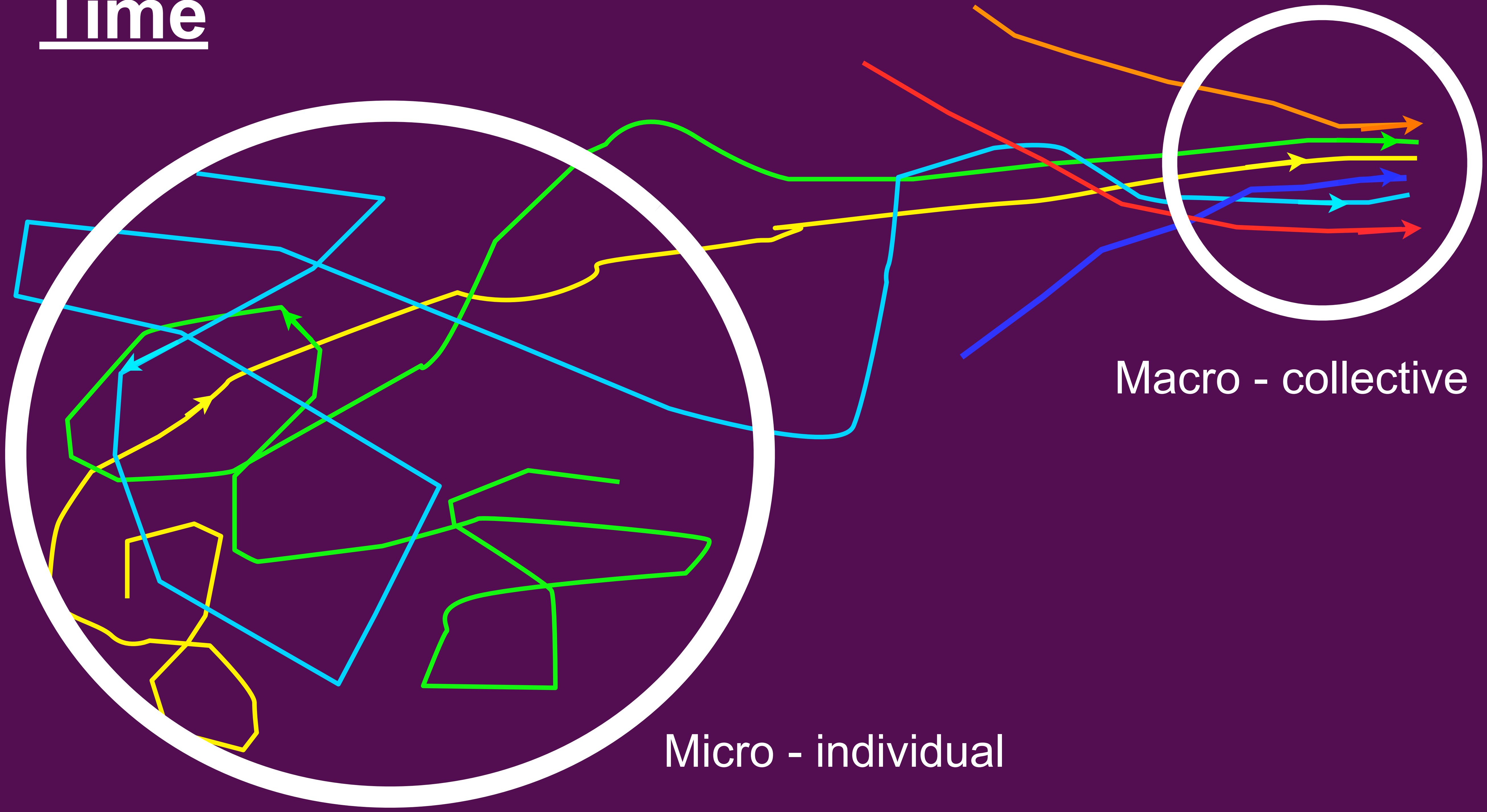

Macro - collective

Micro - individual

Time is in a sense an emergent property

Content

- Intermittency
- Stationary versus non-stationary: asymptotic versus transient
- Event distributions: power law or not
- Self-Organised Criticality
- Record dynamics
    - consider a number of systems:
        * thermal (spin glass)
        * magnetic relaxation - superconductors
        * **evolutionary dynamics: model of evolutionary ecology**
        * ants
        * earthquakes

- From micro-time to macro-time

Intermittency

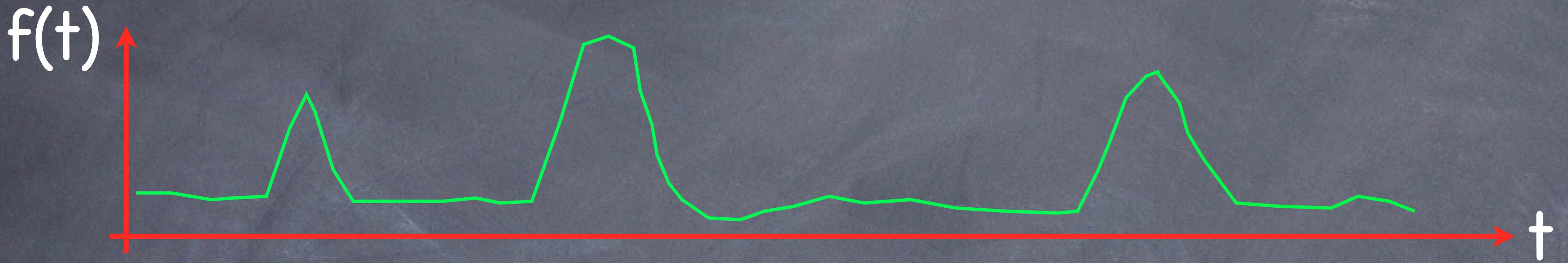

Rain

Earthquakes

Economic crashes

Extinction events

....

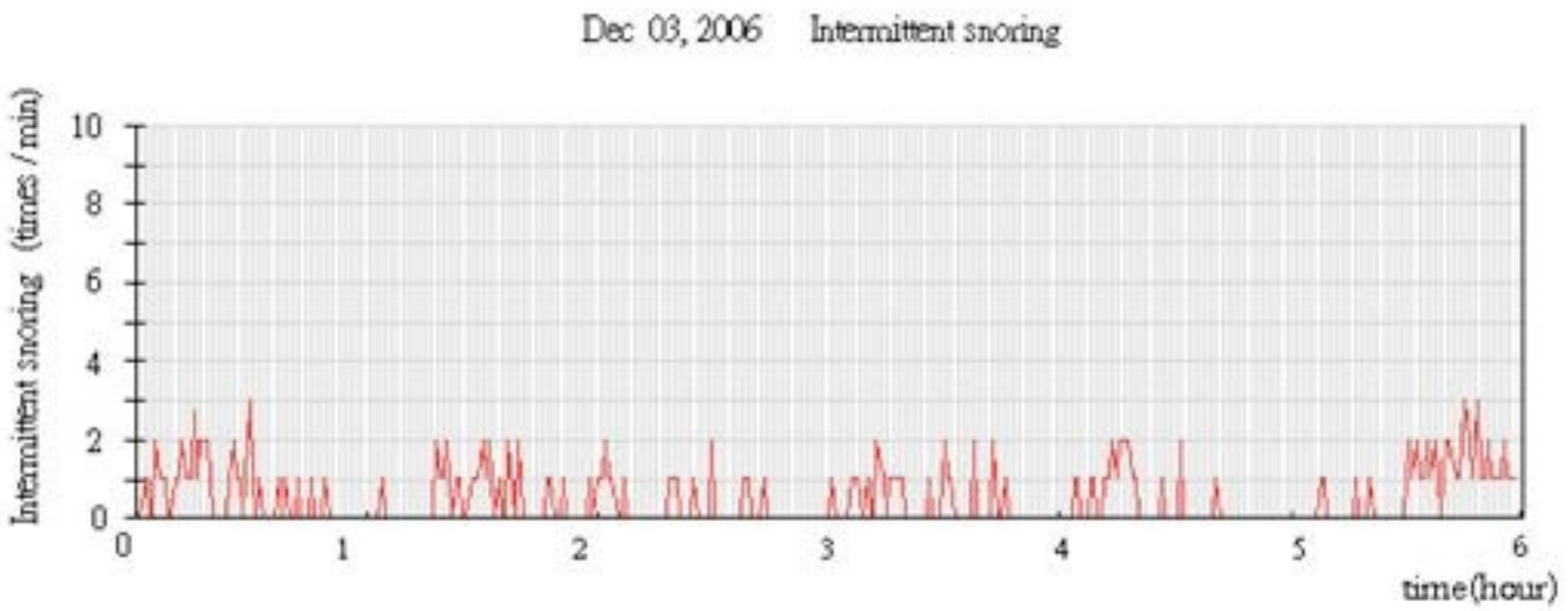

Chih-Ming Cheng, Yeh-Liang Hsu, Chang- Ming Young, Chang-Huei Wu

***Telemedicine and e-Health*, Vol. 14, No. 1, pp. 55-68, January, 2008.**

Stationary versus non-stationary

Stationary: statistics independent of time

$P(x,t) = P(x)$

non-stationary: statistics changes with time

$P(x,t) = P(x,\mathrm{time})$

Dynamics of Complex systems

Driven — versus — Relaxing

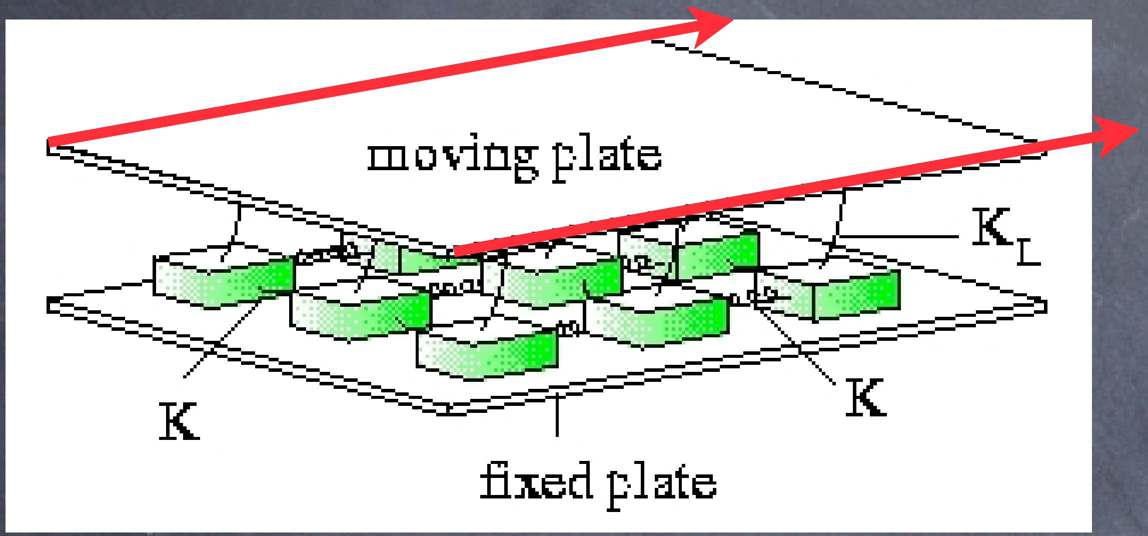

Z. Olami, H.J.S. Feder, and K. Christensen, *Phys. Rev. Lett.* **68**, *1244-1247 (1992). {480}*

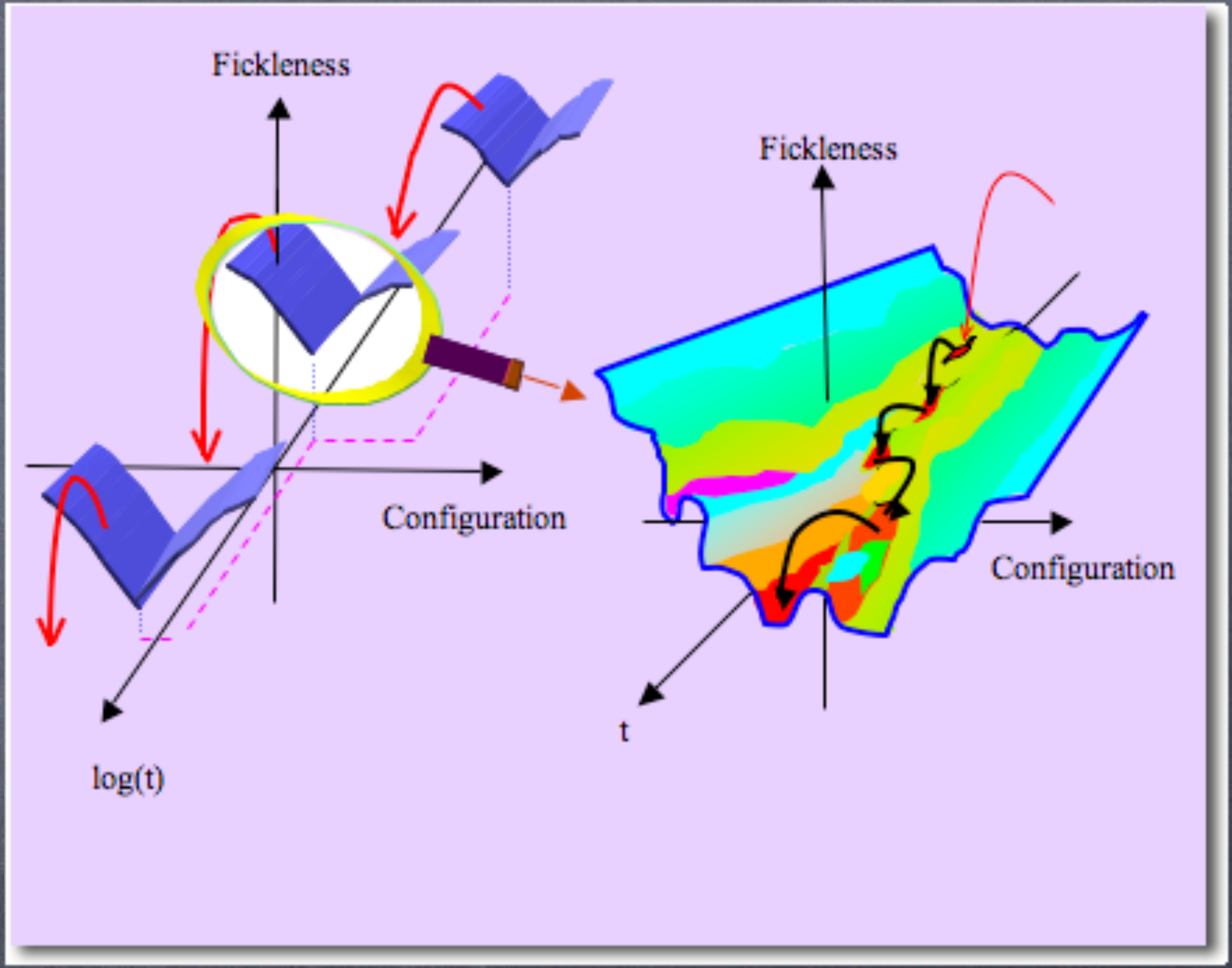

Stationary

Self-organised Criticality

Non-Stationary

Record Dynamics

Event distributions: power law or not

- Rain
- Earthquakes
- Economic crashes
- Extinction events
- ....

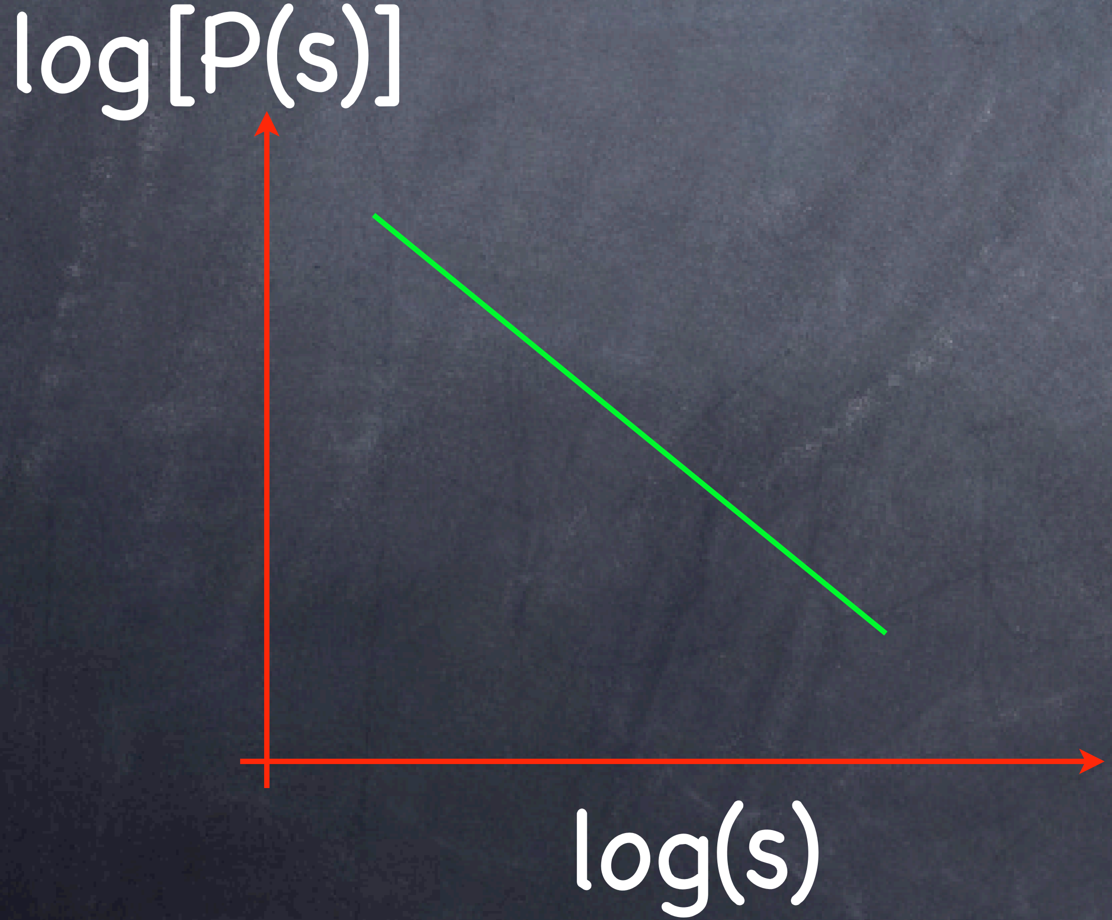

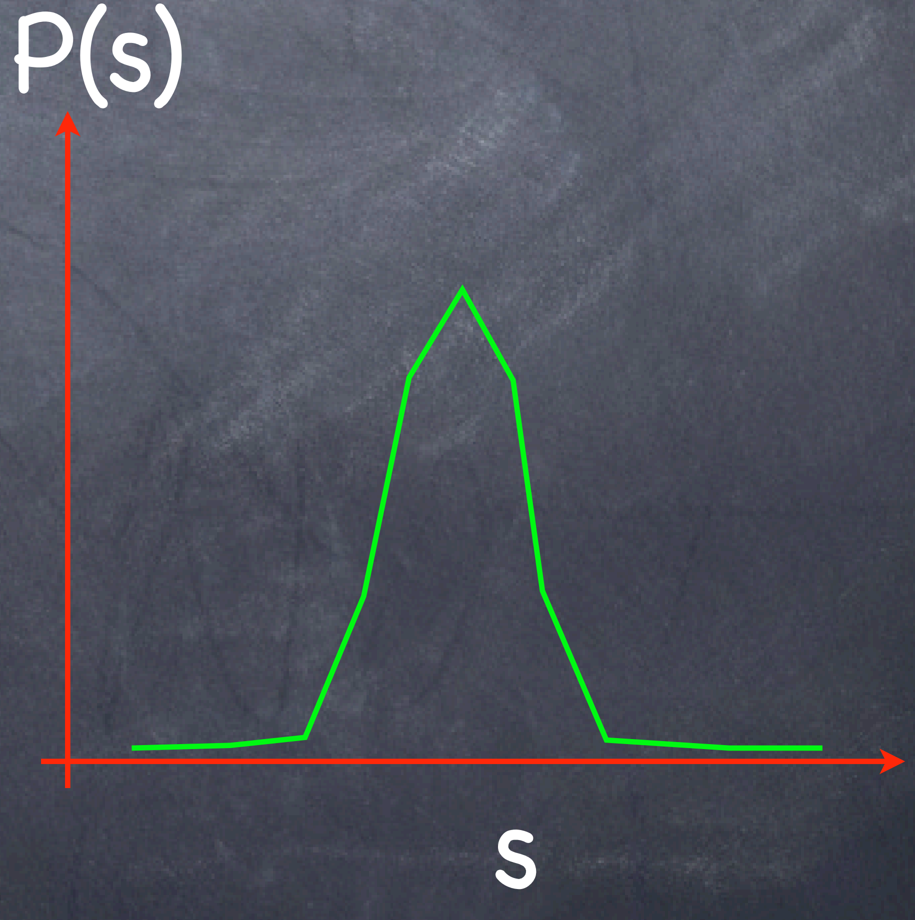

Self-Organised Criticality

System driving themselves (more or less) into state without characteristic scales in time or space.

focus on the stationary state (occurring after some initial transient)
slow drive
intermittent events: “avalanches”
event size distribution

Self-organised Criticality:
suggested as an explanation 1/f and fractals

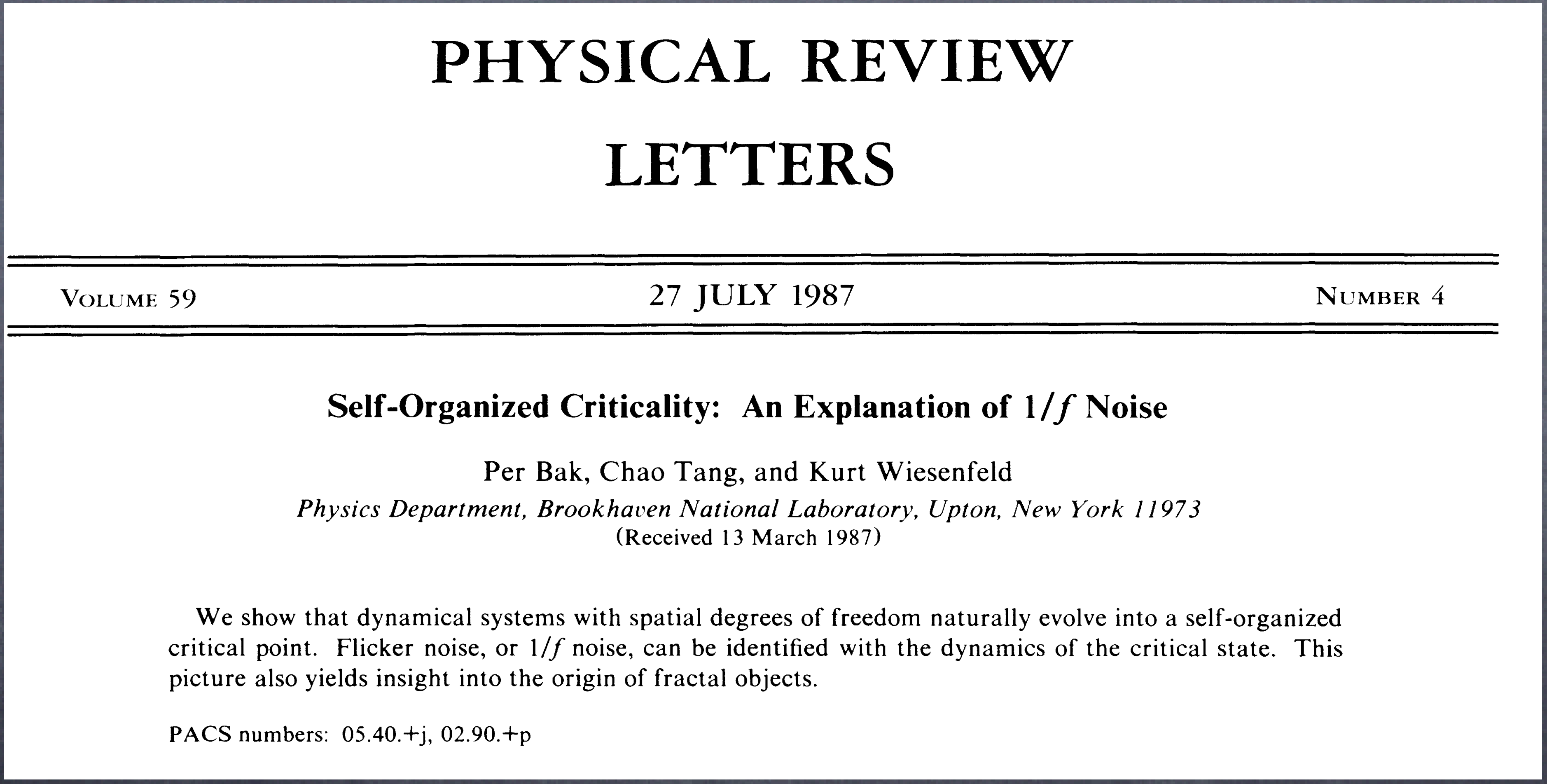

PHYSICAL REVIEW
LETTERS

VOLUME 59 | 27 JULY 1987 | NUMBER 4

Self-Organized Criticality: An Explanation of $1/f$ Noise

Per Bak, Chao Tang, and Kurt Wiesenfeld
Physics Department, Brookhaven National Laboratory, Upton, New York 11973
(Received 13 March 1987)

We show that dynamical systems with spatial degrees of freedom naturally evolve into a self-organized critical point. Flicker noise, or $1/f$ noise, can be identified with the dynamics of the critical state. This picture also yields insight into the origin of fractal objects.

PACS numbers: 05.40.+j, 02.90.+p

The sandpile: No tuning beside slow drive

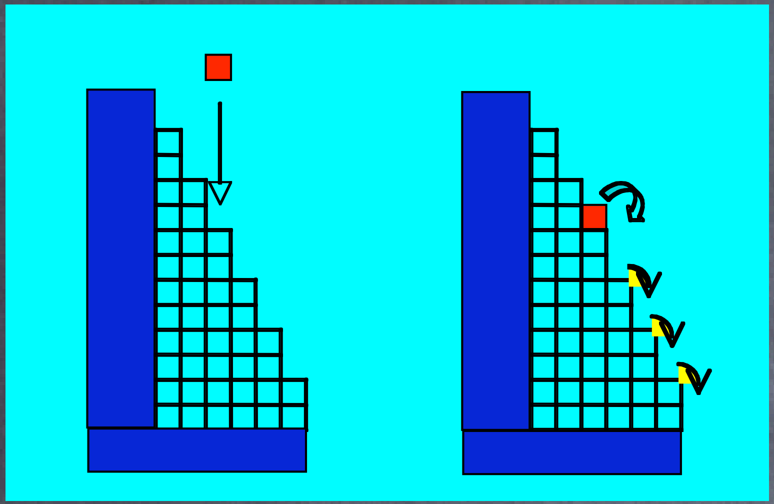

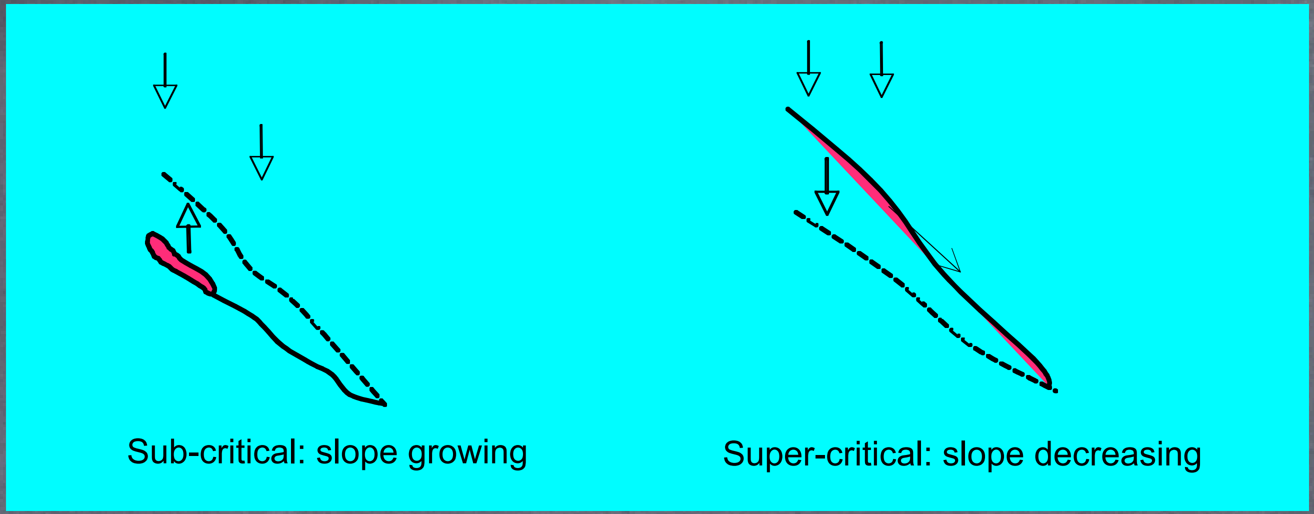
Sub-critical: slope growing

Super-critical: slope decreasing

$$
\begin{aligned}
z(x,y) &\rightarrow z(x,y)-4\\
z(x\pm 1,y) &\rightarrow z(x\pm 1,y)+1\\
z(x,y\pm 1) &\rightarrow z(x,y\pm 1)+1
\end{aligned}
$$

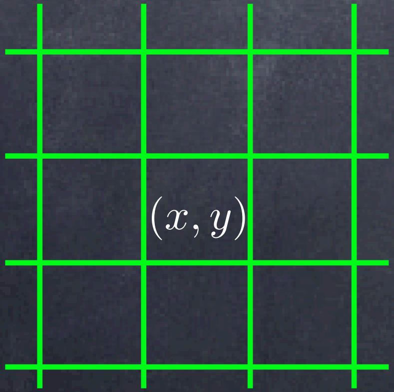

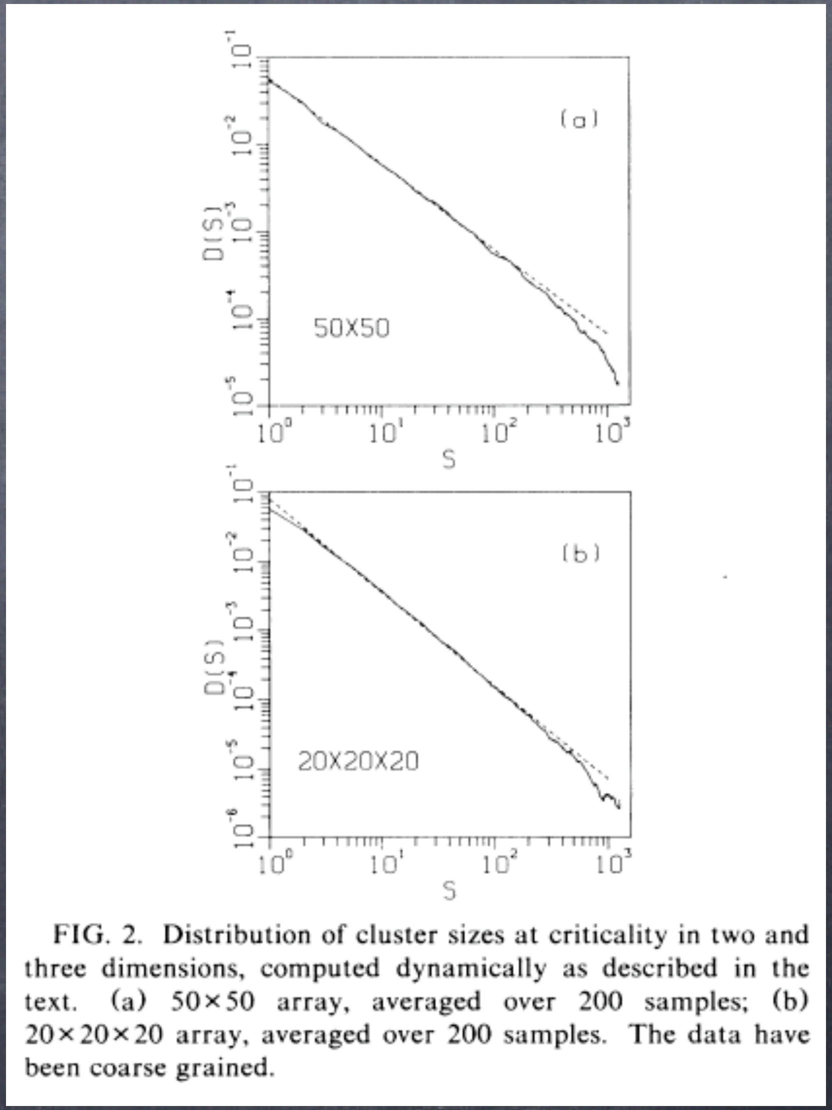

FIG. 2. Distribution of cluster sizes at criticality in two and three dimensions, computed dynamically as described in the text. (a) 50×50 array, averaged over 200 samples; (b) 20×20×20 array, averaged over 200 samples. The data have been coarse grained.

Bak, Tang and Wiesenfeld, PRL 59, 381 (1987)

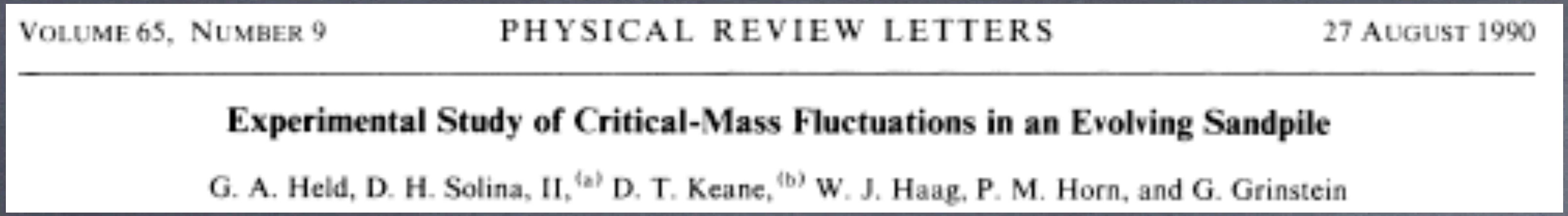
VOLUME 65, NUMBER 9 PHYSICAL REVIEW LETTERS 27 AUGUST 1990

Experimental Study of Critical-Mass Fluctuations in an Evolving Sandpile

G. A. Held, D. H. Solina, II,[a] D. T. Keane,[b] W. J. Haag, P. M. Horn, and G. Grinstein

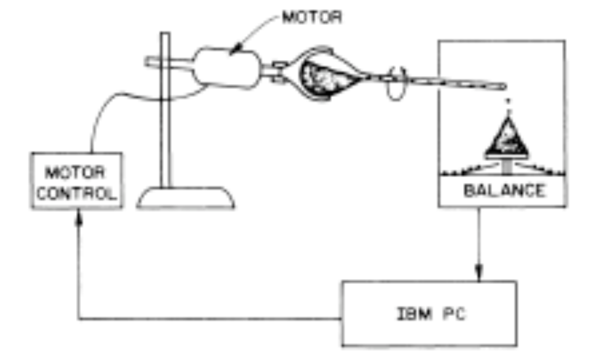

FIG. 1. Schematic illustration of the experimental apparatus.

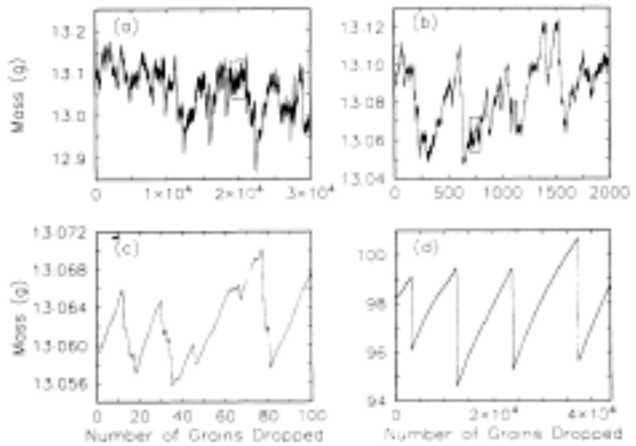

FIG. 2. (a) Mass of the 1.5-in.-diam sandpile as a function of the number of grains dropped onto it. (b) Magnification of the boxed region of (a) between 19 000 and 21 000 grains dropped. (c) Magnification of the boxed region of (b) between 700 and 800 grains dropped. (d) Mass of the 3.0-in.-diam sandpile as a function of the number of grains dropped onto it. The fine-scale mass fluctuations observed for the 1.5-in.-diam sandpile are no longer present.

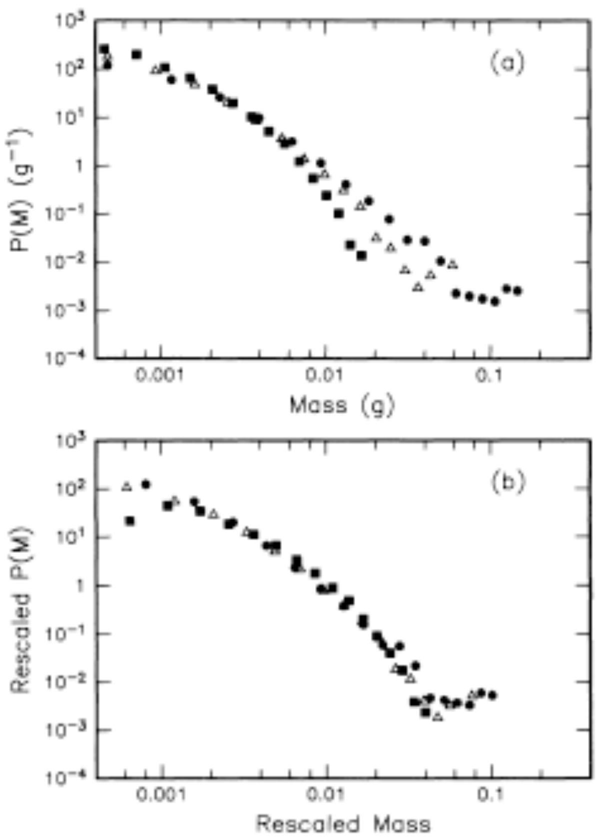

FIG. 3. (a) Probability distribution of avalanches $P(M)$ as a function of avalanche mass M for sandpiles with base diameters of 1.5 (●), 0.75 (△), and 0.38 (■) in. Units of probability density $P(M)$ are g^{-1}. For each base diameter, the range of avalanche sizes ΔM included in a given data point $P(M)$ increases quadratically with mass. (b) The probability distributions from (a) rescaled by Eq. (1) with $\beta = 2\nu = 1.8$. Mass and probability density are rescaled to $ML^{-0.9}$ and $P(M)L^{1.8}$, respectively, where L is the base diameter in inches.

Later

V. Frette, K. Christensen, A. Malthe-Sørenssen, J. Feder, T. Jøssang, and P. Meakin, *Avalanche Dynamics in a Pile of Rice*. *Nature* **379**, 49-52 (1996). {264}

Self-organised Criticality: suggested as an explanation 1/f and fractals

However BTW sandpile: No 1/f as $S(f) \propto 1/f^2$

But deterministic lattice gas

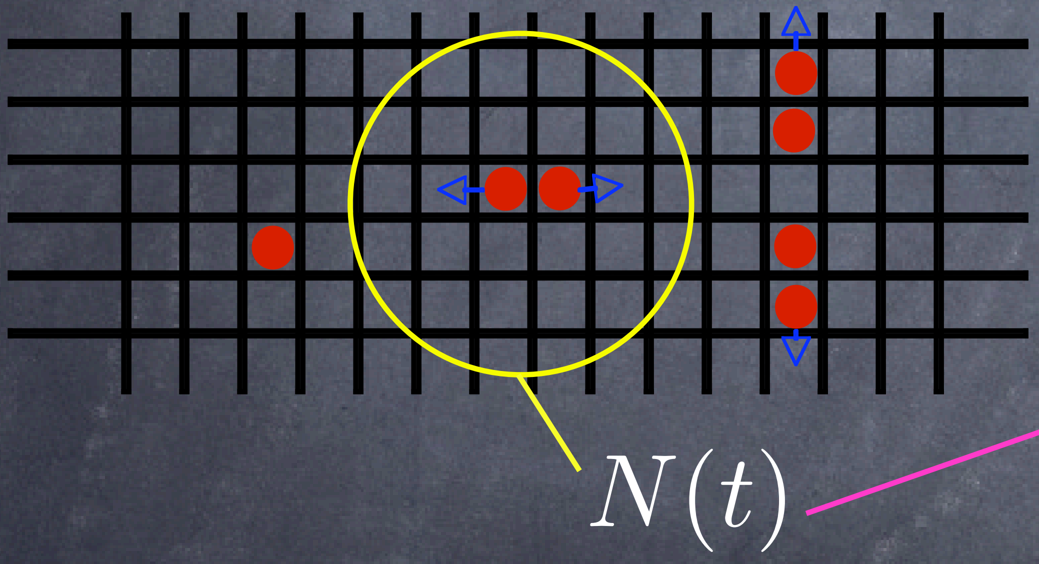

1/f power spec

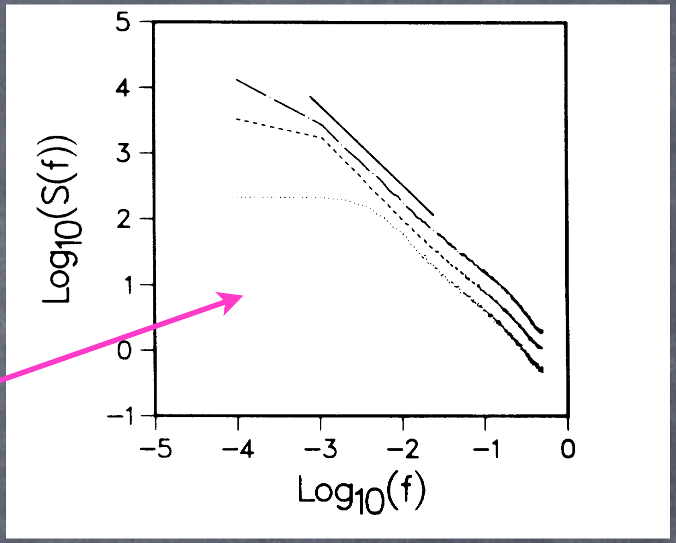

Dissipation occurs on a fractal

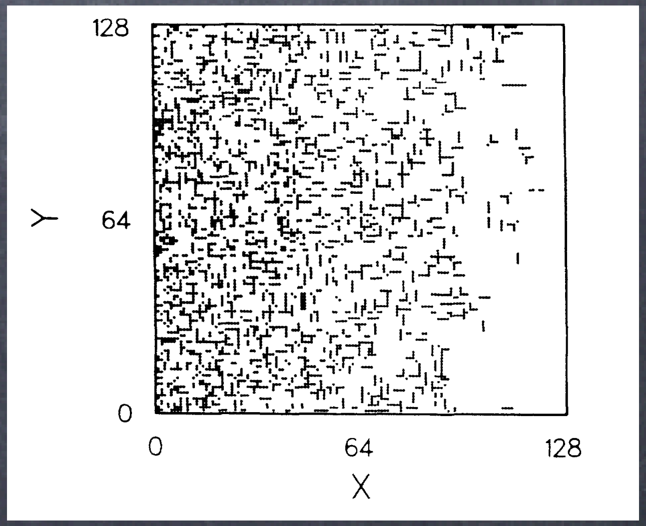

Experiment on fluctuations in vortex density in thin film
Yeh & Kao, PRL, 53, 1590 (1984)

From HJ Jensen PRL 64,1 (1990)

1/f from diffusion

$$\frac{\partial n(\mathbf{x},t)}{\partial t} = \gamma \nabla^2 n(\mathbf{x},t) \quad \text{and} \quad n(\mathbf{x}_B,t) = \eta(\mathbf{x}_0,t)$$

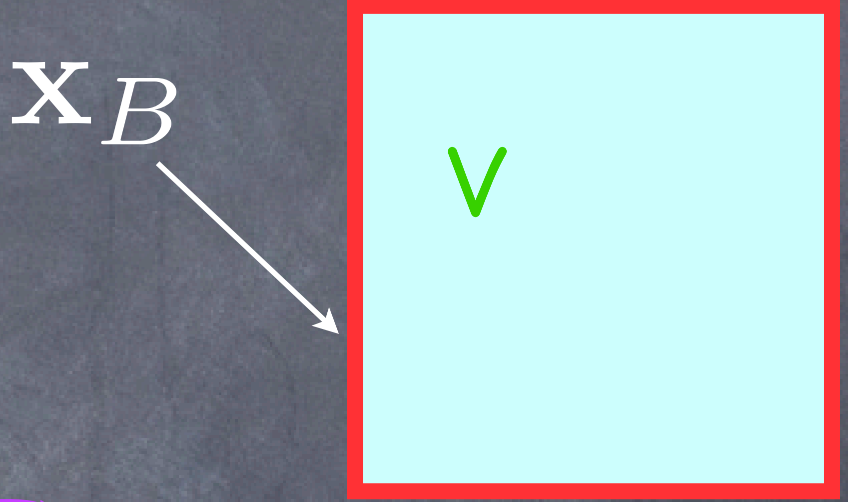

then $N(t) = \int_V d\mathbf{x} n(\mathbf{x},t)$

is 1/f in any dimension.

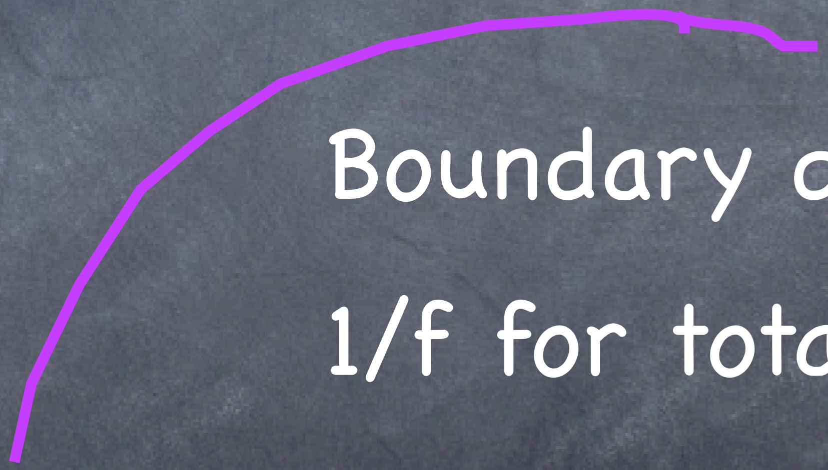

Boundary driven BTW:

1/f for total $z = \sum_i z_i$

for $f < 1/T_{max}$

See e.g.

- Grinstein, Hwa & Jensen, Phys. Rev. A **45** R559 (1992)
- H.J. Jensen, *Self-Organized Criticality*, Cambridge University Press 1998.

But can we be sure a bulk noise term can be ignored?

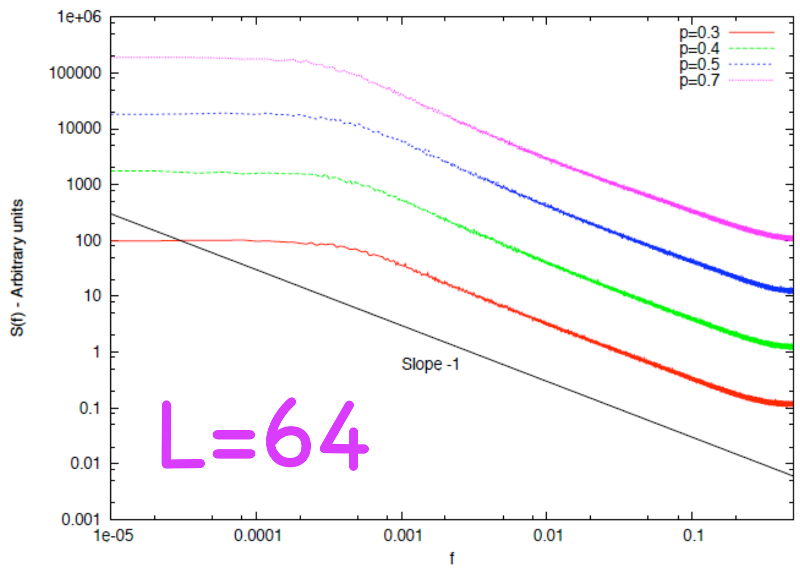

FIG. 12: Scaling behaviour of the spectrum $S(f) \propto f^{-\beta}$ of the total number of particles $N(t)$ in the dDLG for different boundary drives p and particles densities ρ. $S(f)$ has been multiplied by different constants for different drives p to visualise the scaling exponents properly. With small lattice sizes one observes scaling with $\beta = 1$. Lattice size $L = 64$.

Larger systems

From Master thesis
Andrea Giomette

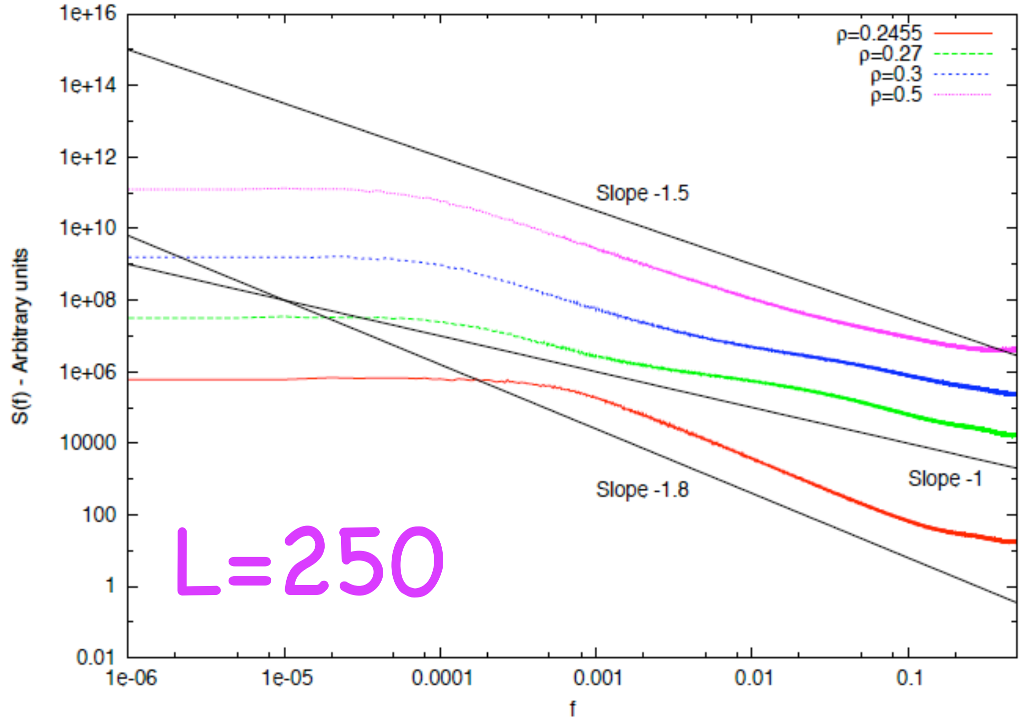

FIG. 16: Scaling behaviour of the spectrum $S(f) \propto f^{-\beta}$ of the total number of particles $N(t)$ in the pDLG for different particle densities ρ. A crossover from $\beta \simeq 1.8$ at $\rho \simeq \rho_c = 0.245$ to $\beta = 3/2$ at $\rho \gg \rho_c$ is observed. $S(f)$ has been multiplied by different constants for different densities ρ to visualise the scaling exponents properly. Lattice size $L = 250$.

Self-Organised Criticality:

Paradigm well represented by e.g. the earthquake dynamics:

- Global very slow drive → gradual build up of local strain.
- Local rigidity or threshold needs to be exceeded

  Abrupt short lived release of the strain through a quake or avalanche

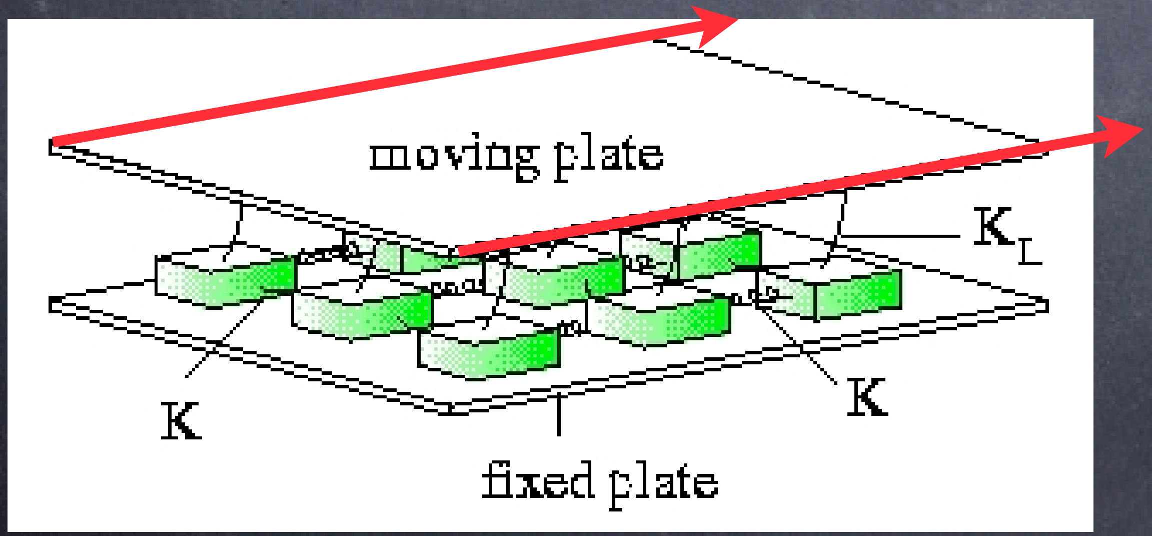

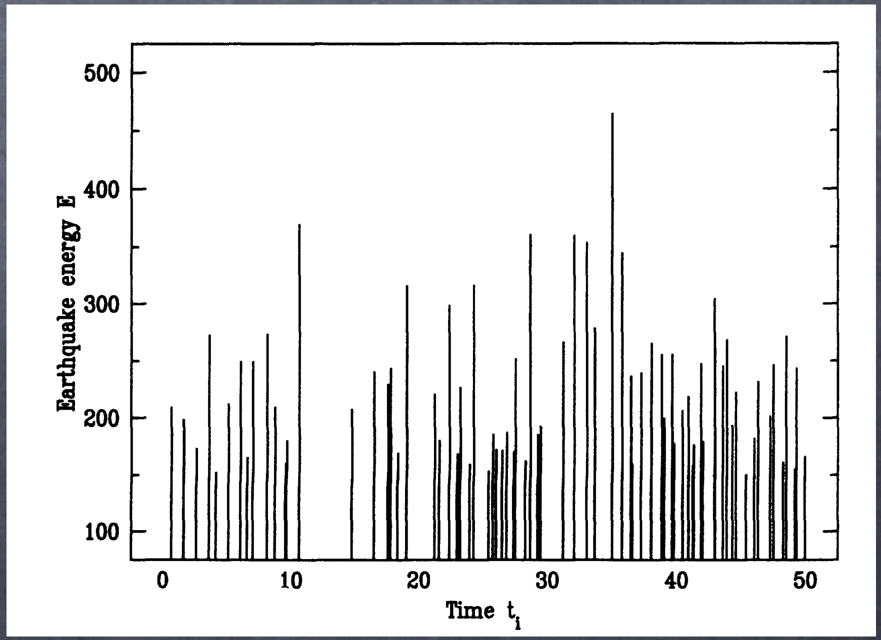

Constant rate of events

From Olami & Christensen, PRA, 46, R1720 (1992)

Focus on the distribution of event sizes

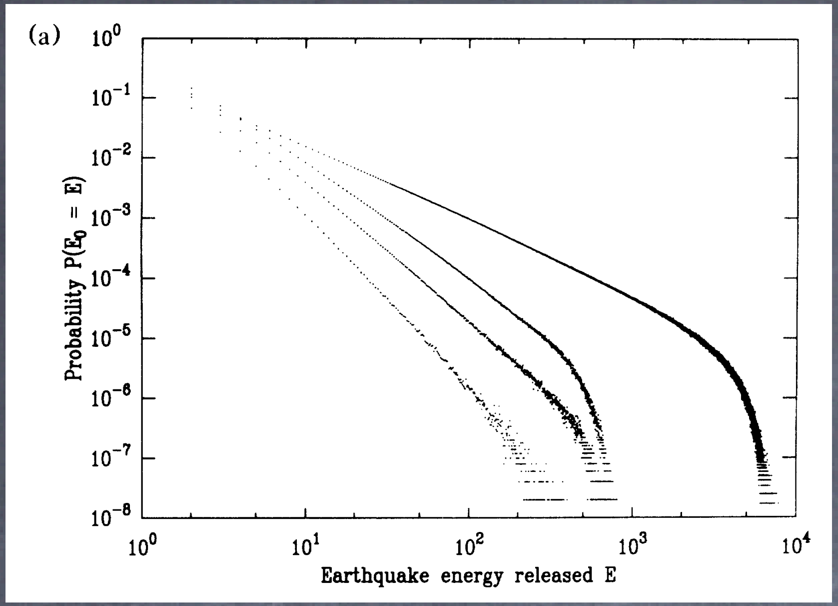

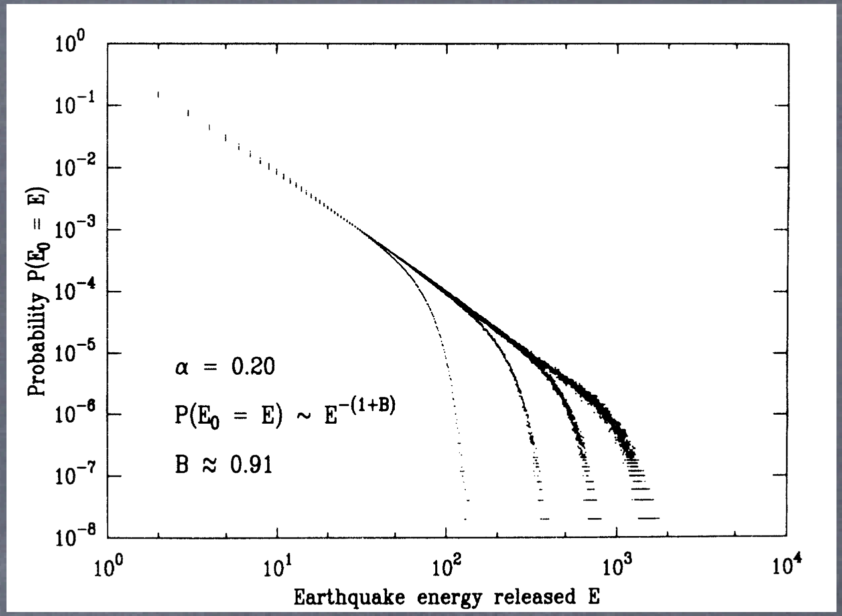

From: Olami, Feder and Christensen PRL 68, 1244 (1992)

Dependence on parameters

Dependence on system size

Power laws → Criticality ↔ Lack of scale

Typically SOC models turned out to exhibit more complicated behaviour.

Drossel-Schwabl

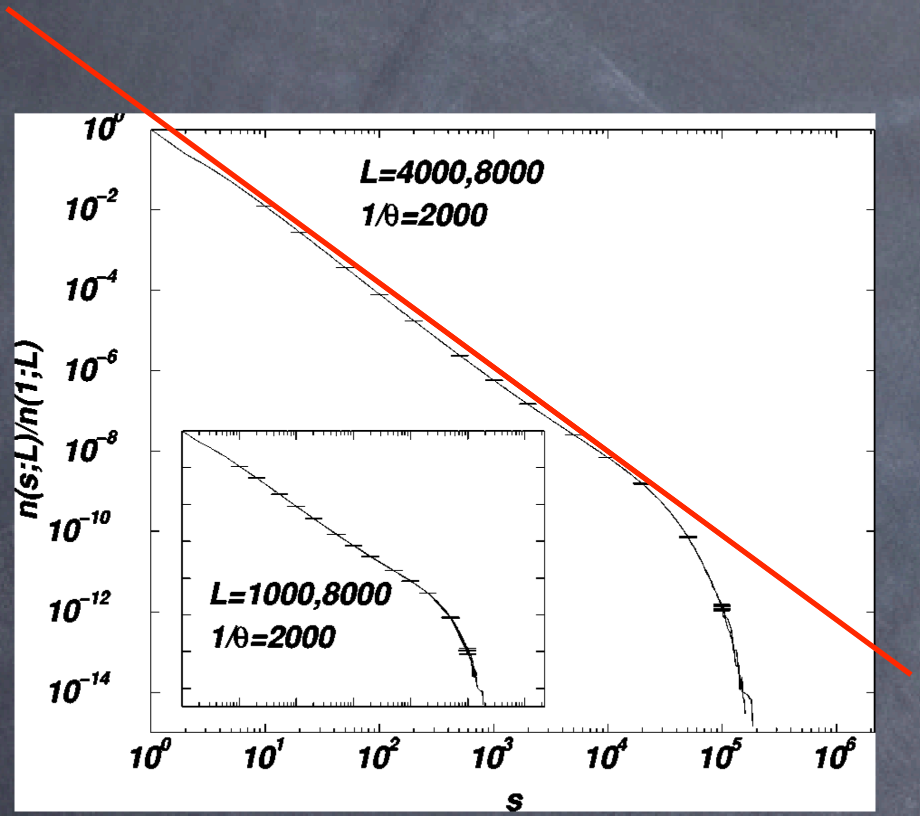

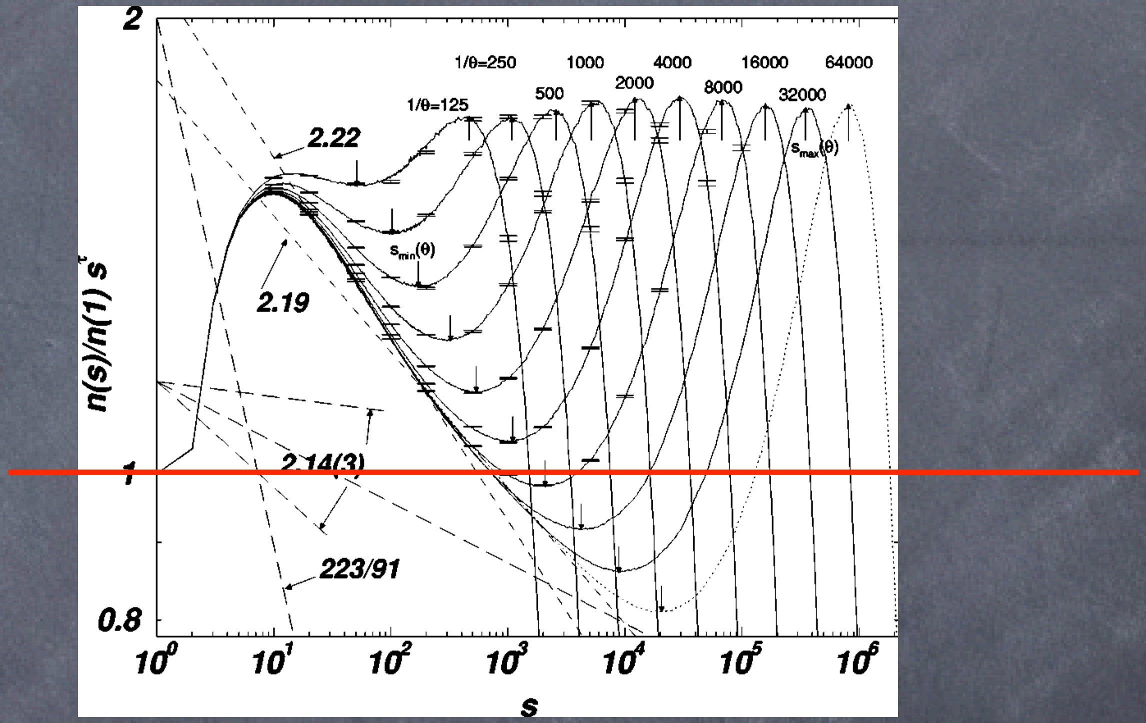

Scaling analysis in systems with L up to 64,000

From Prussner & Jensen, PRE **65**, 056707 (2002)

See also Grassberger, New J Phys **4**, 17 (2002)

J Phys A **26**, 2081 (1993)

- SOC supposed to self-organise to a stationary critical state:
  - no characteristic length scale
  - no characteristic time scale

similar to equilibrium critical phenomena, except (!?!) SOC self-tune.

- Nevertheless, relation to phase transitions has been explored, in particular to absorbing state phase transitions - cf. talk by Gunnar Pruessner.

Record dynamics

Record statistics

-> record dynamics

http://www.frontpagemediaonline.com/images/news/Spring View long jump.jpg

http://www.sdhoc.com/main/articles/highschools/Rosariotrack/Image00088939

Intermittent evolution driven by record large fluctuations

Examples:

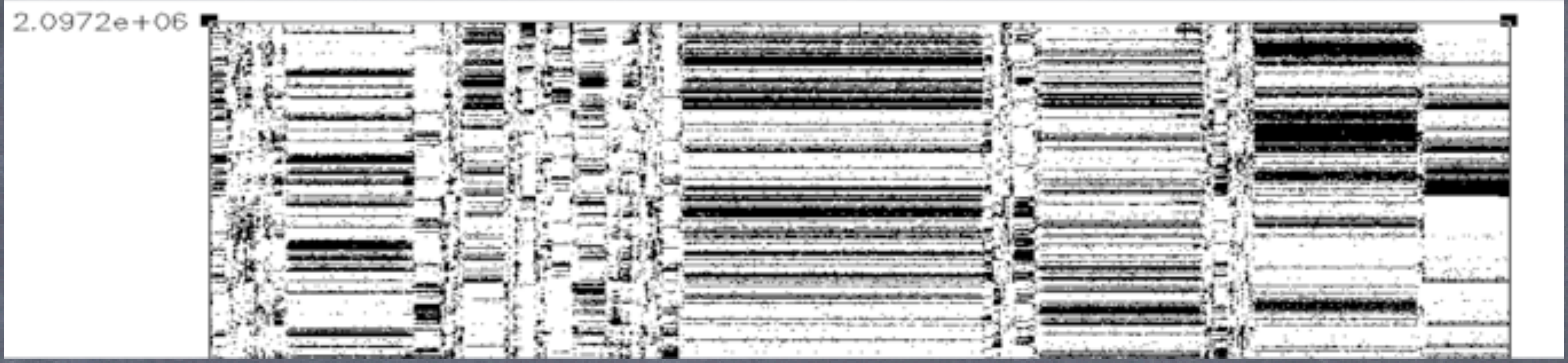

- Spin glasses
- Models of evolutionary ecology
- Models of magnetic relaxation in superconductors
- and more

Record dynamics

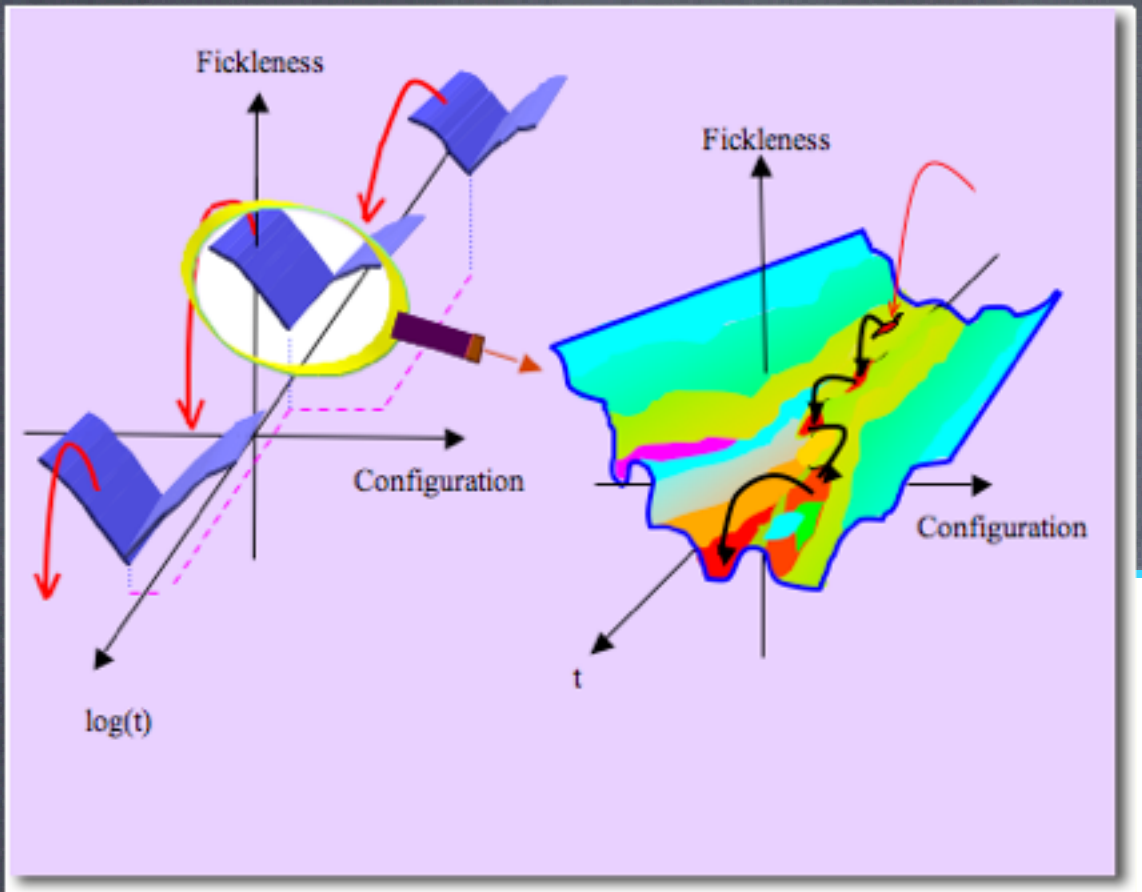

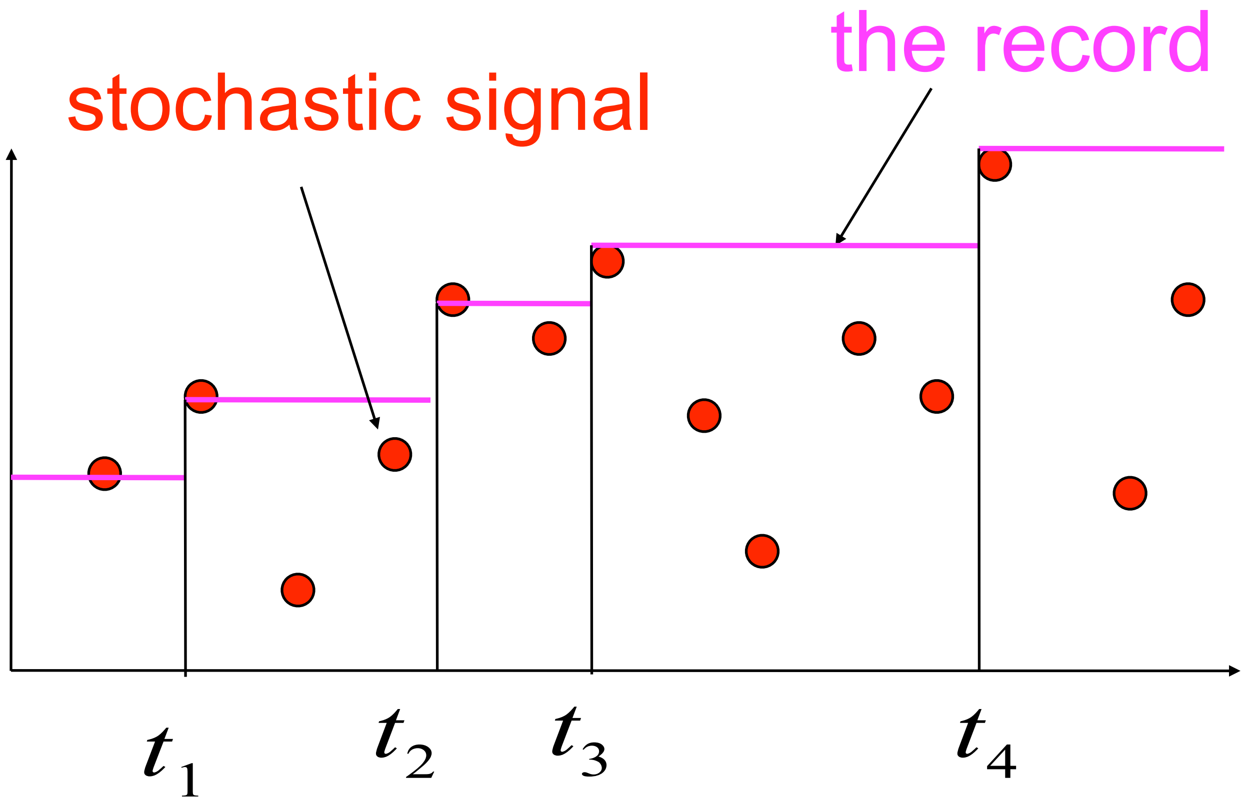

$$\tau = \ln(t_k) - \ln(t_{k-1}) = \ln(\frac{t_k}{t_{k-1}})$$ expo. distrib.

Record dynamics

Distribution of the number of records during *t* time steps independent of the nature of the fluctuating signal:

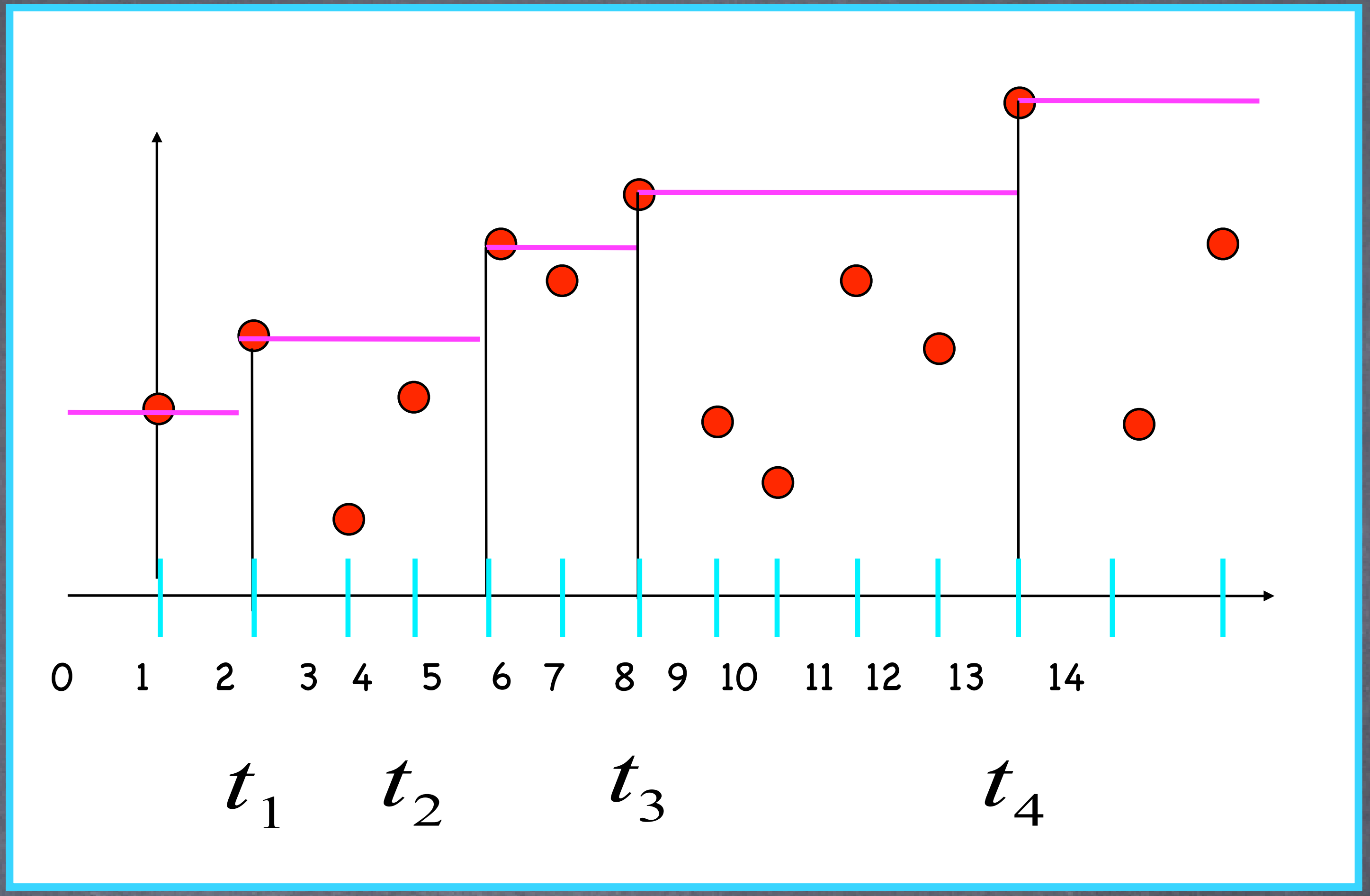

$$P_1(t) = \frac{1}{t}$$

The first out of *t* is the biggest

$$P_{(1,m)}(t) = \frac{1}{(m-1)t}$$

Two records during *t*: one at t=1 with prob (m-1) & one at t=*m* with prob 1/t.

$$\Downarrow$$

$$P_2(t) = \sum_{m=2}^{t} \frac{1}{(m-1)t} \approx \frac{\ln t}{t}$$

Two records during *t*

$$\Downarrow$$

$$P_n(t) \approx \frac{(\ln t)^{n-1}}{(n-1)!}\frac{1}{t} = e^{-}\lambda \frac{\lambda^{n-1}}{(n-1)!}$$

with $\lambda = \ln t$

log Poisson

Record dynamics

$\tau = \ln(t_k) - \ln(t_{k-1}) = ln(t_k/t_{k-1})$ exponentially distributed

- Poisson process in logarithmic time
- Mean and variance

$$\langle Q \rangle \propto \ln t \ \text{ and } \ \langle (Q - \langle Q \rangle)^2 \rangle \propto \ln t$$

- Rate of records constant as function of ln(t)
- Rate decreases $\propto 1/t$
- Non-stationary 1/f fluctuations

Relevance

When systems initially are in a state of high (generalised) internal strain & stress

Anderson, Jensen, Oliveira & Sibani, Compelxity, **10**, 49 (2004)

Examples:

- magnetic relaxation in superconductors
- relaxing spin glass
- evolutionary ecology
- hungry ants
- Omiri after shock law

Record dynamics

Magnetic Relaxation

in

Type II Superconductor

with Nicodemi, Oliveira, Sibani

Type II Superconductor Magnetic Relaxation Experiment

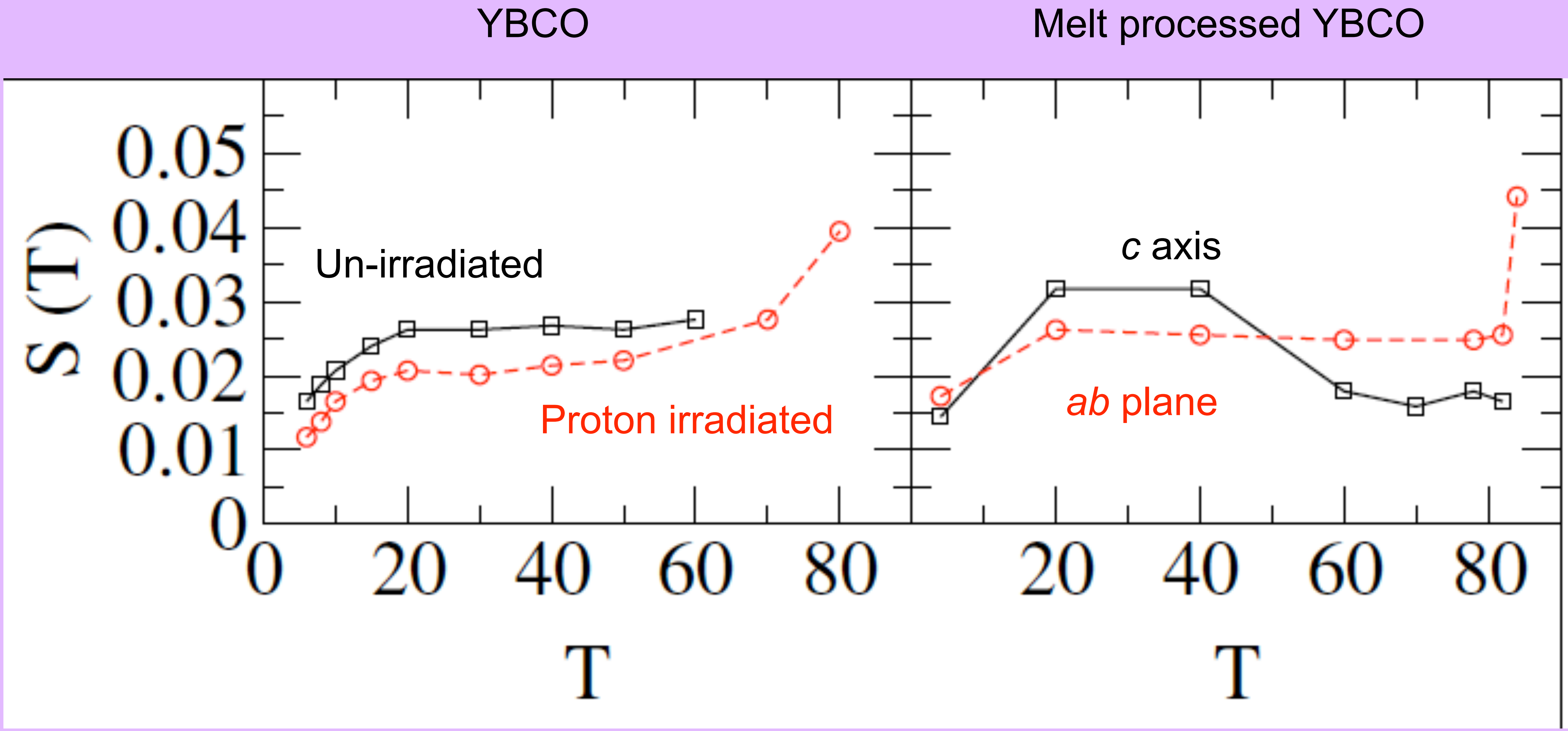

Left: Civale et al. PRL 65, 1164 (1990)

Riht: Kaiser et al. J Cryst Growth 85, 593 (1987)

Restricted **O**ccupancy **M**odel

Monte Carlo Kawasaki dynamics on stack of coarse grained superconducting planes

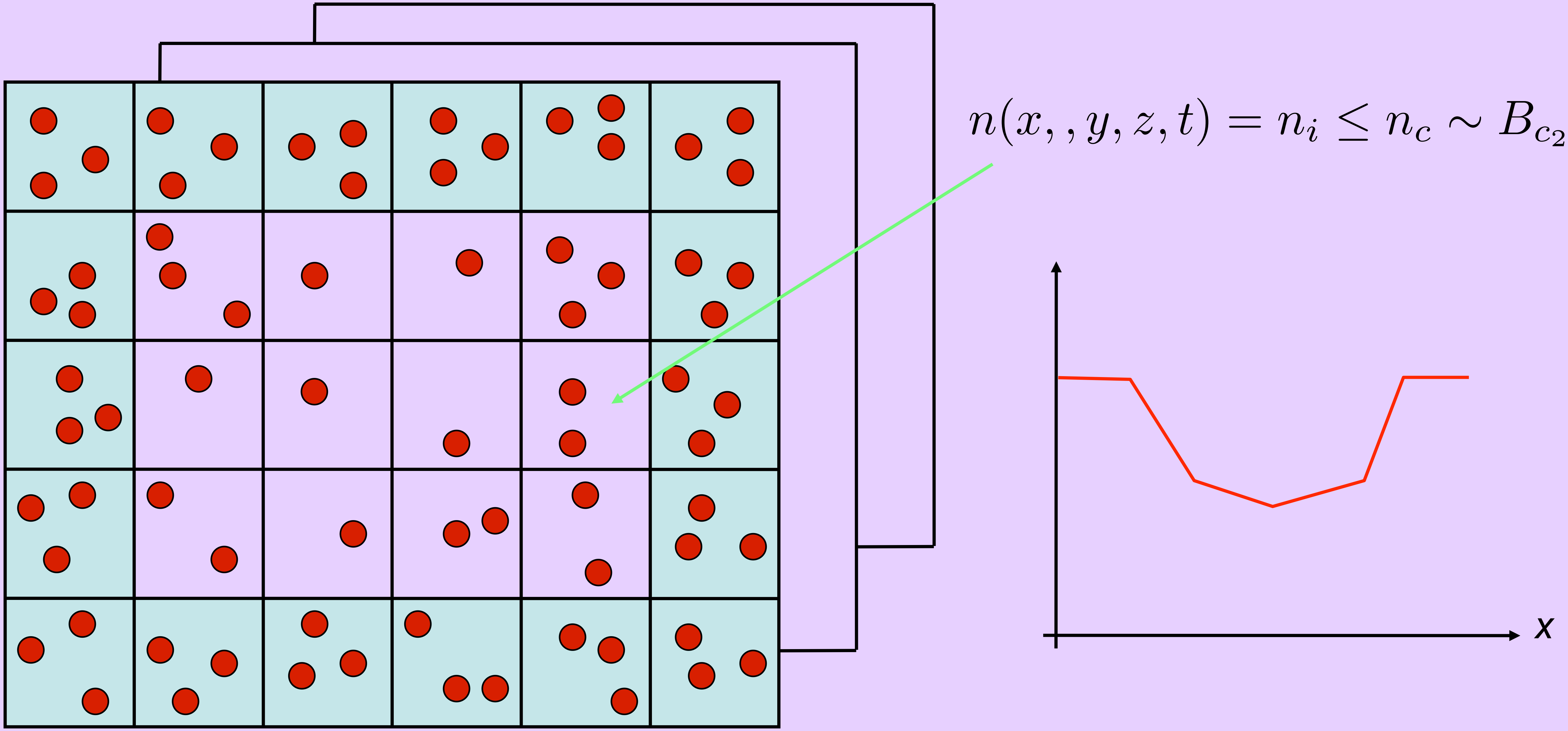

$$n(x,,y,z,t) = n_i \leq n_c \sim B_{c_2}$$

For 2D, zero temp.deterministic lattice gas see Jensen: PRL **64**, 3103 (1990)
For 2D, zero temp. cellular automaton see Bassler & Paczuski: PRL **81**, 3761 (1998)

ROM

Hamiltonian

$$H = \sum_i n_i A_{ij} n_j - \sum_i A_{ii} n_i - \sum_i A_i^p n_i + \sum_{\langle ij \rangle_z} A_2 (n_i - n_j)^2$$

Here

$$0 \le n_i < N_{c2} = B_{c2} l_0^2 / \varphi_0$$

M. Nicodemi and H.J. Jensen, *Equilibrium and off-equilibrium dynamics in a model for vortices in superconductors*. Phys. Rev. B **65** 144517 (2002).

H.J. Jensen and M. Nicodemi, *Memory effects in repsonse functions of driven vortex matter*, Europhys. Lett. **57** 348 (2002).

M. Nicodemi and H. J. Jensen, *Aging and memory phenomena in magnetic and transport properties of vortex matter*, J. Phys. A **34** 8425 (2001).

H.J. Jensen and M. Nicodemi, *Off equilibrium glassy properties of vortex creep in superconductors*. Europhysics Lett. **54** 566 (2001)

M. Nicodemi and H.J. Jensen, *Creep of superconducting vortices in the limit of vanishing temperature: A fingerprint of off equilibrium dynamics*. Phys. Rev. Lett. **86** 4378-4381 (2001).

M. Nicodemi and H.J. Jensen, *Off equilibrium magnetic properties in a system of repulsive particles for vortices in superconductors*, J. Phys. A. **34** L11 (2001).

H.J. Jensen and M. Nicodemi *Second magnetisation peak relaxation in a model for vortices in superconductors*. Physica C **341-348** 1065-1066 (2000)

ROM: Temperature independent creep

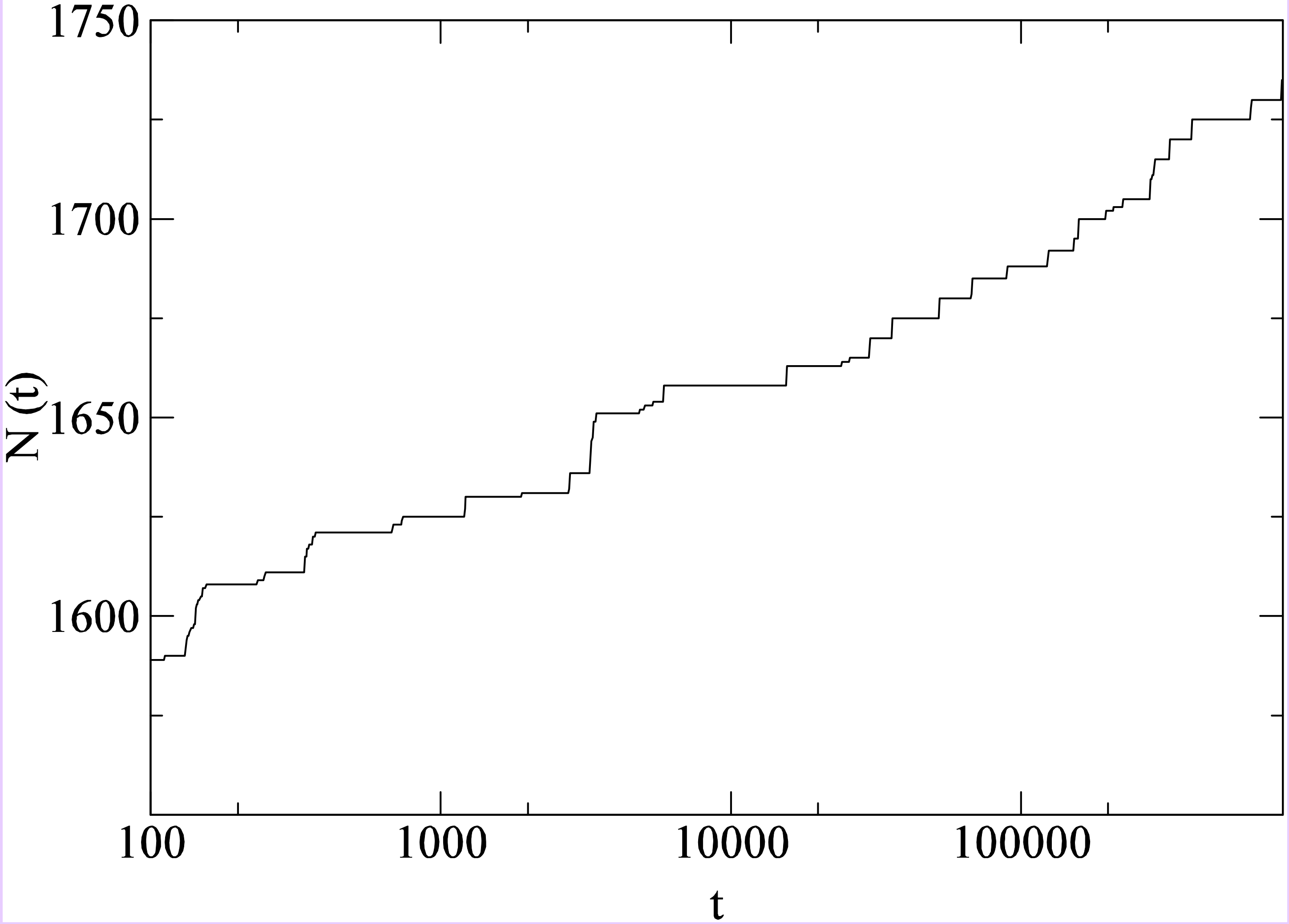

Realisations of record dynamics

ROM: Temperature independent creep

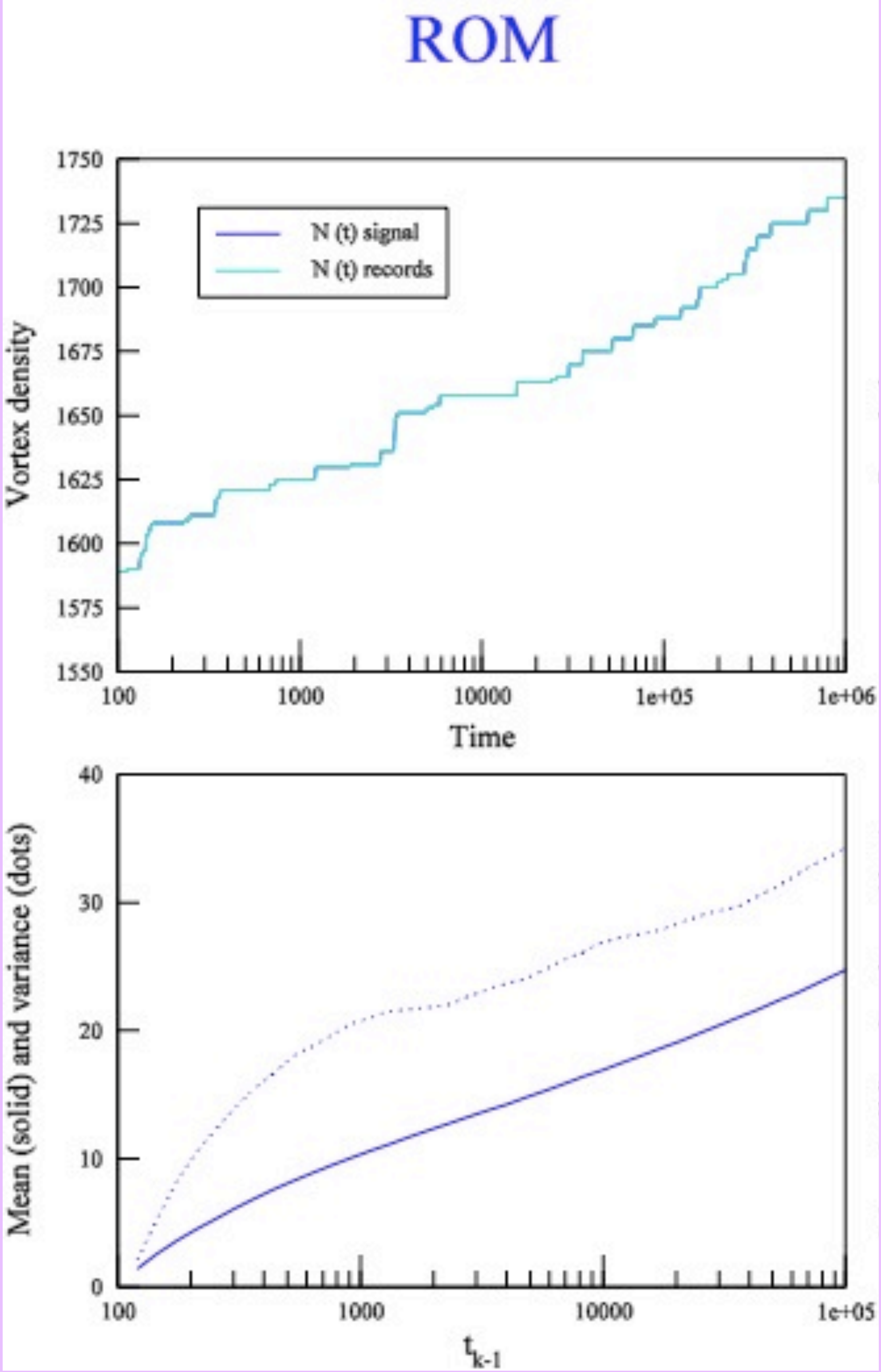

Further evidence

The cumulative distribution of the log waiting times.
Comparison with exponential distribution.

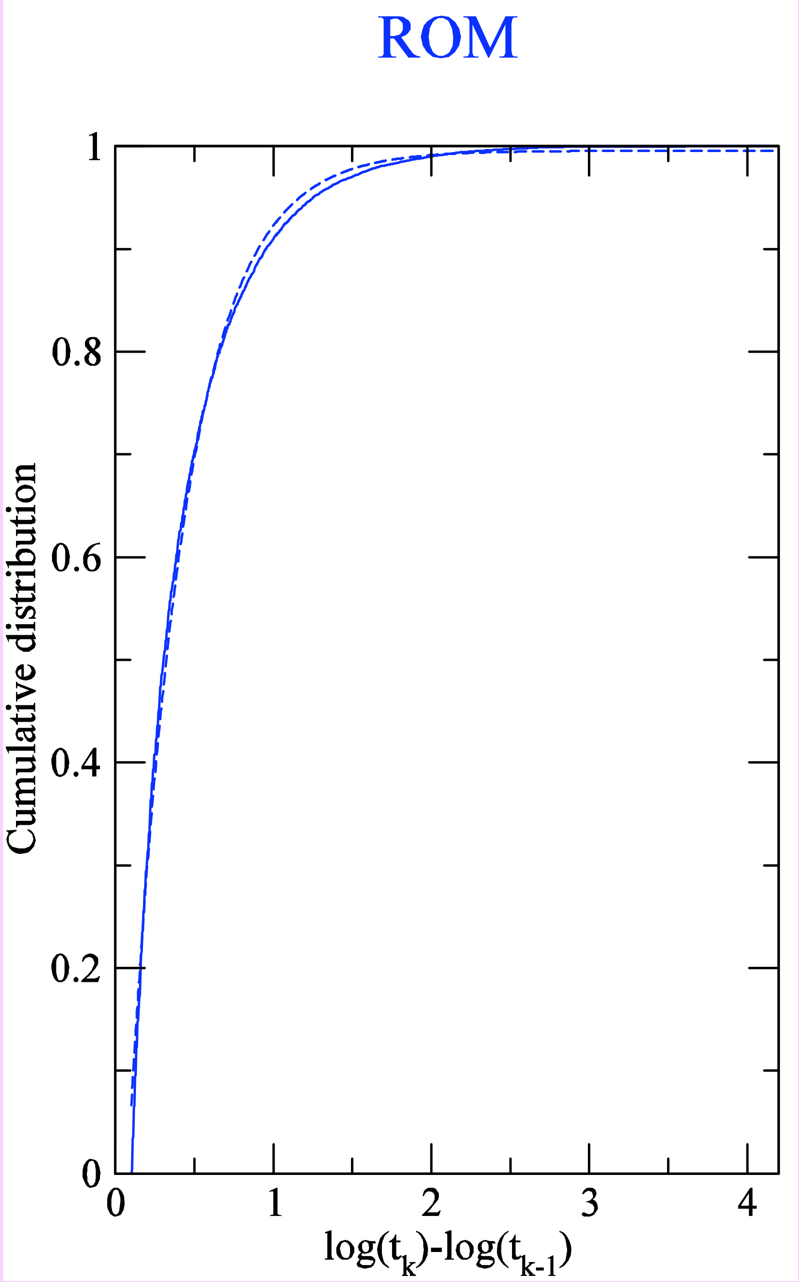

Number of vortices in the bulk as function of time

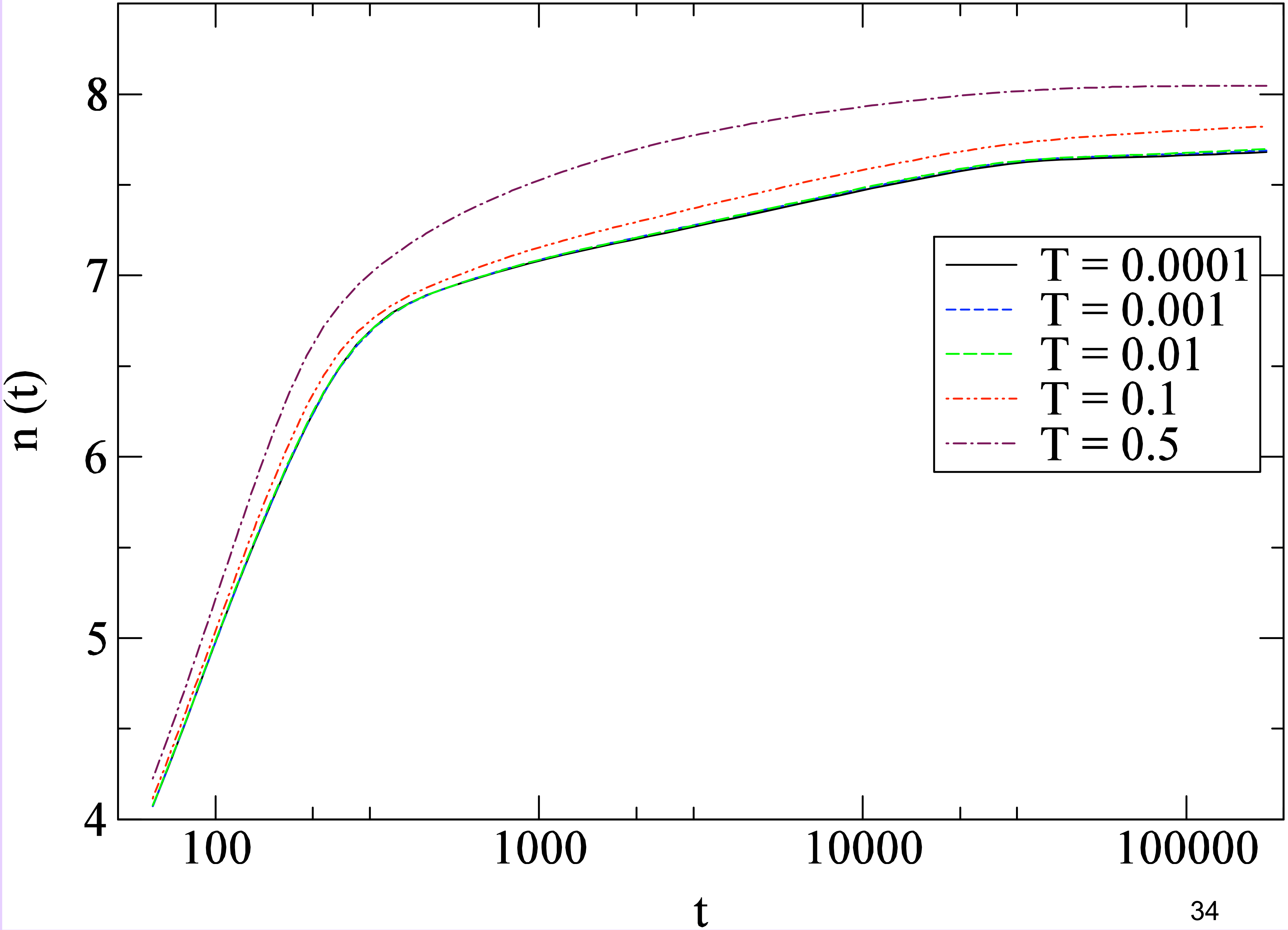

Quake statistics and the total number vortices entering.

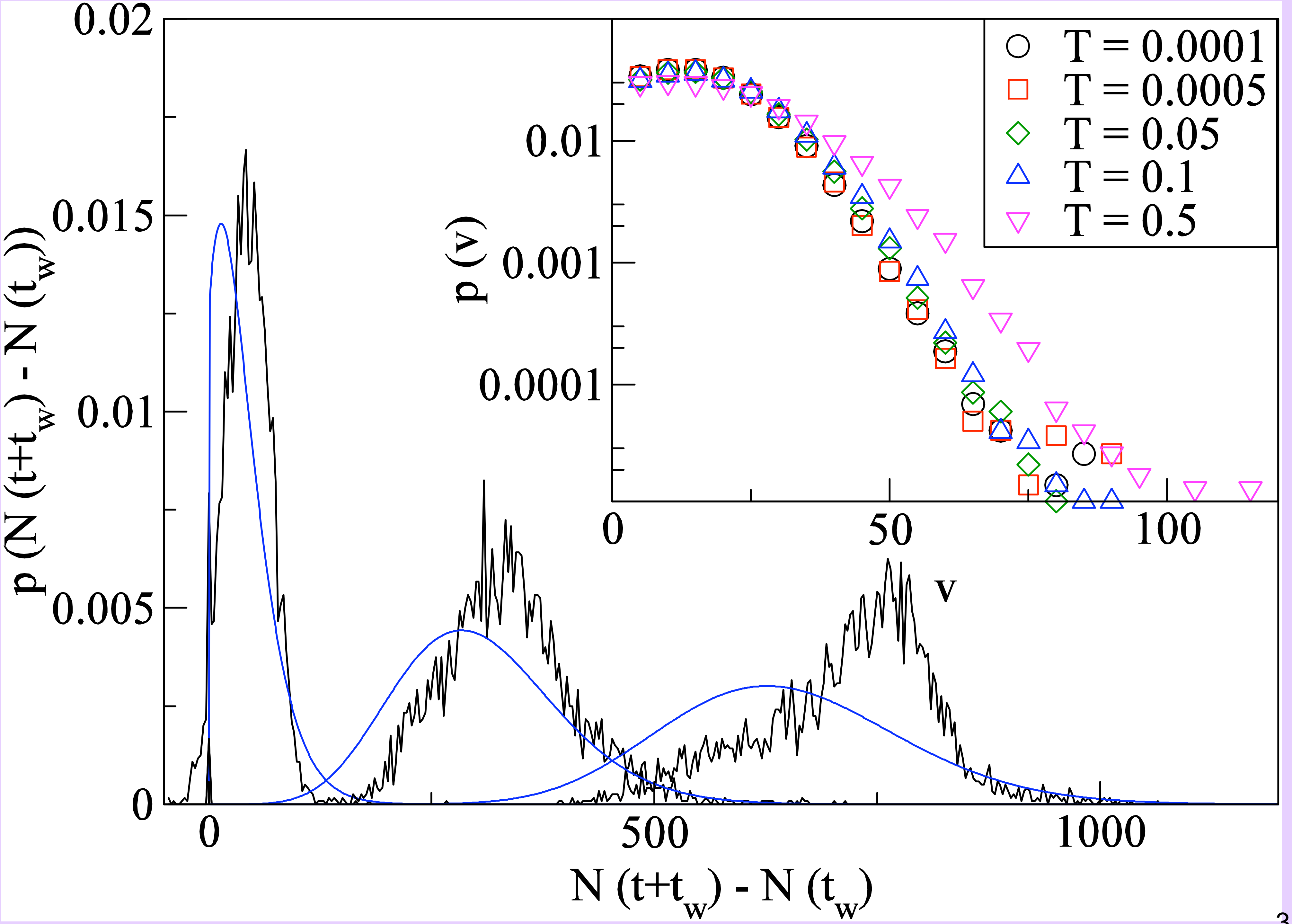

The magnetic creep rate: $S = \dfrac{d\ln(M)}{d\ln(t)}$ where $M(t) = |N(t) - N_{ext}|$

comparison with experiment

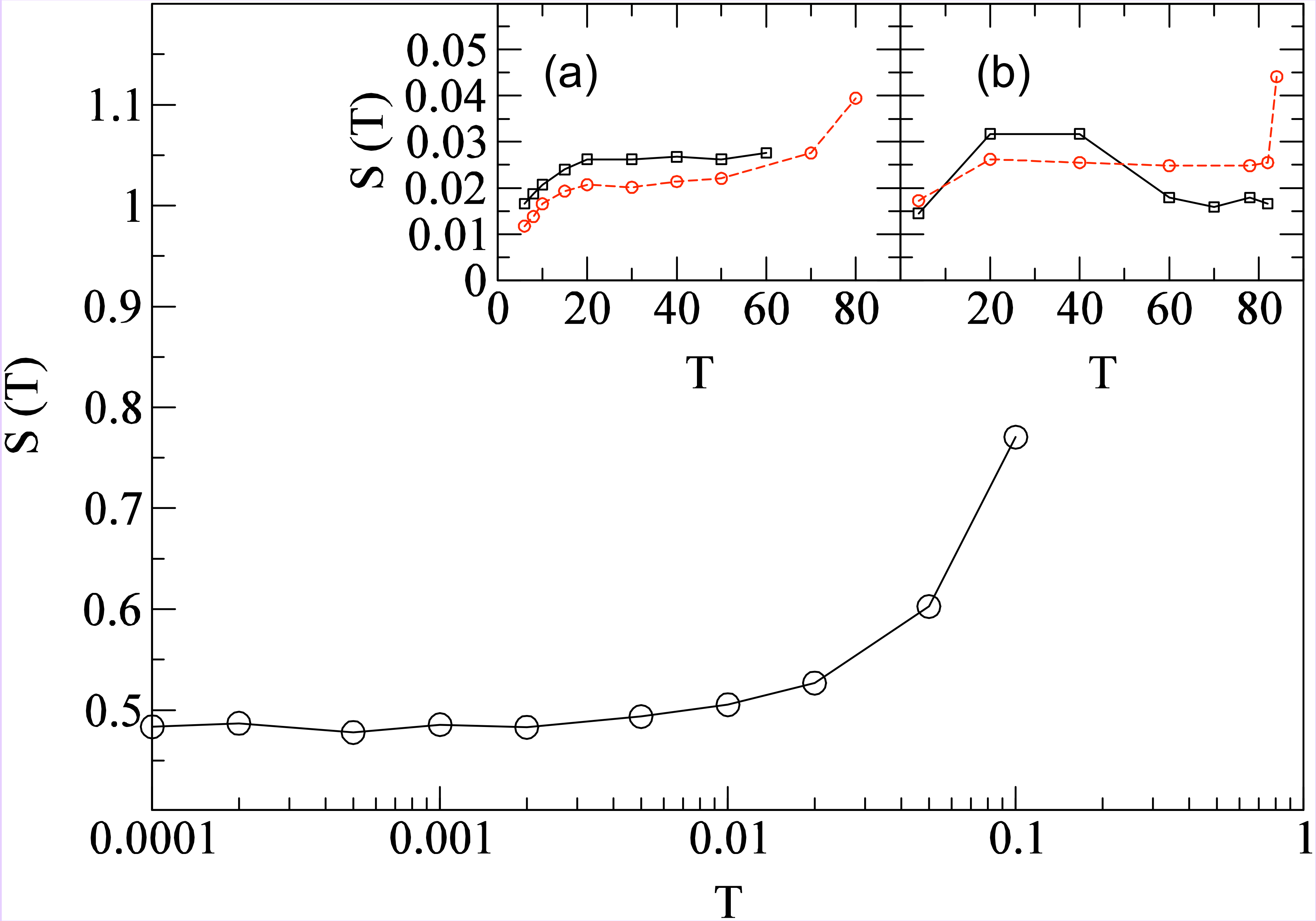

Experim. data from

(a) Civale et al.
PRL 65, 1164 (1990)

(b) Kaiser et al. J Cryst
Growth 85, 593 (1987)

From Oliveira, Jensen, Nicodemi & Sibani PRB 71, 104526 (2005)

Record dynamics

Spin Glass

with Sibani

Spin glass

Microscopic magnetic moments – or spins – coupled together with random coupling constants.

The Hamiltonian:

$$H = -\frac{1}{2}\sum_{ij} J_{ij}\mathbf{S}_i \cdot \mathbf{S}_j \quad \text{where} \quad \mathbf{S}_i,\ \mathbf{S}_j = \pm 1$$

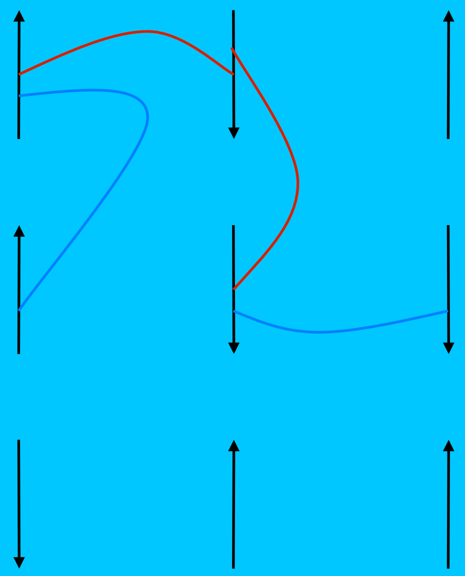

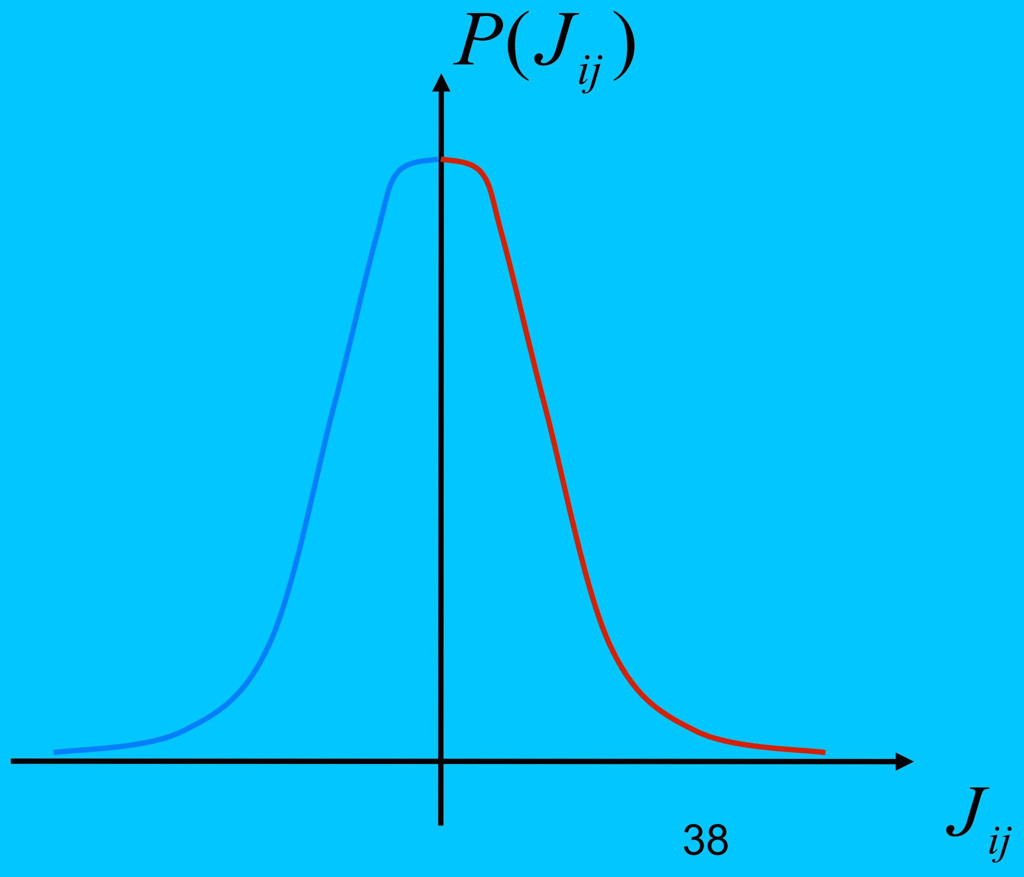

Spin glass

Quench from high temperature:

time < 0: T = high

time > 0: T = very low

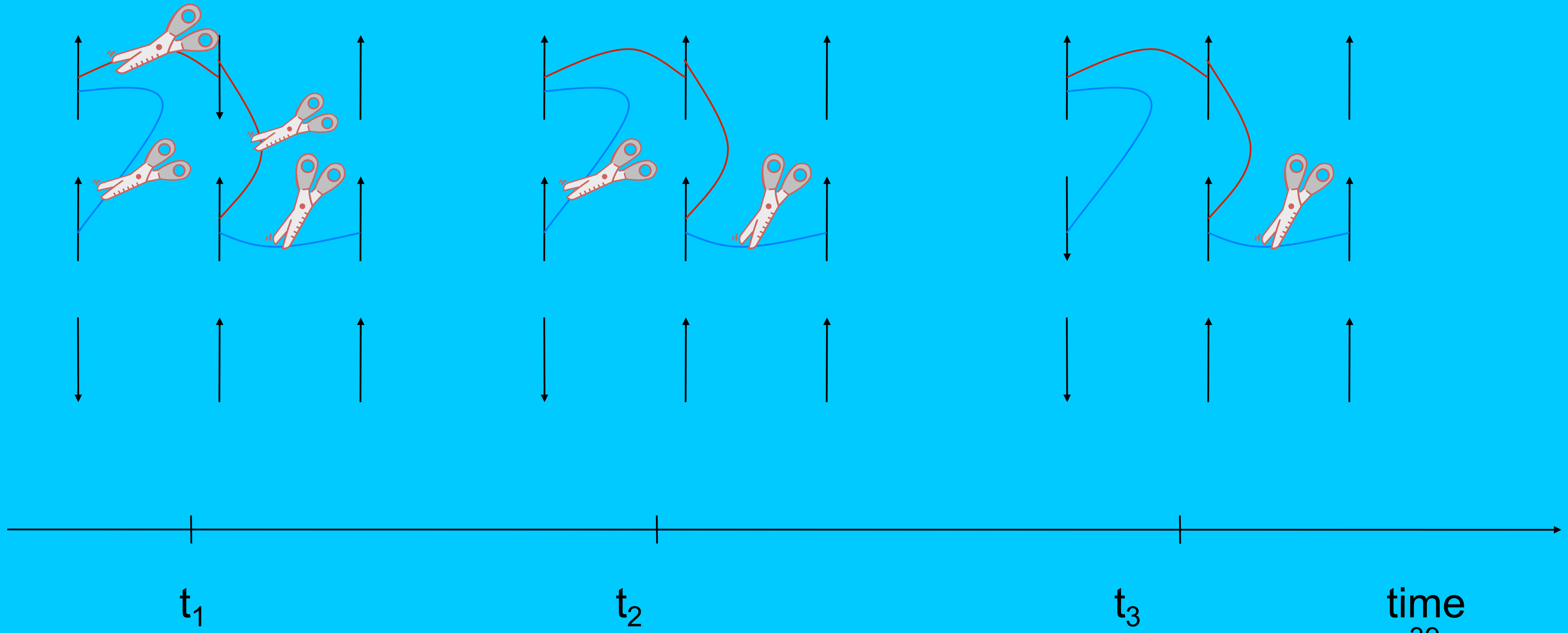

Spin glass: heat transfer

Protocol: Quench from high temp. at time t= 0.

Measure heat transfer, *H*, between spin glass and reservoir during time interval

$$[t_w, t_w + \delta t]$$

- If $\delta t << t_w$ Gaussian p(H)
- If $\delta t \approx t_w$ exponential tail

Spin glass: heat transfer

$\delta t << t_w$

$\delta t \approx t_w$

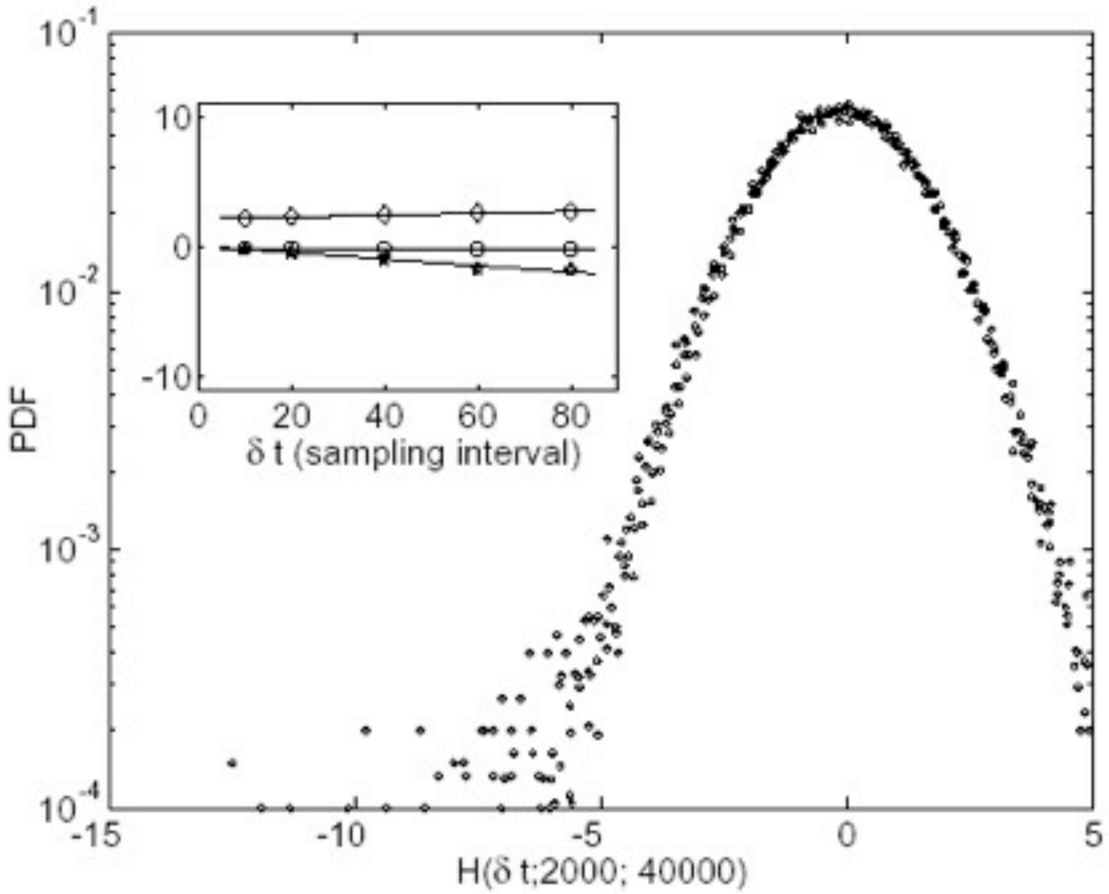

Fig. 1

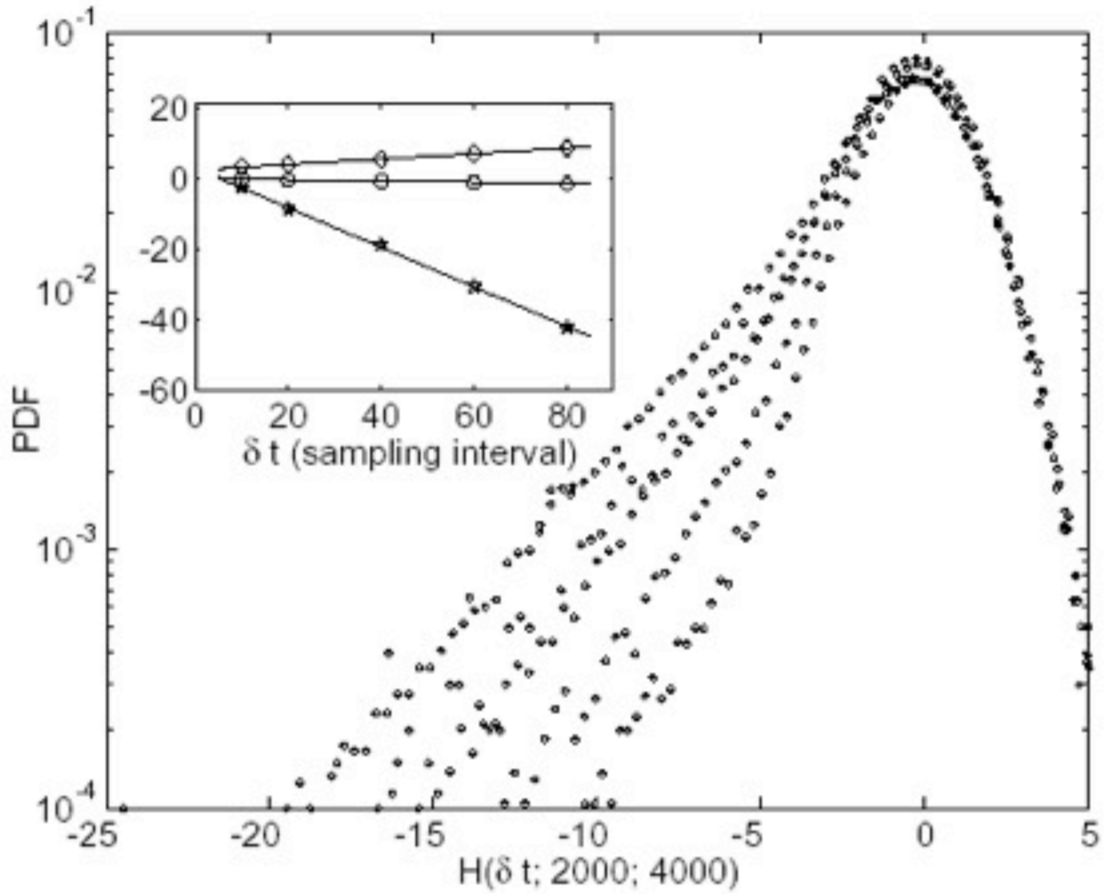

Fig. 2

From Sibani & Jensen, EPL 69, 563 (2005)

Break ?

Record dynamics

Adaptation

Tangled Nature

What next:

- Motivation
- The Tangled Nature Model
- Phenomenology

Why Tangled Nature ?

Last paragraph to the Origin of Species

It is interesting to contemplate a tangled bank, clothed with many plants of many kinds, with birds singing on the bushes, with various insects flitting about, and with worms crawling through the damp earth, and to reflect that these elaborately constructed forms, so different from each other, and dependent upon each other in so complex a manner, have all been produced by laws acting around us.

Evolutionary ecology:

- Interacting organisms + Evolution → Evolving bio-net
- Each type will see an ever changing environment

Focus on system level properties

- ✓ stability
- ✓ mode of evolution
- ✓ nature of the adaptation
- ✓ ecological characteristics: SAD, SAR, Connectance,...

Motivation - Lifetimes

- Lifetime of taxa

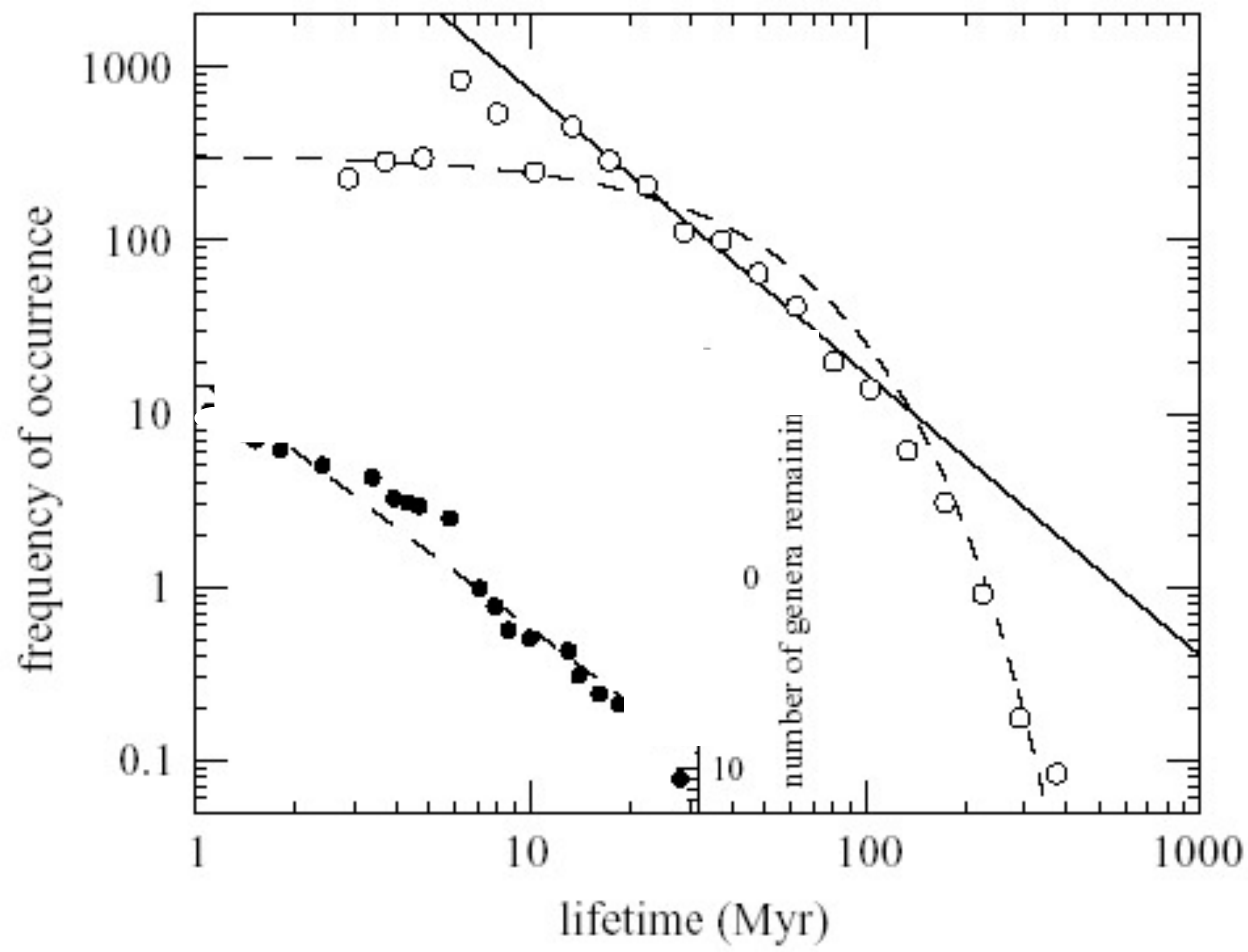

Fossil record: Frequency distribution of lifetimes of marine genus.

From:

Newman and Sibani, Proc. Roy. Soc. B. **266**, 1593 (1999)

Motivation - Tempo and mode

- Time dependent extinction rate

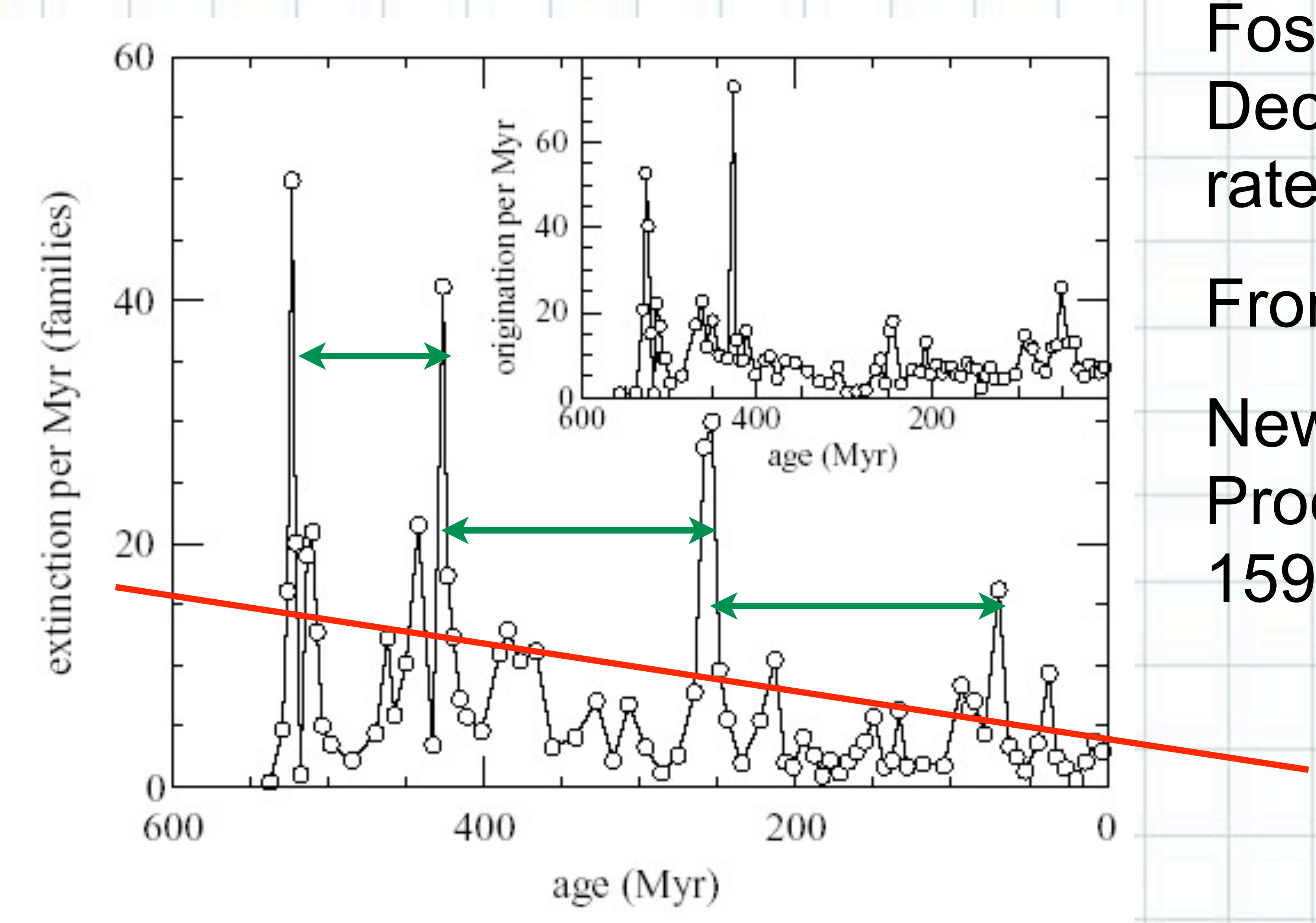

Fossil record: Decreasing extinction rate.

From:

Newman and Sibani, Proc. Roy. Soc. B. **266**, 1593 (1999)

Motivation - Ecology

- Species area relation

$$\# S \propto A^{z}$$

Bird species versus area; Czech Republic.

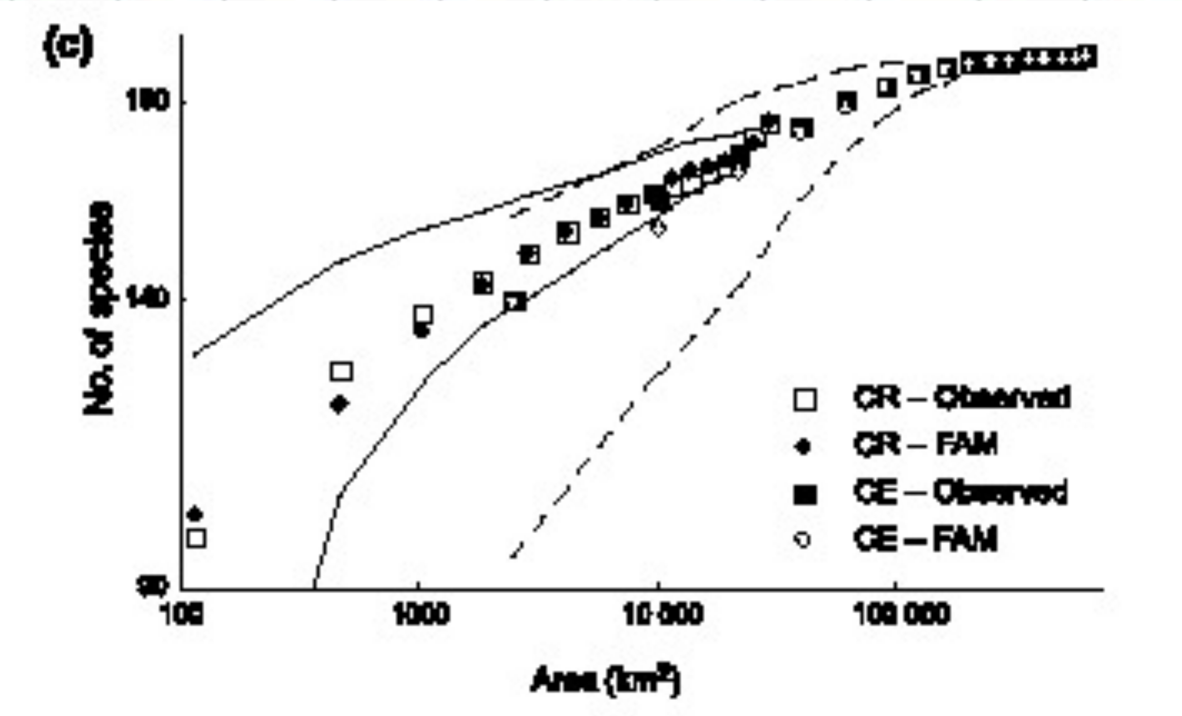

From:

A Stizling and D Storch

Ecol. Lett. **7**, 60 (2004)

Model

Collaborators:

Simon Laird, Daniel Lawson, Paul Anderson, Kim Christensen, Matt Hall, Simone A di Collobiano, Paolo Sibani, Dominic, Jones

Interaction and co-evolution

The Tangled Nature model

- Individuals reproducing in type space
- Your success depends on who you are amongst

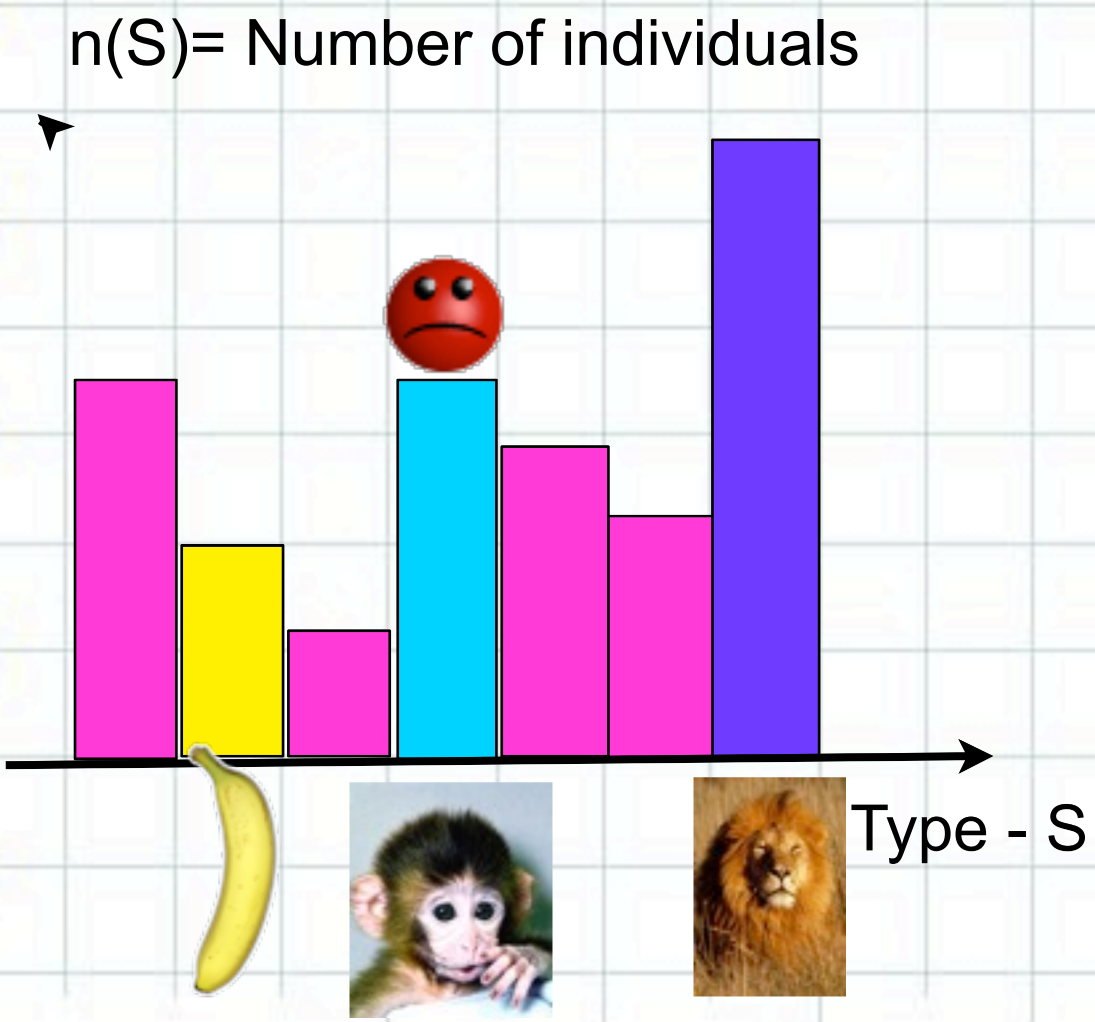

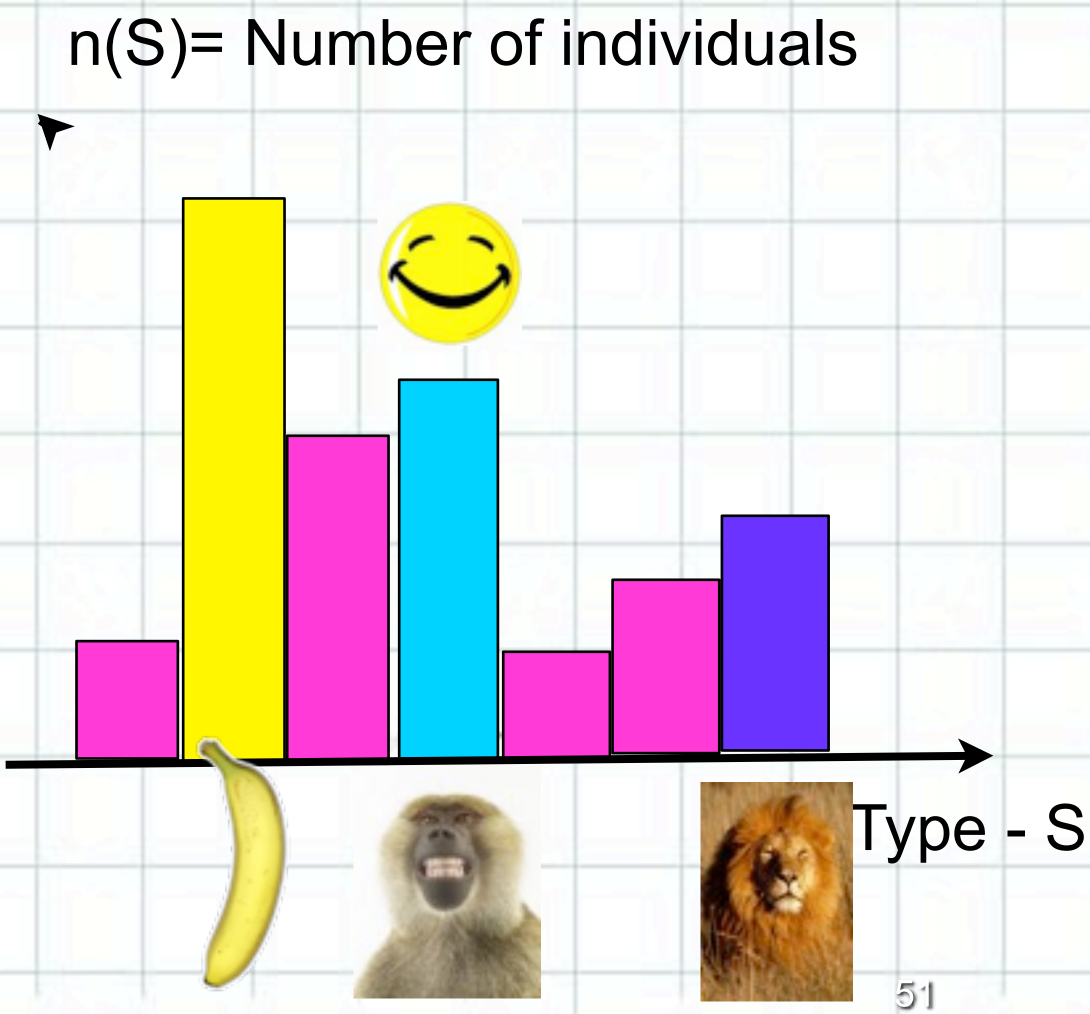

Definition

Individuals $\mathbf{S}^{\alpha} = (S_1^{\alpha}, S_2^{\alpha}, \ldots, S_L^{\alpha})$, where $S_i^{\alpha} = \pm 1$

and $\alpha = 1,2,\ldots,N(t)$

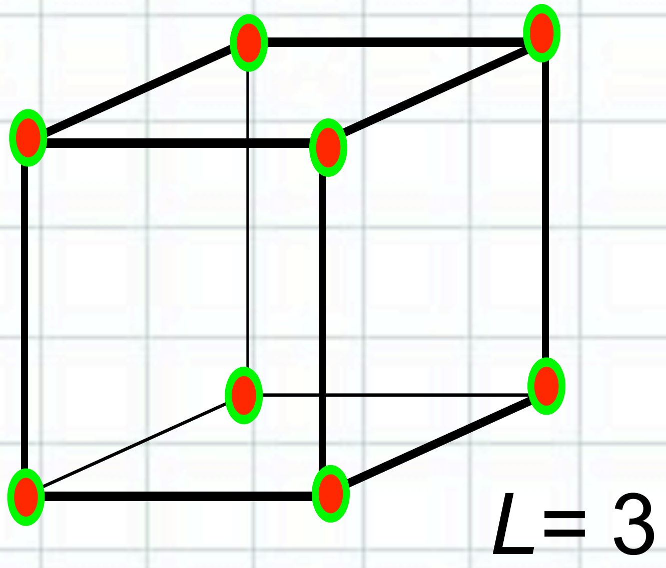

Dynamics – a time step

Annihilation

Choose indiv. at random, remove with probability

$$p_{kill} = const$$

Reproduction:

- Choose indiv. at random
- Determine

$$H(\mathbf{S}^\alpha, t) = \frac{k}{N(t)} \sum_{\mathbf{S}} J(\mathbf{S}^\alpha, \mathbf{S}) n(\mathbf{S}, t) - \mu N(t)$$

$n(\mathbf{S}, t) =$ occupancy at the location $\mathbf{S}$

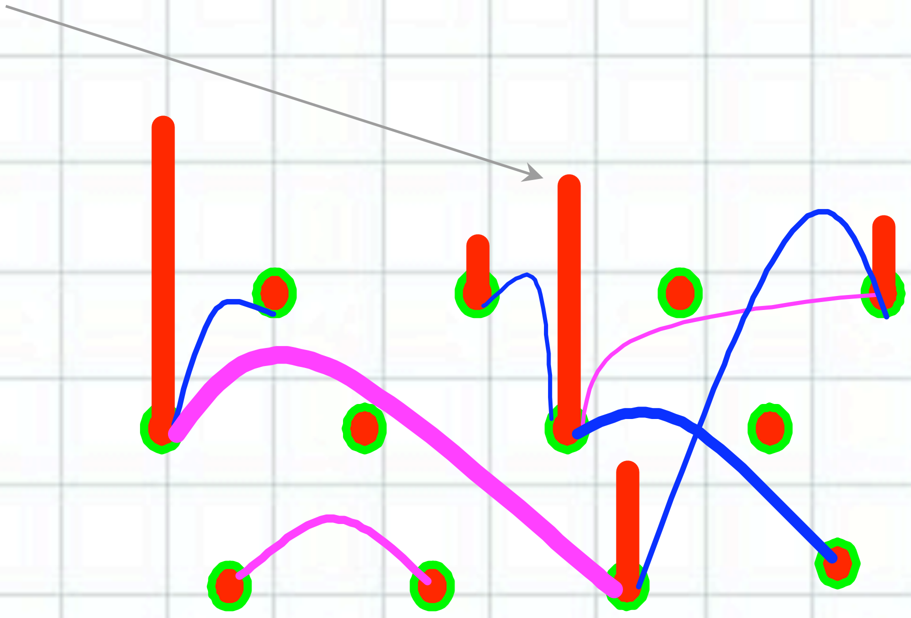

The coupling matrix J(S,*S'*)

- ☑ Either consider J(S,*S'*) to be uncorrelated
- ☑ or to vary smoothly through type space
- ☑ and sparse or dense

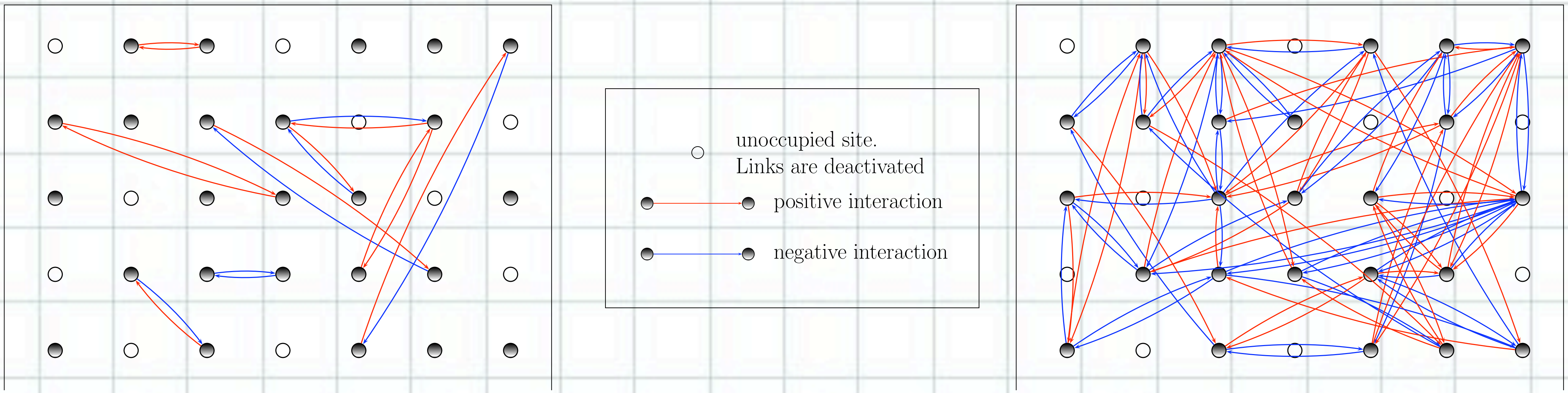

from $H(\mathbf{S}^\alpha,t)$ reproduction probability

$$p_{off}(\mathbf{S}^\alpha,t)=\frac{\exp[H(\mathbf{S}^\alpha,t)]}{1+\exp[H(\mathbf{S}^\alpha,t)]}\in[0,1]$$

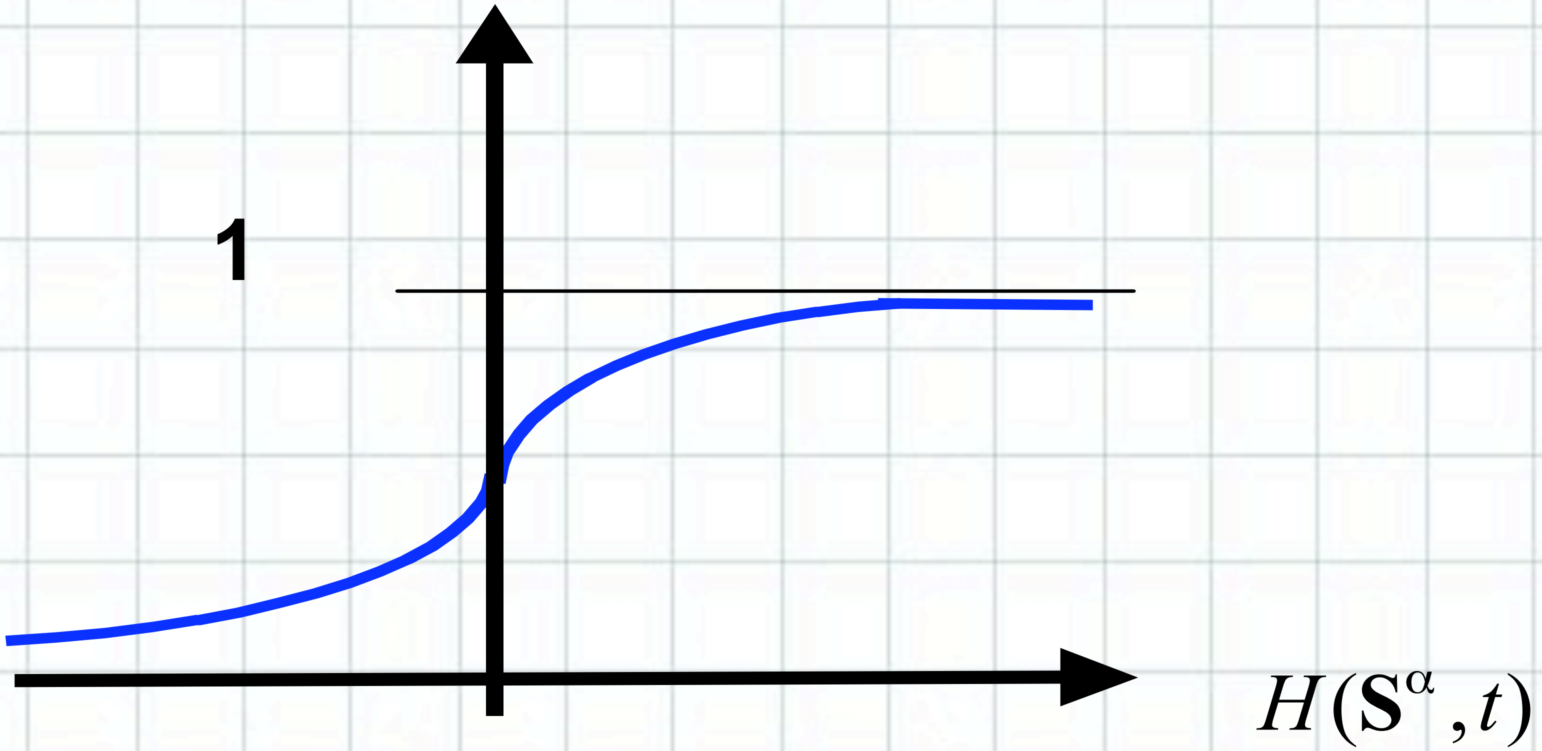

Segregation in genotype space

Initiation

Only one genotype

Jn term = 0

$$H = \frac{k}{N(t)} \sum_{s} Jn - \mu\, N(t)$$

N(t) adjusts

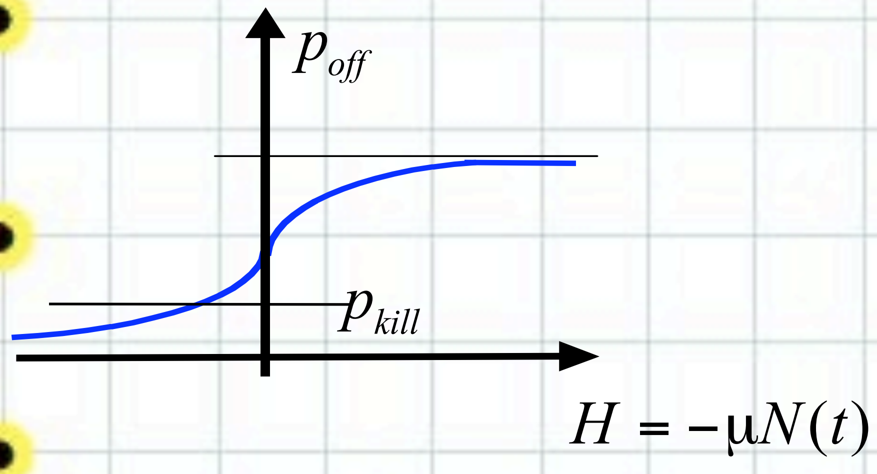

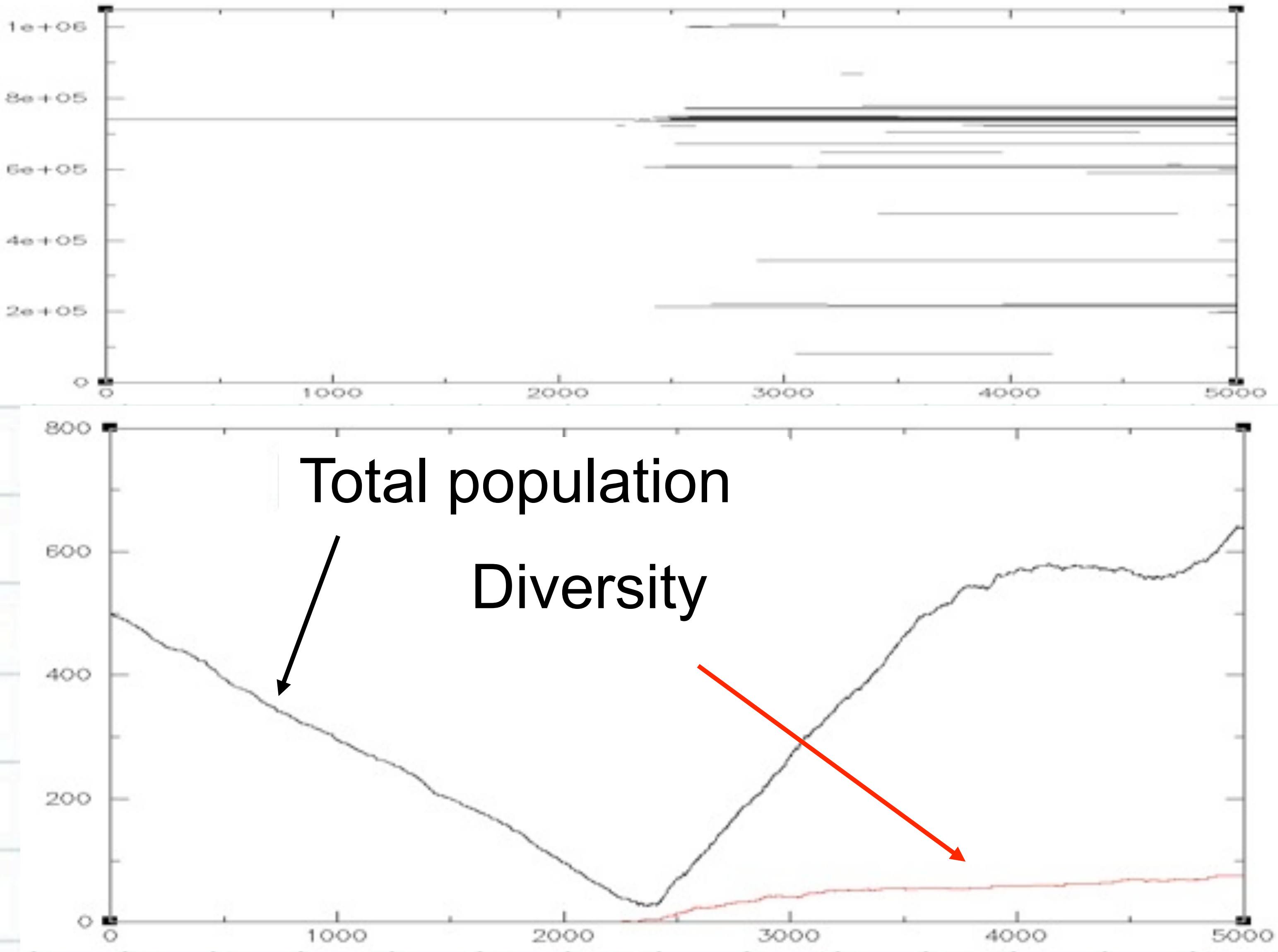

Time steps

Macro dynamics:

Non correlated

Graph courtesy to Matt Hall

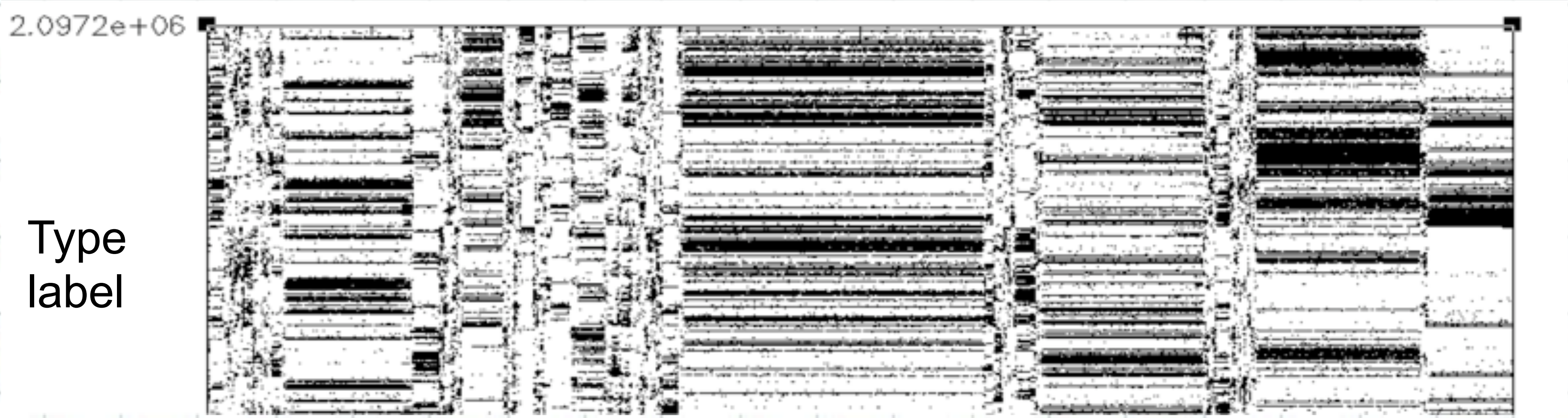

 # generations

1 generation = $N(t)/p_{kill}$

Origin of drift?

Effect of mutation

Let $H = \tilde{J} - \mu N$, then the effect of a mutation is

$$H \mapsto H + \delta \tilde{J}.$$

→ Symmetric fluctuations $prob(\delta \tilde{J}) = prob(-\delta \tilde{J})$

leads to asymmetri

$$p_{off}(H_0 + \delta \tilde{J}) - p_{kill} >$$

$$p_{kill} - p_{off}(H_0 - \delta \tilde{J})$$

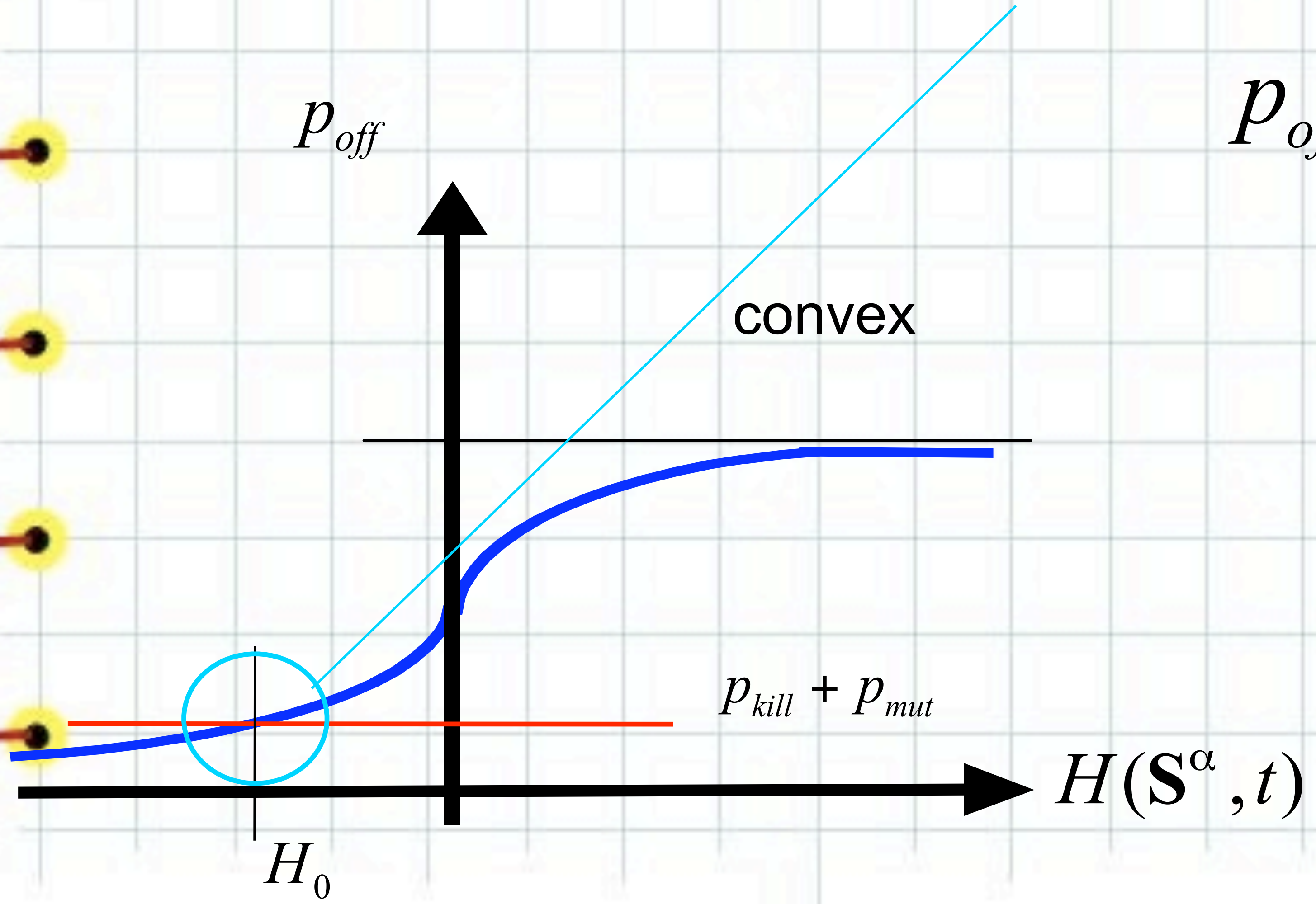

Dynamics:

The functional form of

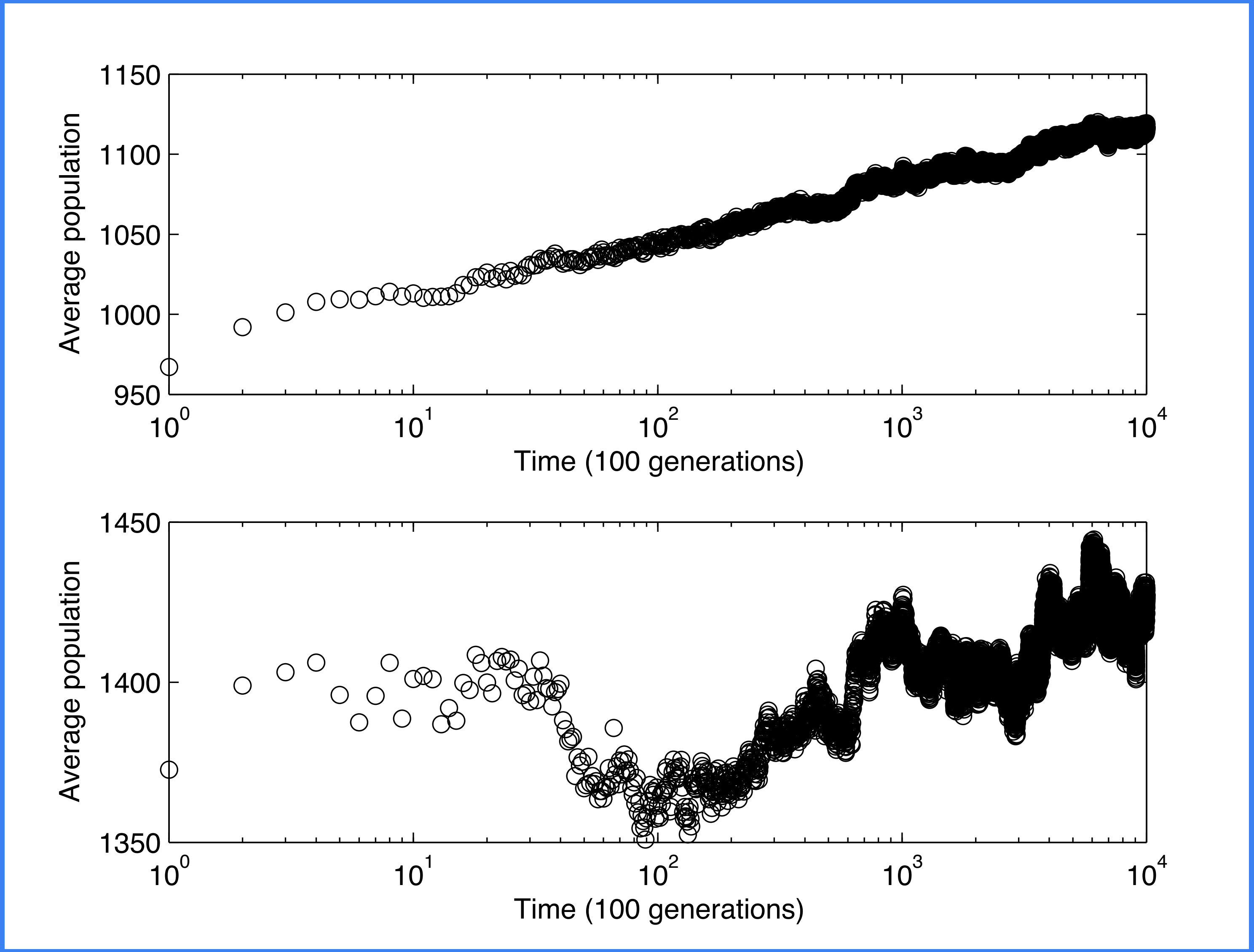

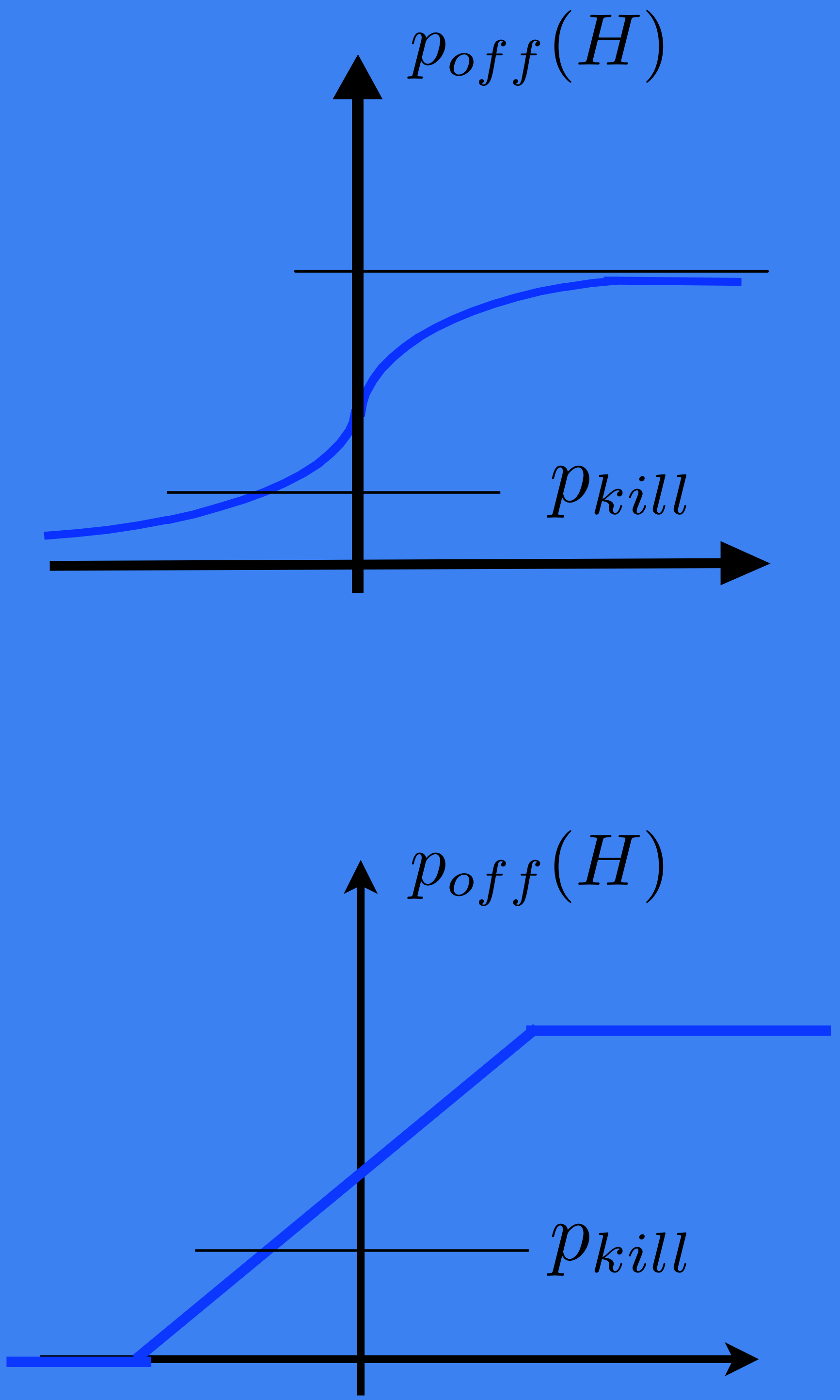

Dominic Jones

Intermittency:

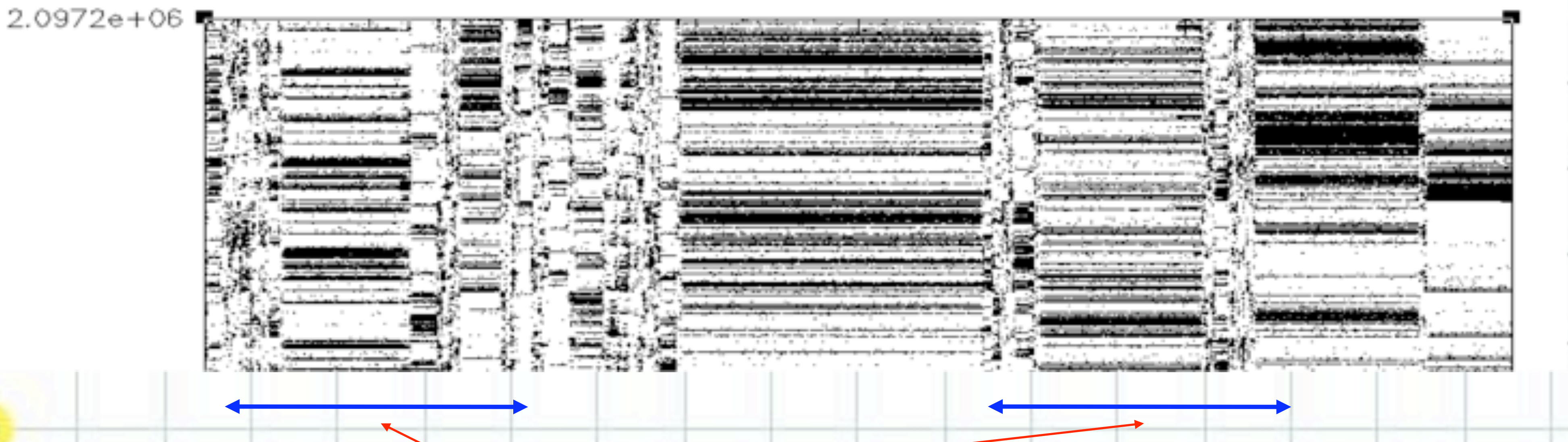

# of transitions in window

Matt Hall

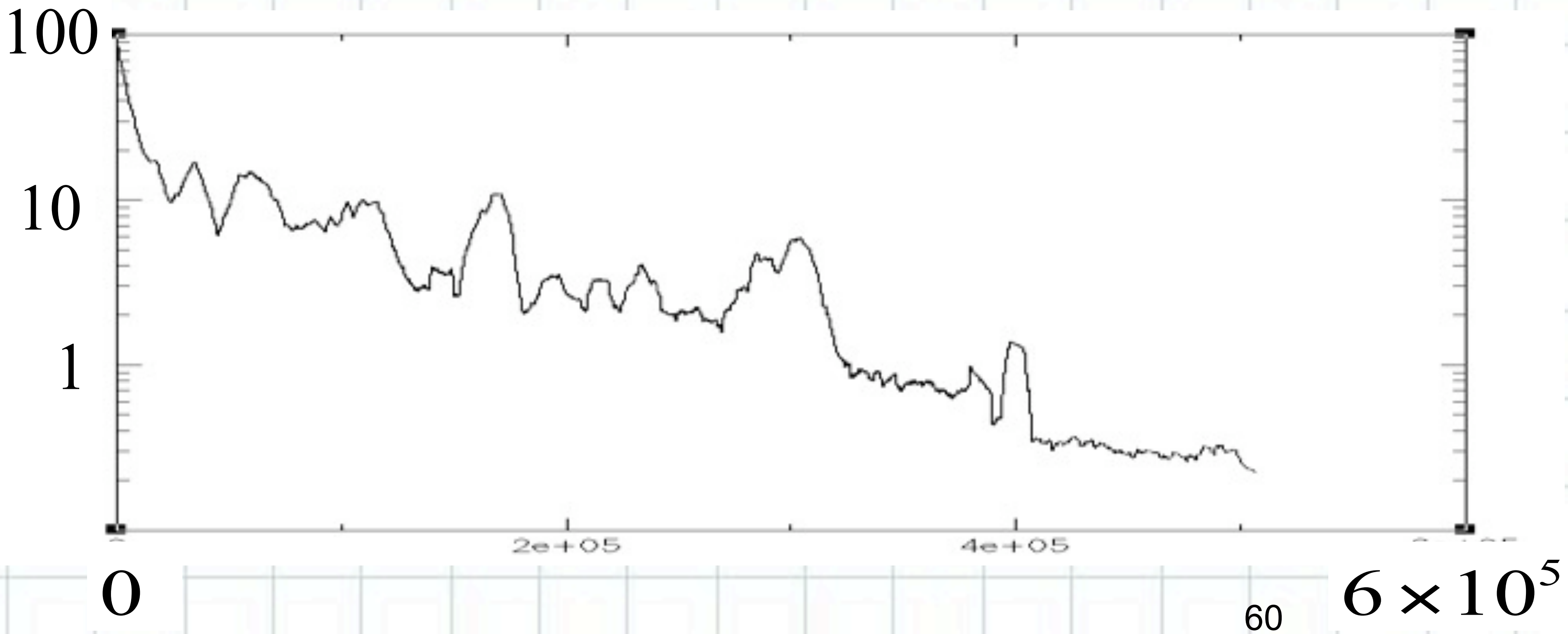

1 generation
= $N(t)/p_{kill}$

Complex dynamics:

Intermittent, non-stationary

Jumping through collective adaptation space: quake driven

Transitions

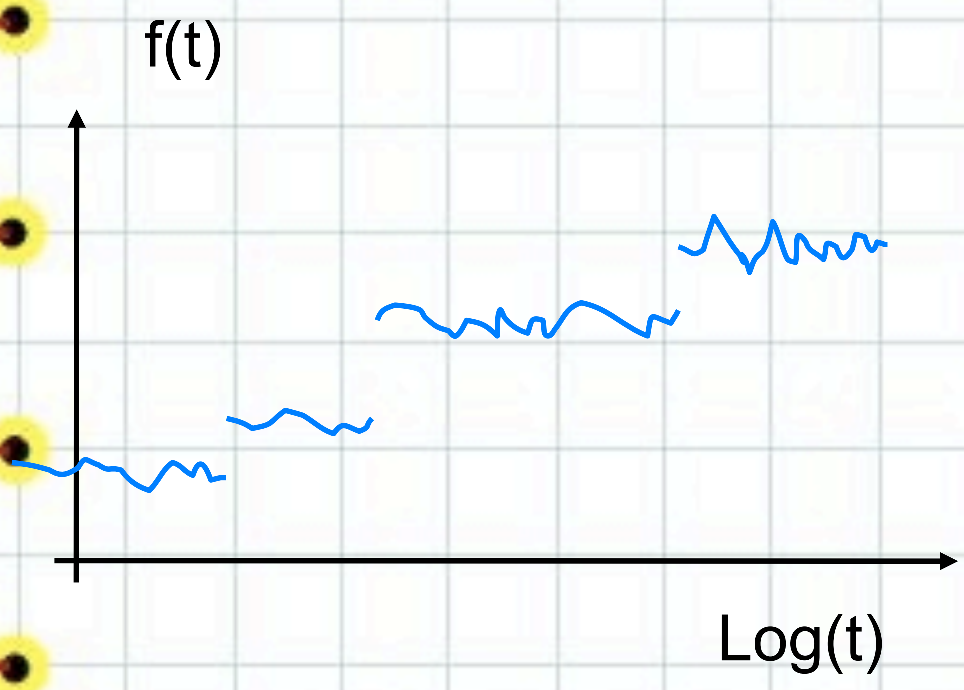

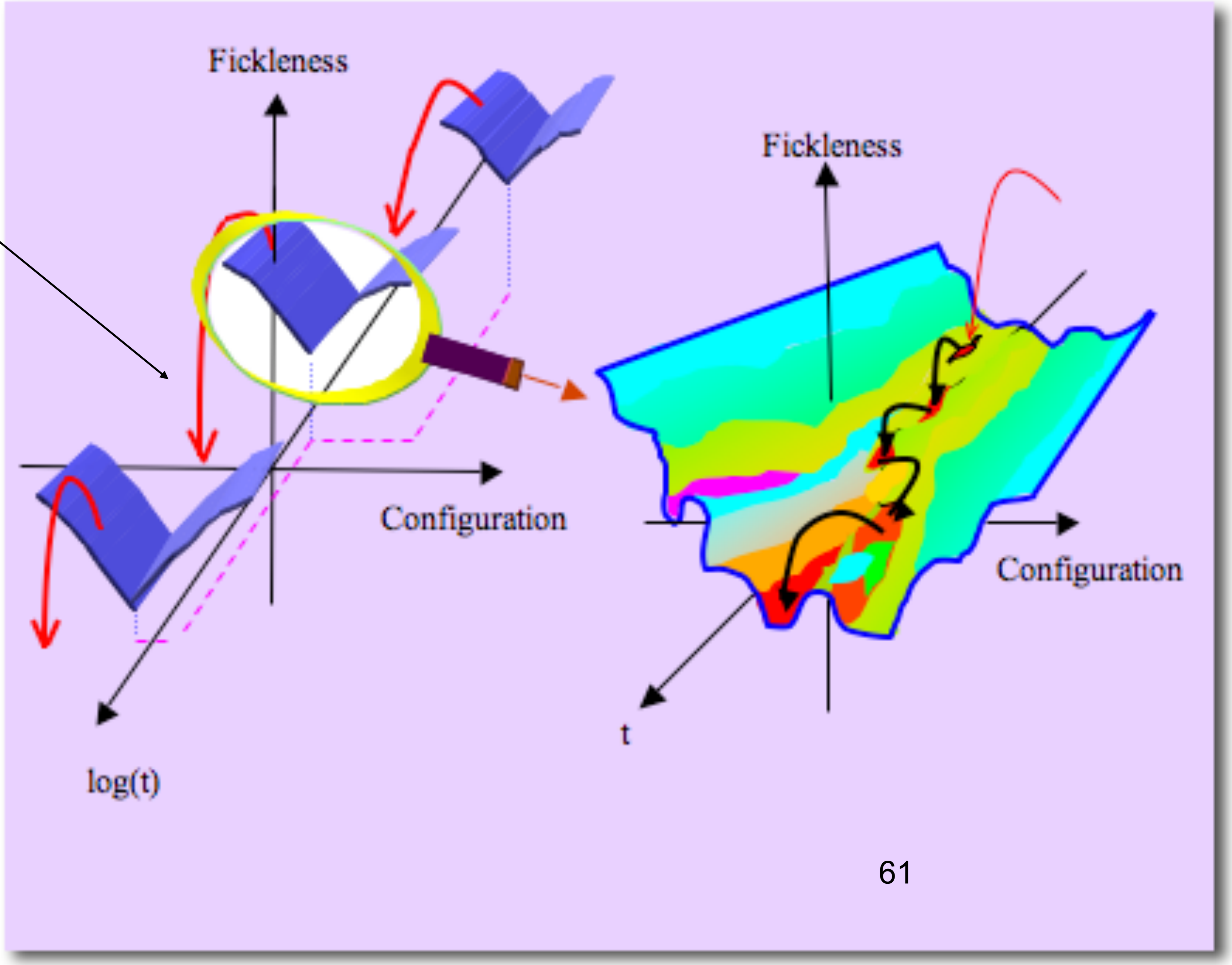

Macro dynamics:

Non correlated

Graph courtesy to Matt Hall

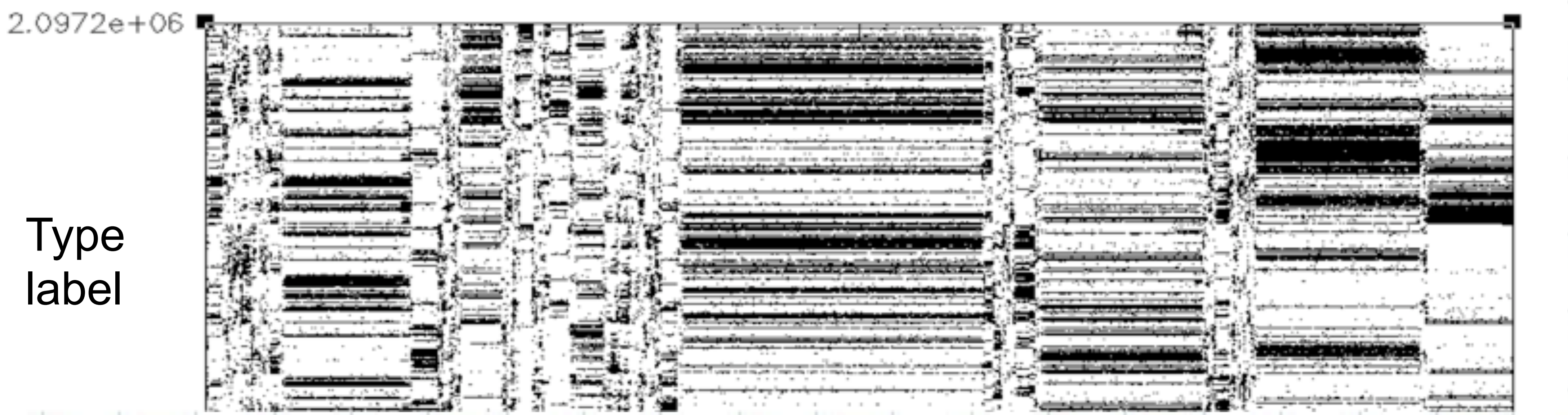

 # generations

1 generation = $N(t)/p_{kill}$

Record dynamics:

Ratio *r* remains non-zero

$$r = (t_k - t_{k-1}) / t_{k-1}$$

Cumulative Distribution

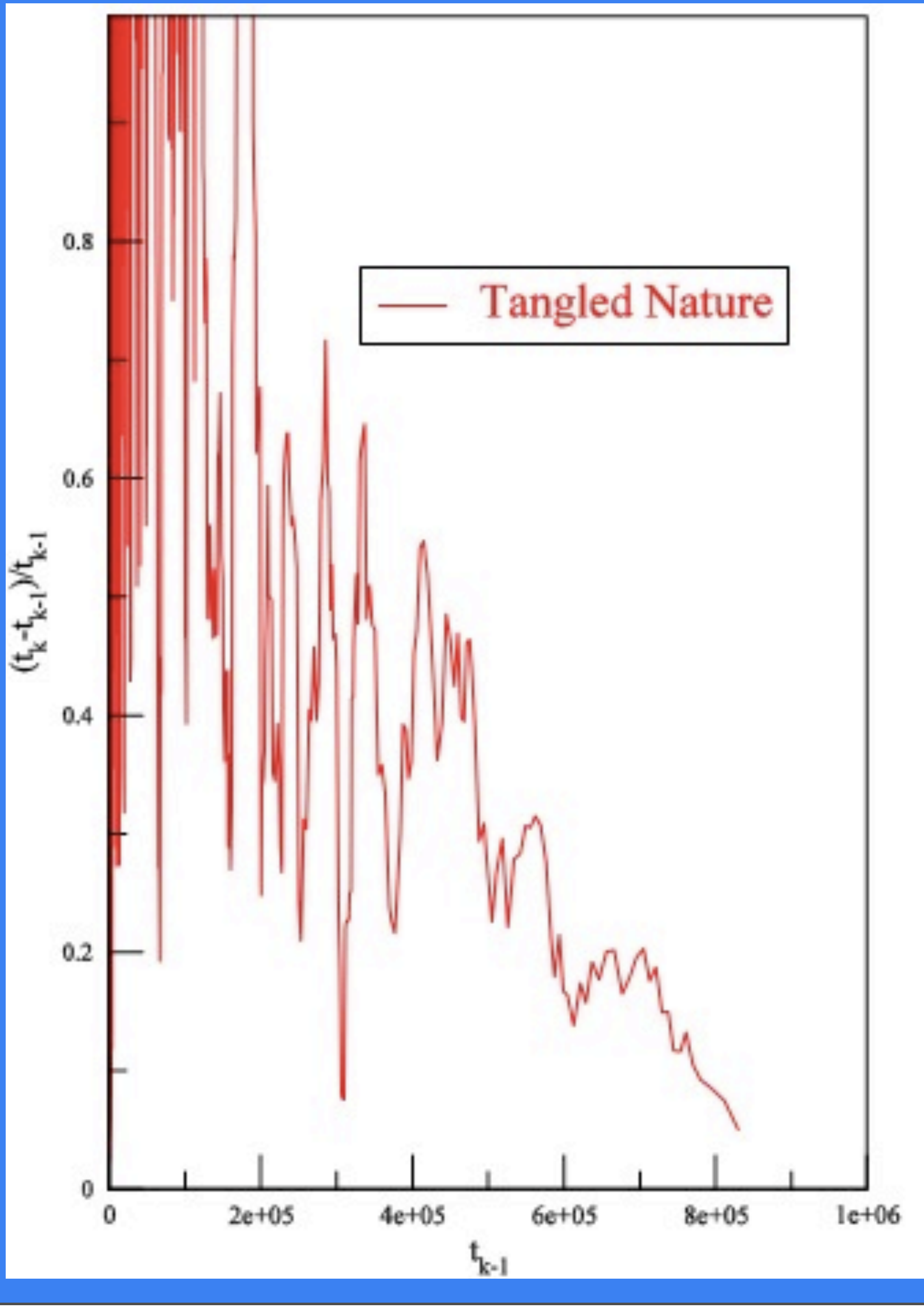

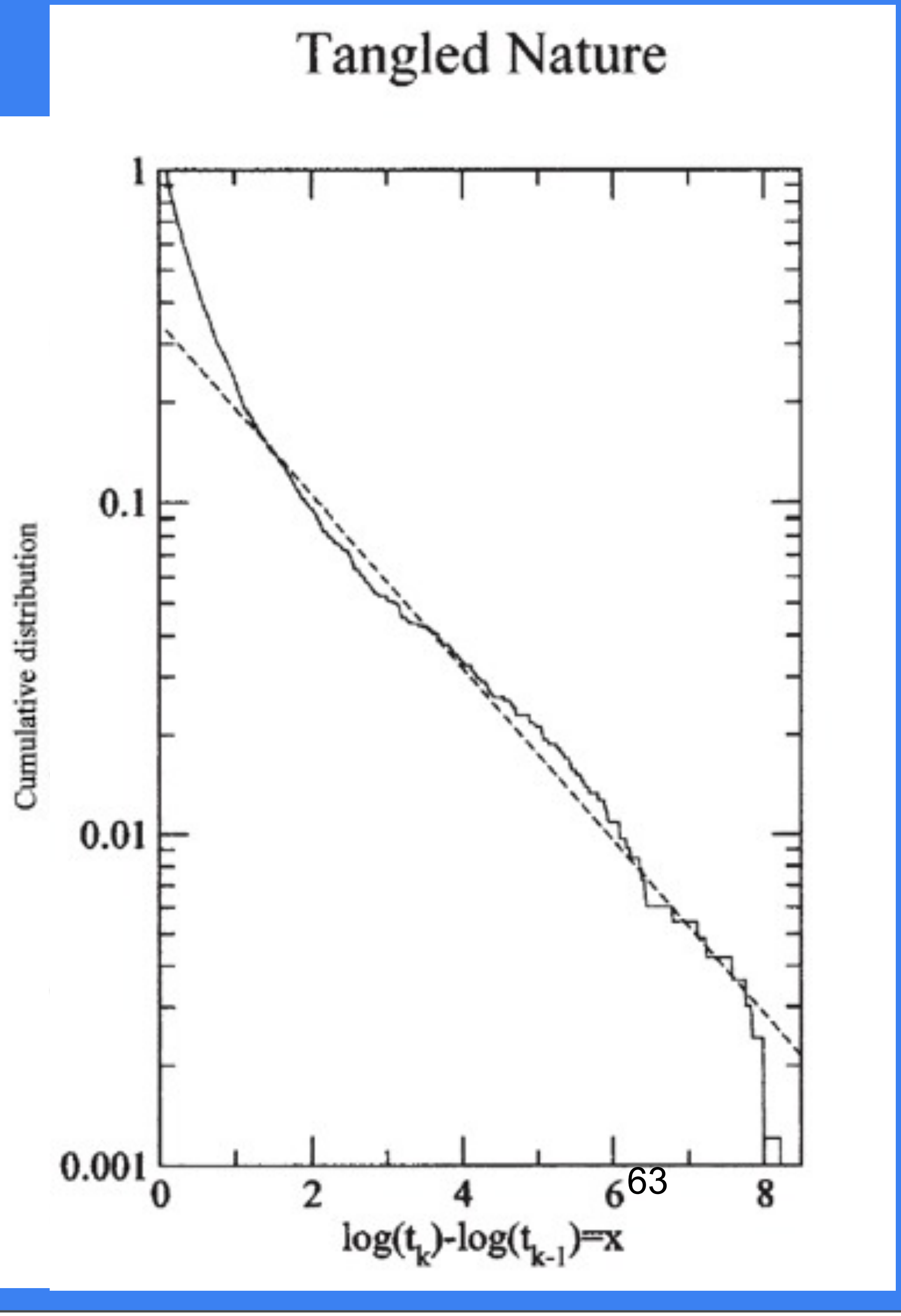

Paul Anderson

Stability

Tangled Nature -

Macro dynamics - the transitions

Non correlated

Graph courtesy to Matt Hall

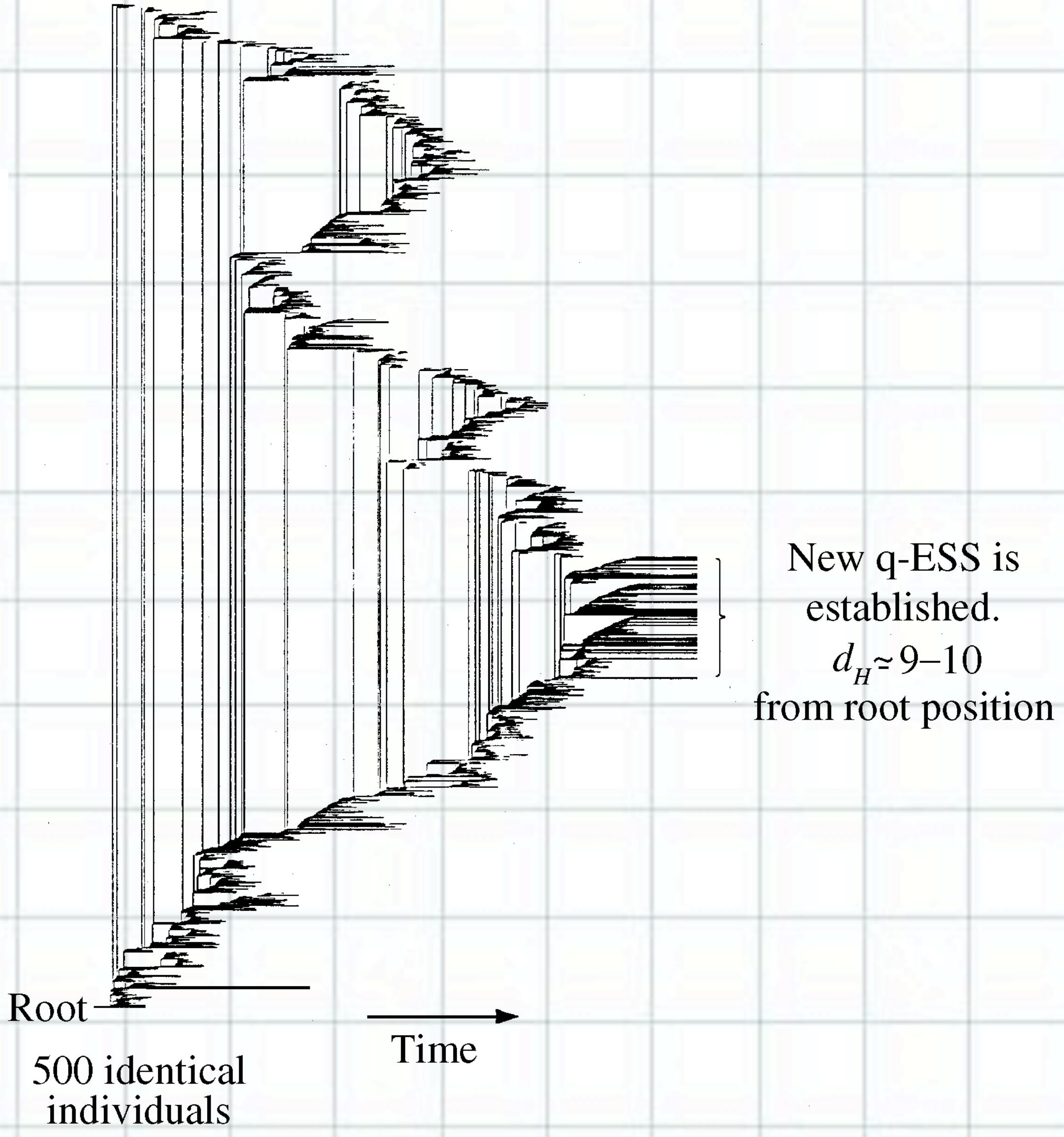

Stability of the q-ESS:

Consider simple adiabatic approximation.

Stability of genotype S assuming: $n(S',t)$ independent of t for $S' \neq S$

Consider $$\frac{\partial n(S,t)}{\partial t} = [p_{off}(n(S,t),t) - p_{kill} - p_{mut}]\frac{n(S,t)}{N(t)}$$

Stationary solution $n_0(S)$ corresponds to $p_{off}(n_0(S)) - p_{kill} - p_{mut} = 0$

Fluctuation $$\delta = n(S,t) - n_0(S)$$

Fulfil $$\dot{\delta} = A\frac{n_0}{N_0}\delta$$

with $A = -(1 - p_{mut})(p_{off})^2 e^{-H_0}(\frac{J}{N_0^{\,2}} + \mu) < 0$ **i.e. stability**

Transitions between q-ESS caused by co-evolutionary collective fluctuations

$n(S',t)$ needs to be considered

dependent of t for $S' \neq S$

The error threshold

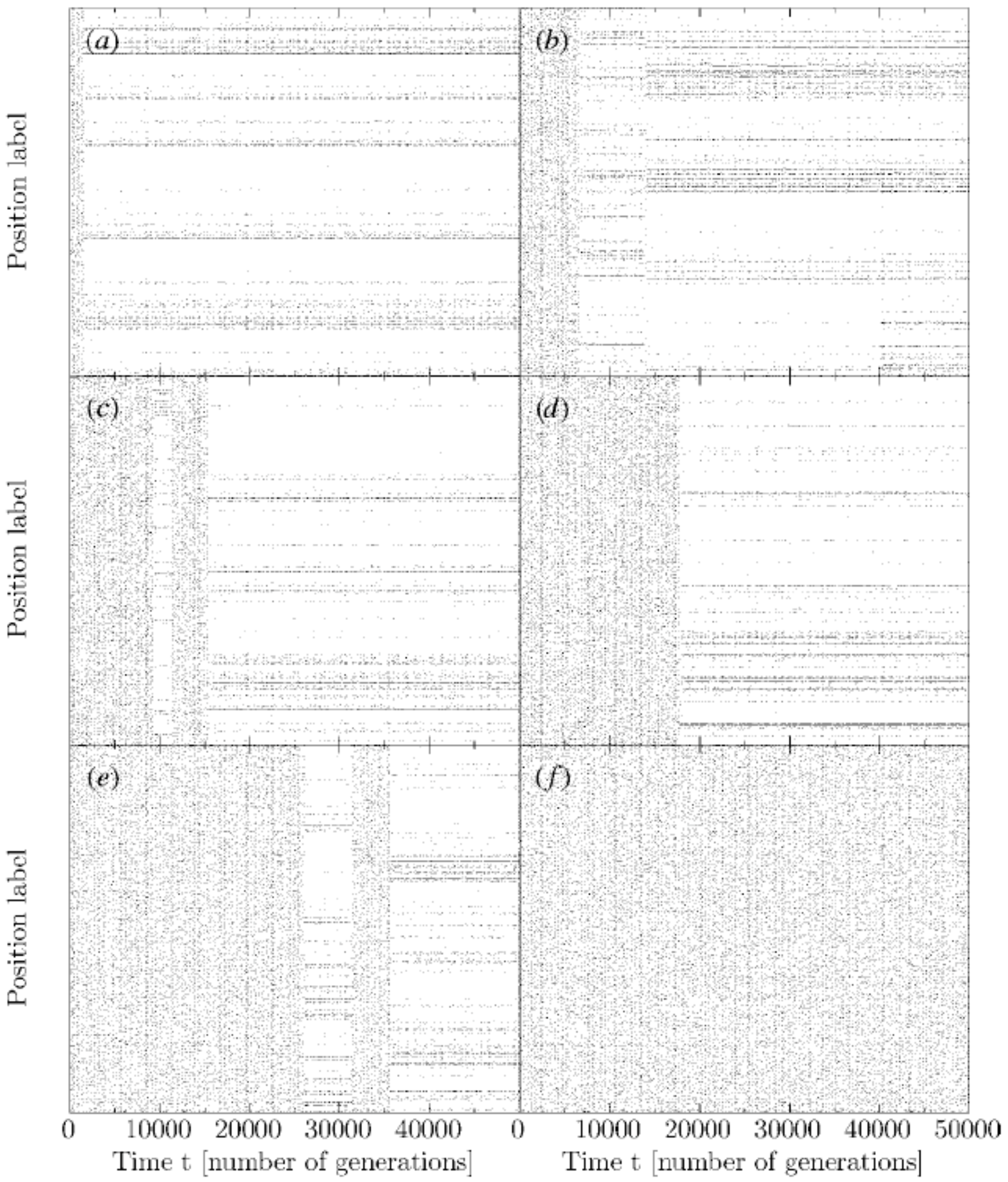

Figure 3. Occupation plots for different values of the mutation rate. The *y*-axis refers to an arbitrary enumeration of all positions in genotype space. Occupied positions are indicated by a black dot. Results shown are for $p_{\mathrm{kill}} = 0.2$, $\mu = 1/1000 \cdot \ln\left(\frac{1-p_{\mathrm{kill}}}{p_{\mathrm{kill}}}\right)$ and $C = 0.05$. (*a*) Mutation rate: $p_{\mathrm{mut}} = 0.009$. The initial transient is extended. (*b*) Mutation rate: $p_{\mathrm{mut}} = 0.009\,25$. The initial transient has the same extension of any q-ESS state. (*c*) Mutation rate: $p_{\mathrm{mut}} = 0.0095$. The transition between two q-ESS state are extended. (*d*) Mutation rate: $p_{\mathrm{mut}} = 0.01$. The initial transient is very extended. (*e*) Mutation rate $p_{\mathrm{mut}} = 0.0104$. The initial transient and any transitions are extensively hectic. (*f*) Mutation rate $p_{\mathrm{mut}} = 0.0108$. There is no q-ESS state.

Too large mutation rate prevents qEES to establish.

Mean field analysis:

$$p_0 = (1 - p_{mut})^L$$

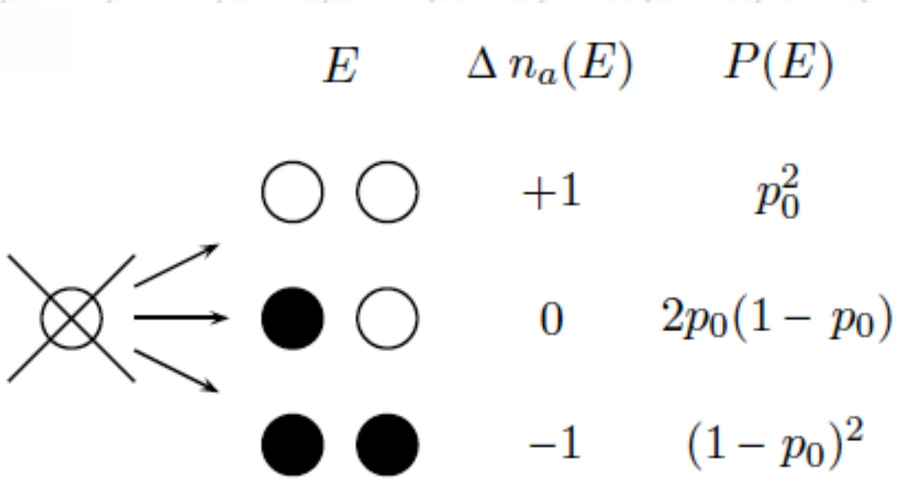

	E	$\Delta\, n_a(E)$	$P(E)$
	○ ○	$+1$	p_0^2
	● ○	0	$2p_0(1-p_0)$
	● ●	-1	$(1-p_0)^2$

Number of individuals on site *a*

$$\Delta n_a = +1 p_o^2 + (-1)(1-P_0)^2 = 2p_0 - 1$$

$$\Downarrow$$

$$n_a(t+1) = n_a(t) + \frac{n_a(t)}{\sum_a' n_{a'}(t)} [p_{off}^a(t)(2p_0 - 1) - p_{kill}]$$

Collobiano, Christensen and Jensen, J Phys A **36**, 883, (2003) Assume steady state, time average and use

$$\langle \frac{n_a(t)}{\sum_a' n_{a'}(t)} p_{off}^a(t)\rangle = \langle \frac{n_a(t)}{\sum_a' n_{a'}(t)}\rangle \langle p_{off}^a(t)\rangle$$

then we obtain

$$p_q = \frac{p_{kill}}{2(1-p_{mut})^L - 1}$$

for the on average off-spring probability for those site which are able to counterbalance the kill by off-spring production.
Leading to a corresponding weight function *H* for the wild-types in the q-ESS

$$H_q = \ln(\frac{p_q}{1-p_q}) = \ln(\frac{p_{kill}}{2(1-p_{mut})^L - 1 - p_{kill}})$$

In the hectic states we assume the a simple balance between reproduction and killing

$$p_{off} = p_{kill}$$

or $$H_{hectic} = \ln(\frac{p_{kill}}{1-p_{kill}})$$

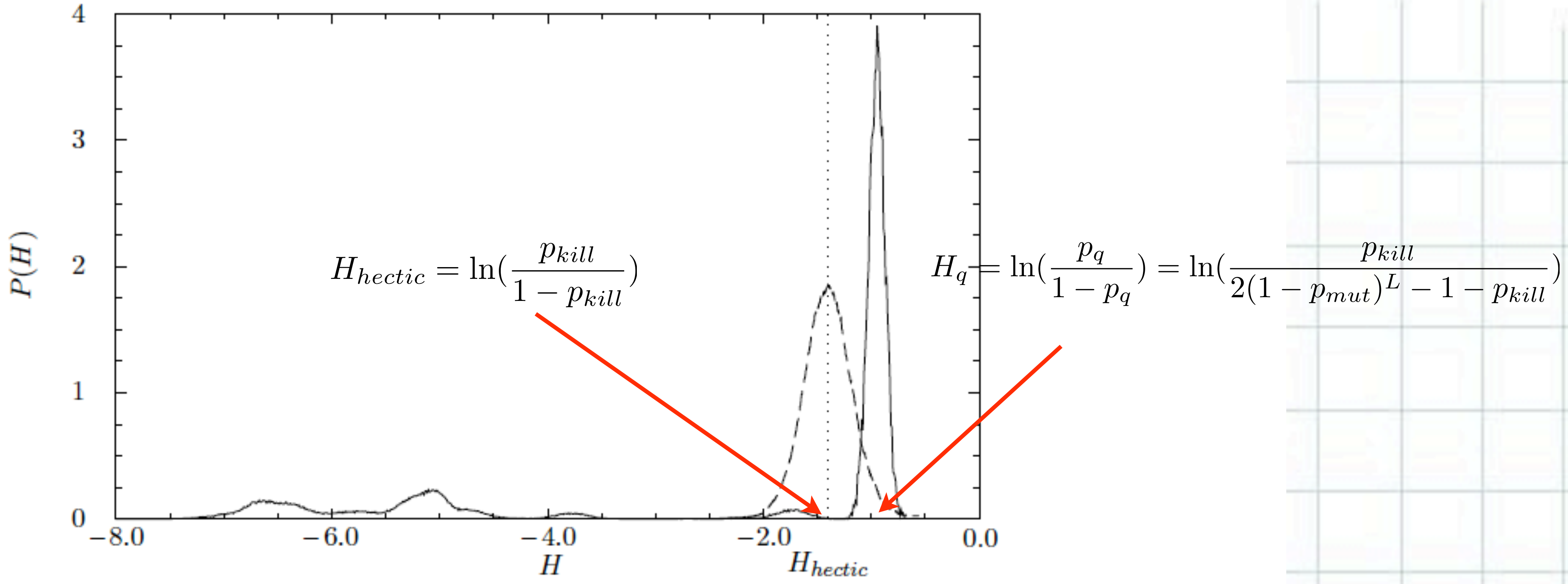

$H_{hectic} = \ln(\frac{p_{kill}}{1-p_{kill}})$

$H_q = \ln(\frac{p_q}{1-p_q}) = \ln(\frac{p_{kill}}{2(1-p_{mut})^L - 1 - p_{kill}})$

Figure 2. The probability density function of the weight function $H = \ln\left(\frac{p_{\text{off}}}{1-p_{\text{off}}}\right)$ during a q-ESS state of a simulation (solid line) and during a transition between two q-ESS states (dashed line). During a q-ESS state (solid line) positions range in two sets: unfit positions, for which the weight function is lower than −3.0 and fit positions, for which the fitness is greater then the average value $\langle H \rangle = \ln\left(\frac{1-p_{\text{kill}}}{p_{\text{kill}}}\right) \approx -1.38 = H_{\text{hectic}}$, indicated by a vertical dotted line. During a transition (dashed line) the fitness of all positions is normally distributed around H_{hectic} where all positions reproduce (on average) at the same rate, equal to the killing rate. Note the support of the weight function in the hectic phase exceeds H_q, ensuring that the positions in genotype space are able to fulfil the q-ESS balance equation (13). The parameters (for precise definitions, see [14, 15]) are $p_{\text{kill}} = 0.2$, $\mu = 1/1000 \cdot \ln\left(\frac{1-p_{\text{kill}}}{p_{\text{kill}}}\right) \approx 0.0014$, $C = 10.0$ and $p_{\text{mut}} = 0.008$.

A hectic transition can only develop into a q-ESS if hectic peak overlaps with q-EES peak

$$H_{hectic} + \alpha k \geq H_q$$

We assume width of hectic peak proportional to with of distribution of *J* given by *k*

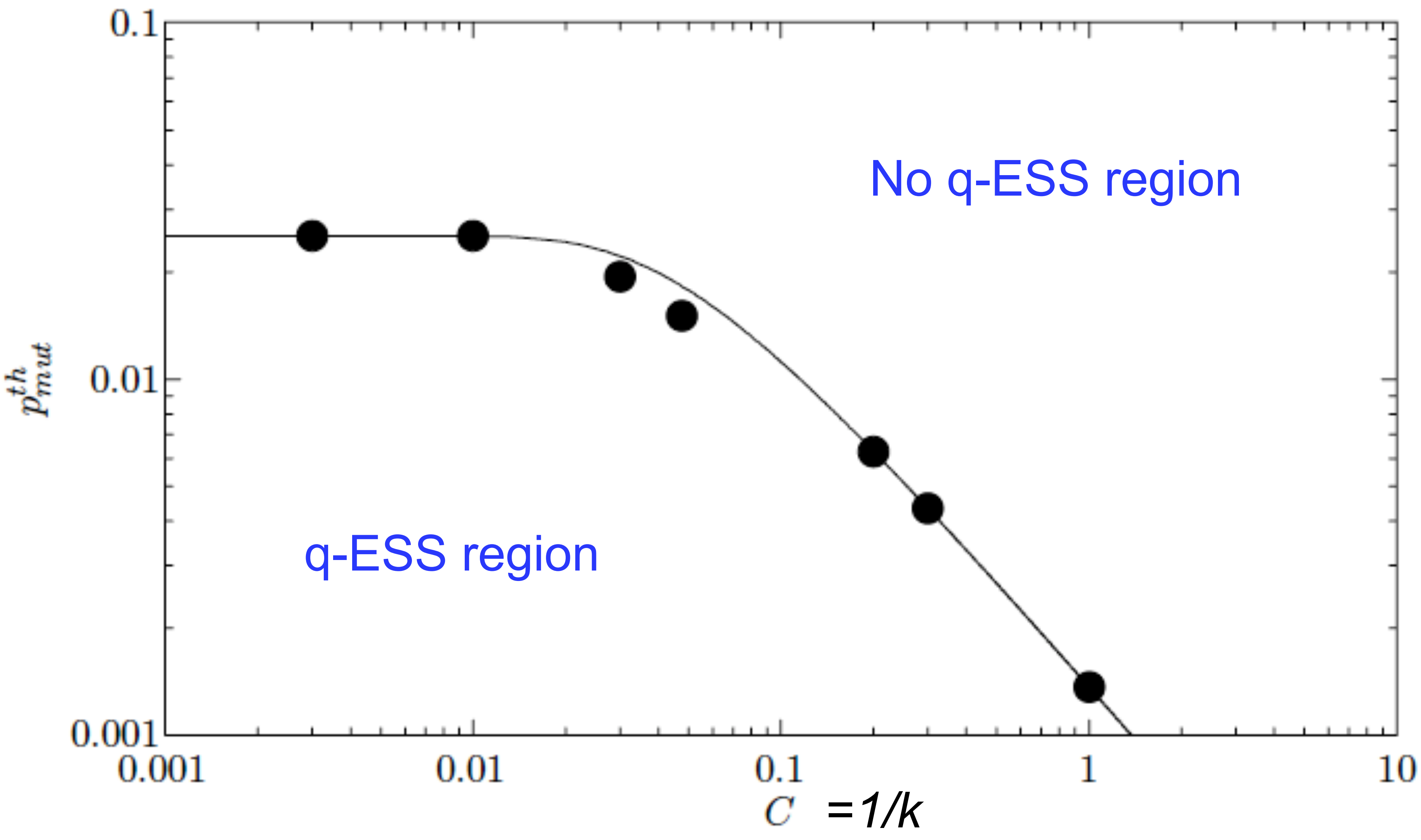

Figure 4. The computational determination of the error threshold. The loss of q-ESS states occurs for mutation rates above the solid circles. The data, compared with the theoretically predicted error threshold $p_{\mathrm{mut}}^{\mathrm{th}}$ (solid line), indicate a value of $\alpha = 0.07$, see equation (18). The parameters of the simulations are $L = 20$, $\mu = 0.005$ and $p_{\mathrm{kill}} = 0.2$.

α is used as fitting parameter

Dynamics - correlations:

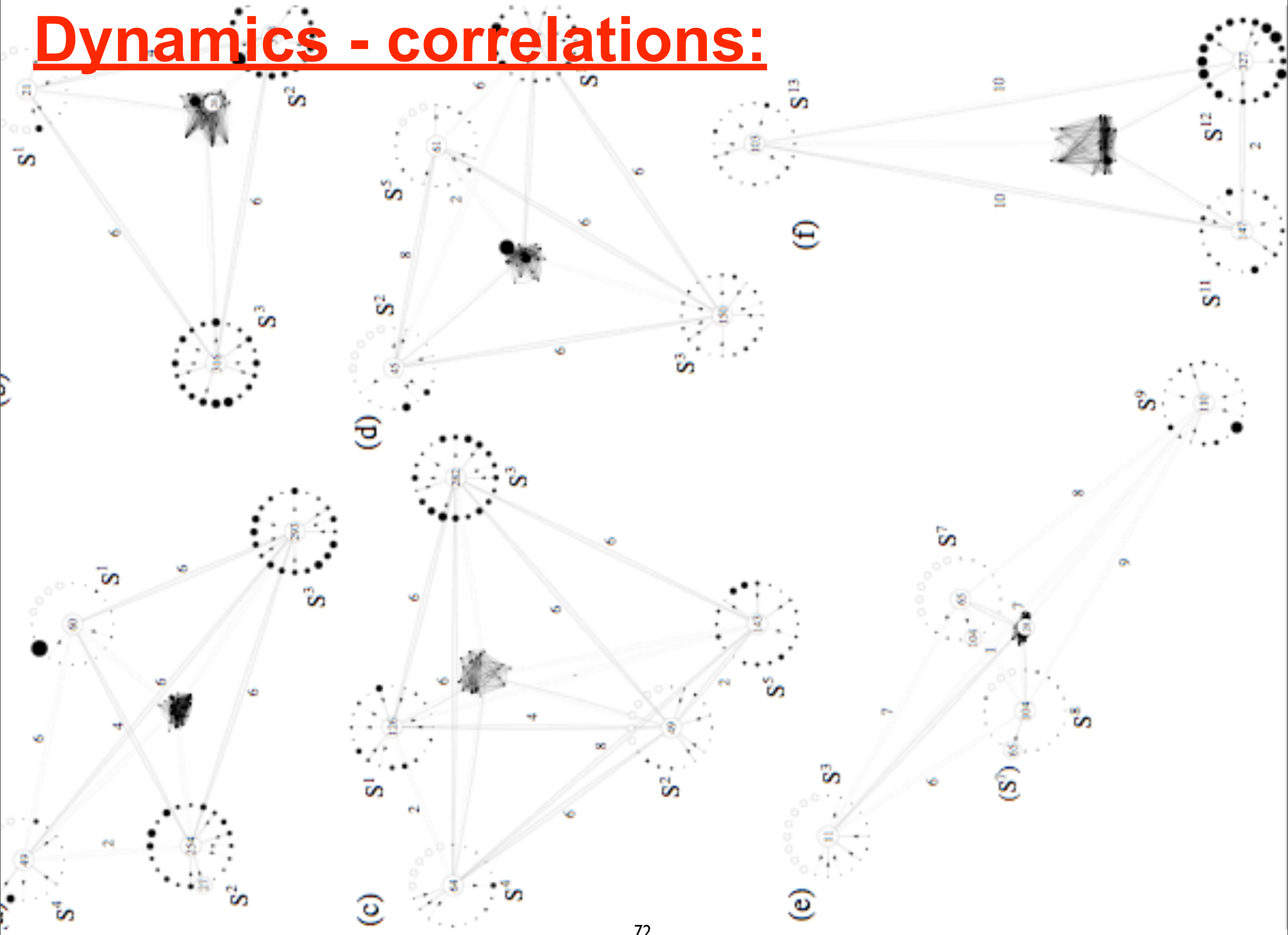

Dynamics - correlations:

The evolution of
the correlations

$$I = \sum_{J_1, J_2} P(J_1, J_2) \log\left[\frac{P(J_1, J_2)}{P(J_1)P(J_2)}\right]$$

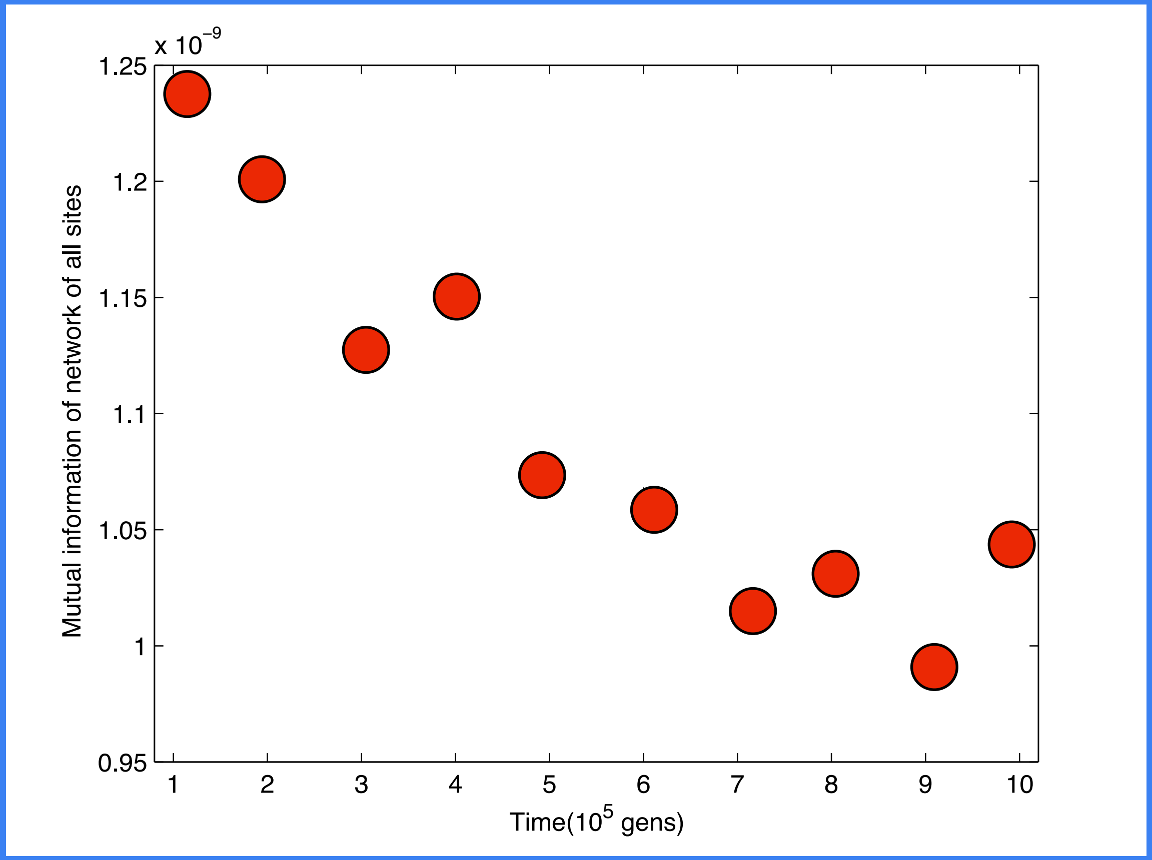

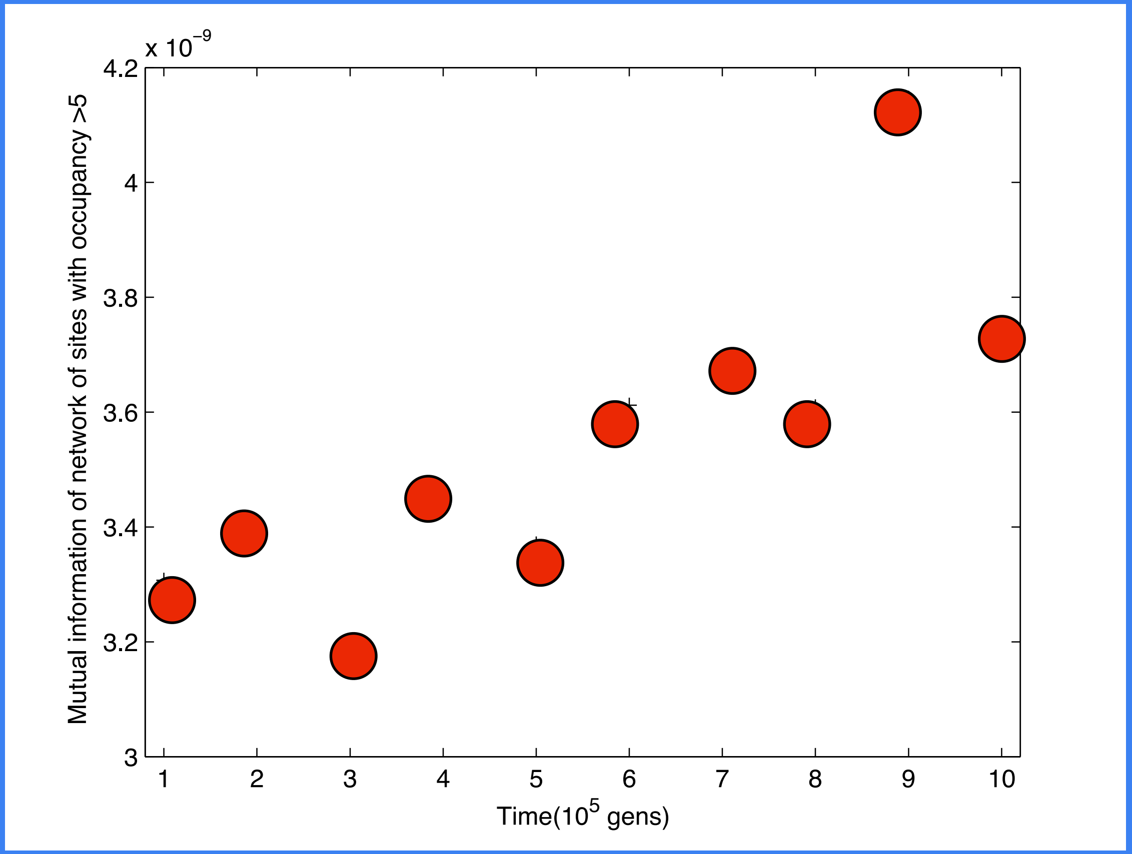

Mutual information of all

Mutual information of core

Dominic Jones

Time evolution of

Distribution of active coupling strengths

Non correlated

Low connectivity

High connectivity

From Anderson & Jensen
J Theor Biol. **232**, 551 (2005)

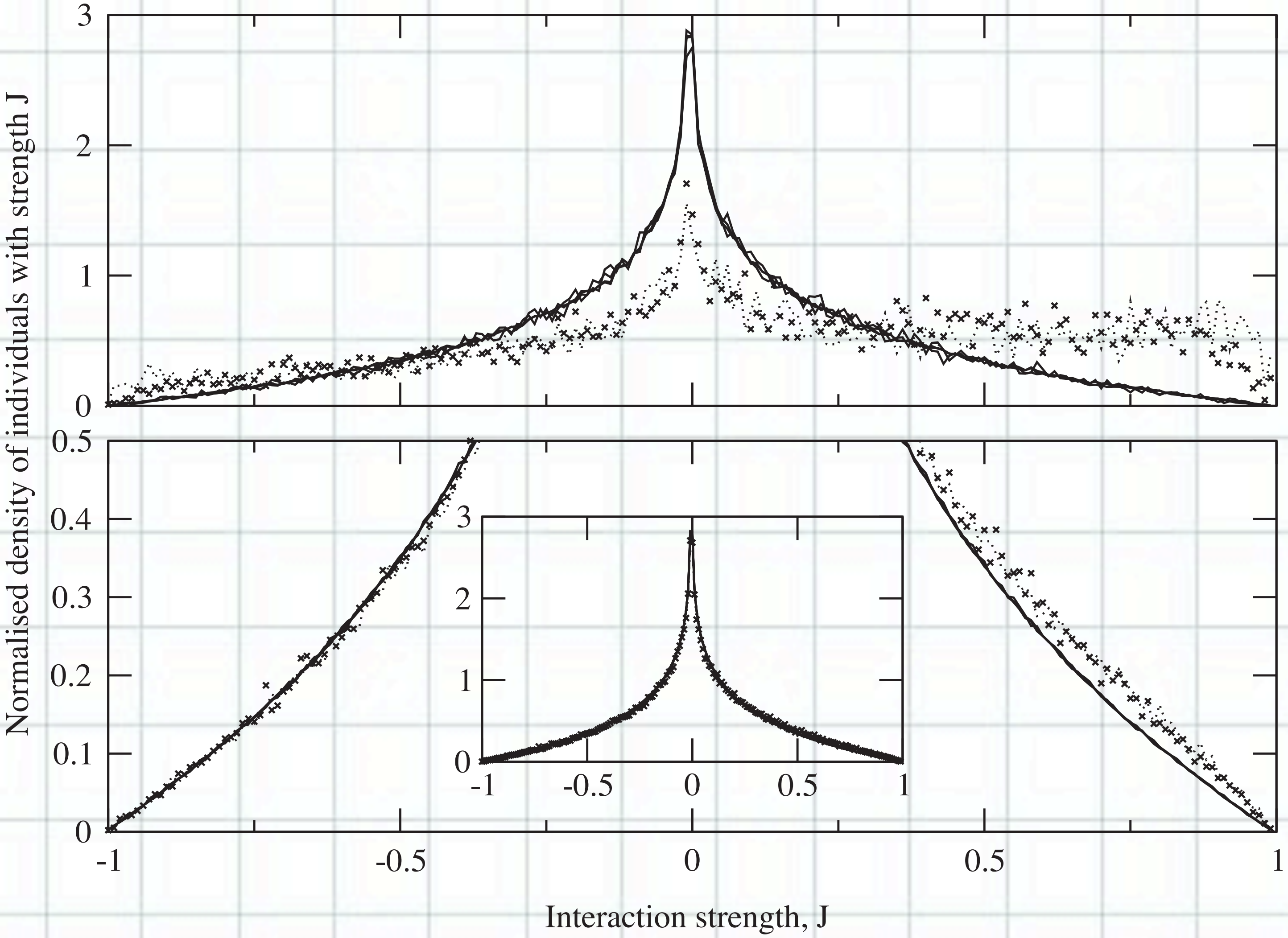

Fig. 3. Interaction distributions. Top: Distribution of interaction strengths between individuals for $\theta = 0.005$. Bottom: $\theta = 0.25$. Inset: Entire distribution. Solid lines, random; crosses, simulation at $t = 500$; dotted lines, simulation at $t = 500,000$. All plots are normalized so that their area is one. For high θ, a significant increase in positive interactions is seen. For low θ, a change is seen but for trivial reasons.

Time evolution of

Distribution of active coupling strengths

Correlated

High connectivity

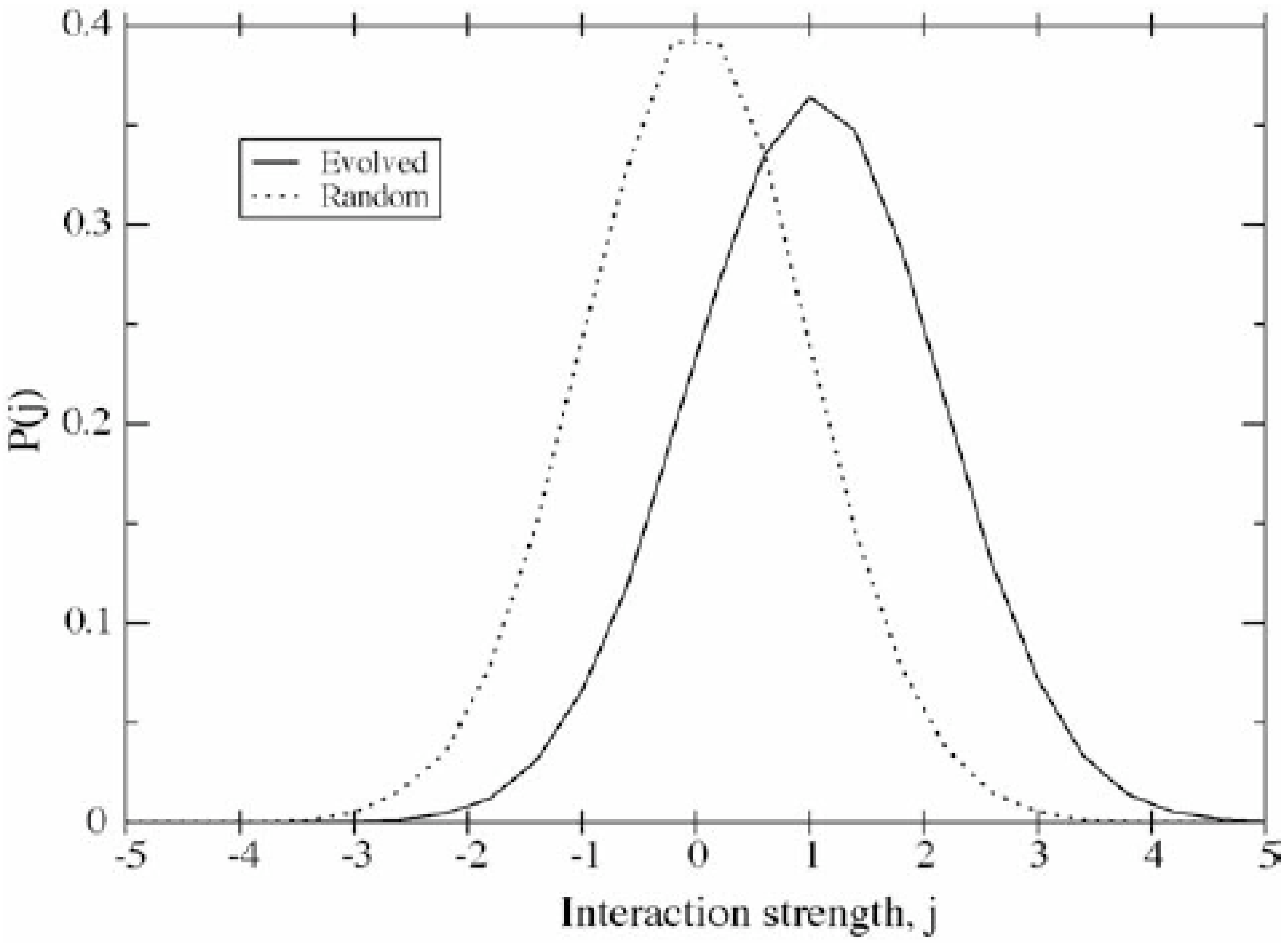

From Laird & Jensen, Ecol Compl. **3**, 253 (2006)

Time evolution of

Species abundance distribution

Non Correlated

From Anderson & Jensen
J Theor Biol. **232**, 551 (2005)

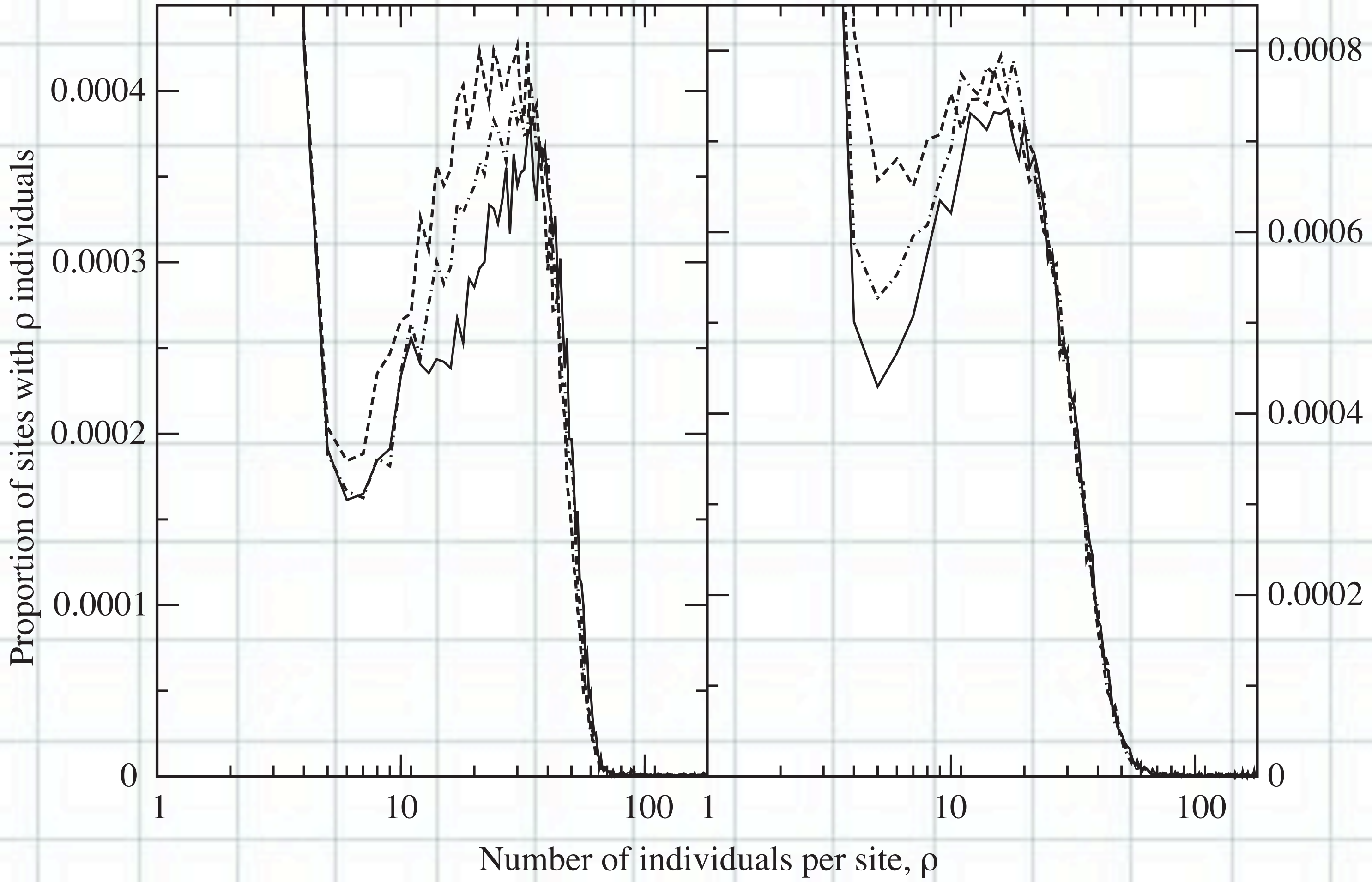

Fig. 5. Species abundance distributions. Species abundance distributions for the simulations only. Dashed line, $t = 500$; dashed–dotted line, $t = 5000$; solid line, $t = 500,000$. Low θ on the left, high θ on the right. The ecologically realistic log-normal form is only seen for high θ.

Low connectivity High connectivity

The evolved degree distribution

Correlated

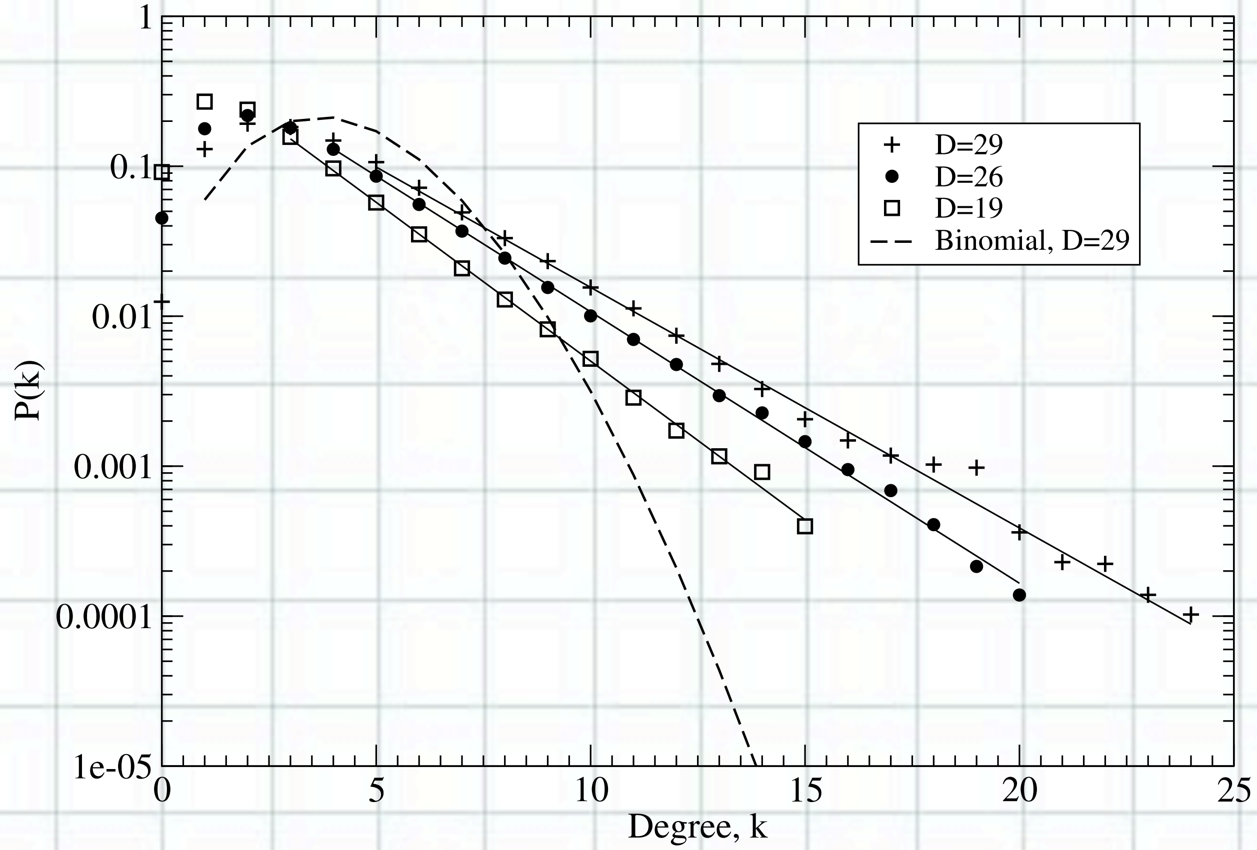

Figure 1: Degree distributions for the Tangled Nature model simulations. Shown are ensemble averaged data taken from all networks with diversity, $D = \{19, 26, 29\}$ over 50 simulation runs of 10^6 generations each. The exponential forms are highlighted by comparison with a binomial distribution of $D = 29$ and equivalent connectance, $C \simeq 0.145$ to the simulation data of the same diversity.

Exponential becomes 1/k in limit of vanishing mutation rate

From Laird & Jensen, Ecol. Model. In Press
See also Laird & Jensen, EPL, **76**, 710 (2006)

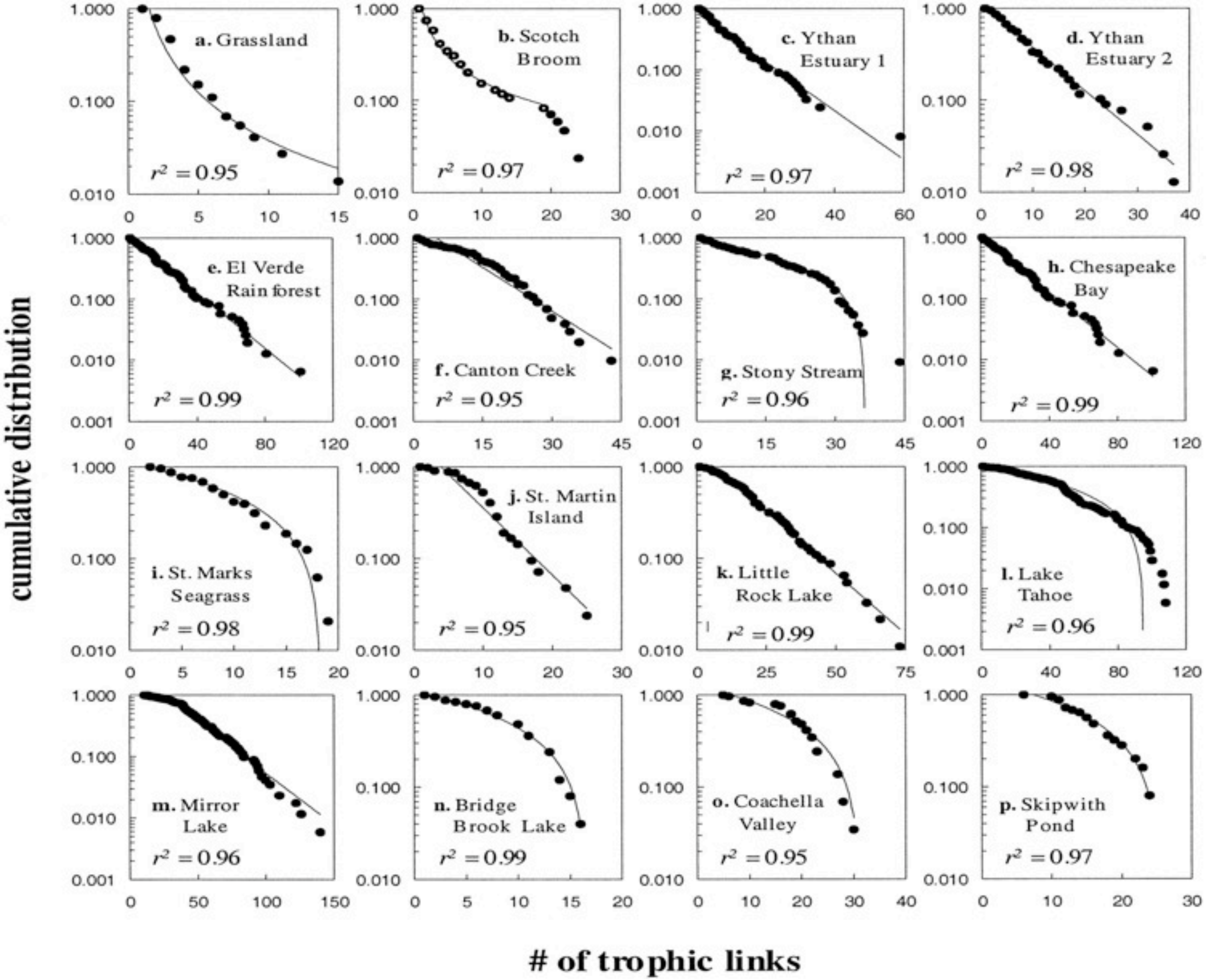

Dunne, Jennifer A. et al. (2002) Proc. Natl. Acad. Sci. USA 99, 12917-12922

The evolved connectance

Correlated

$$\langle C \rangle = \frac{\#\ \text{Edges}}{\#\ \text{Possible Edges}}$$

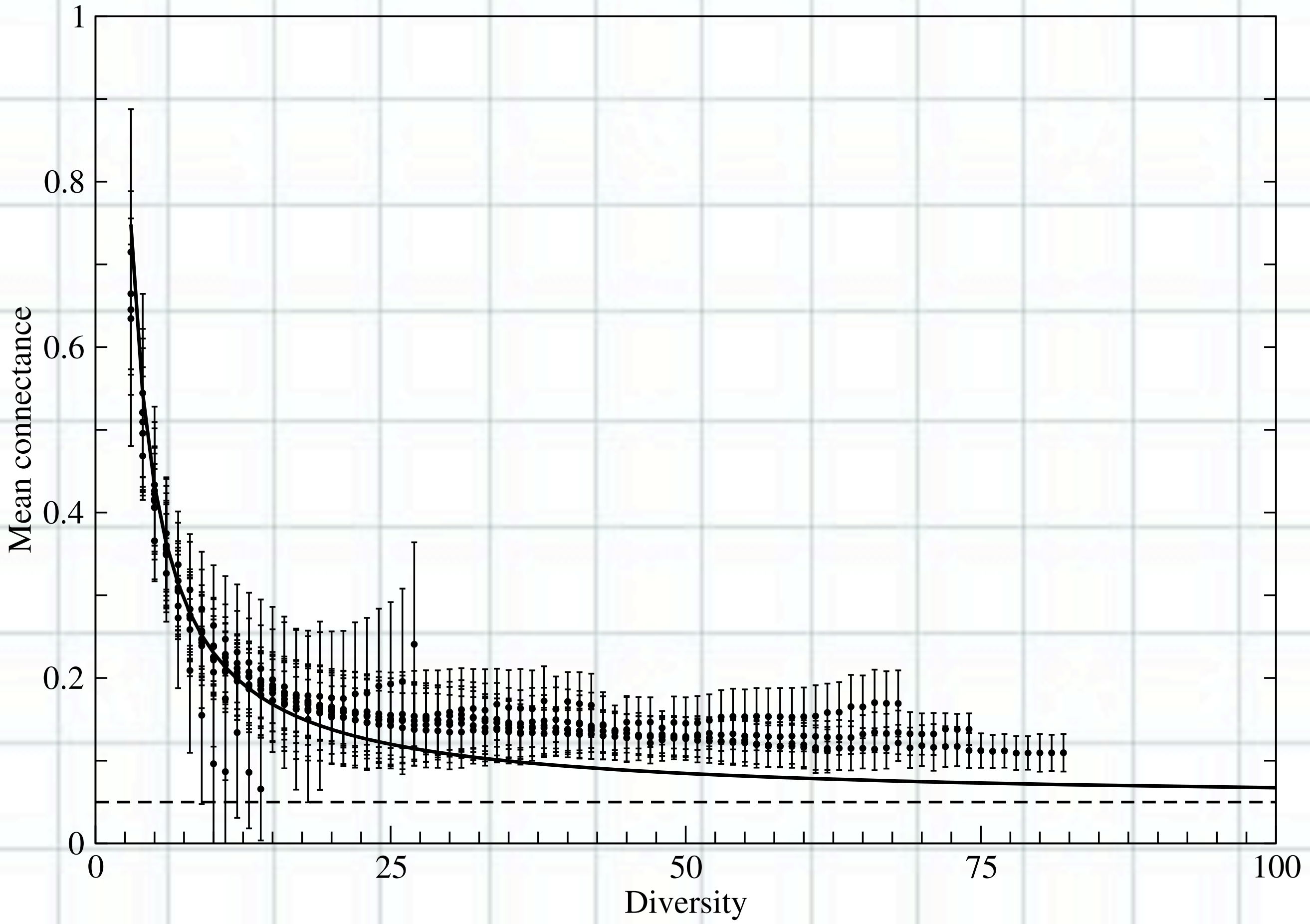

Figure 4: Plot of ensemble-averaged mean connectances, $< C >$ against species diversity. Error bars represent the standard error. The lower dotted line marks the null system connectance, $C_J = 0.05$, which the evolved systems clearly surpass. The overlaid functional form is that given by Eq.(8) using the correct background connectance, $C_J = 0.05$ and with a value of, $s = 5.5$ for the selection parameter.

From Laird & Jensen, Ecol Compl. **3**, 253 (2006)

Connectance

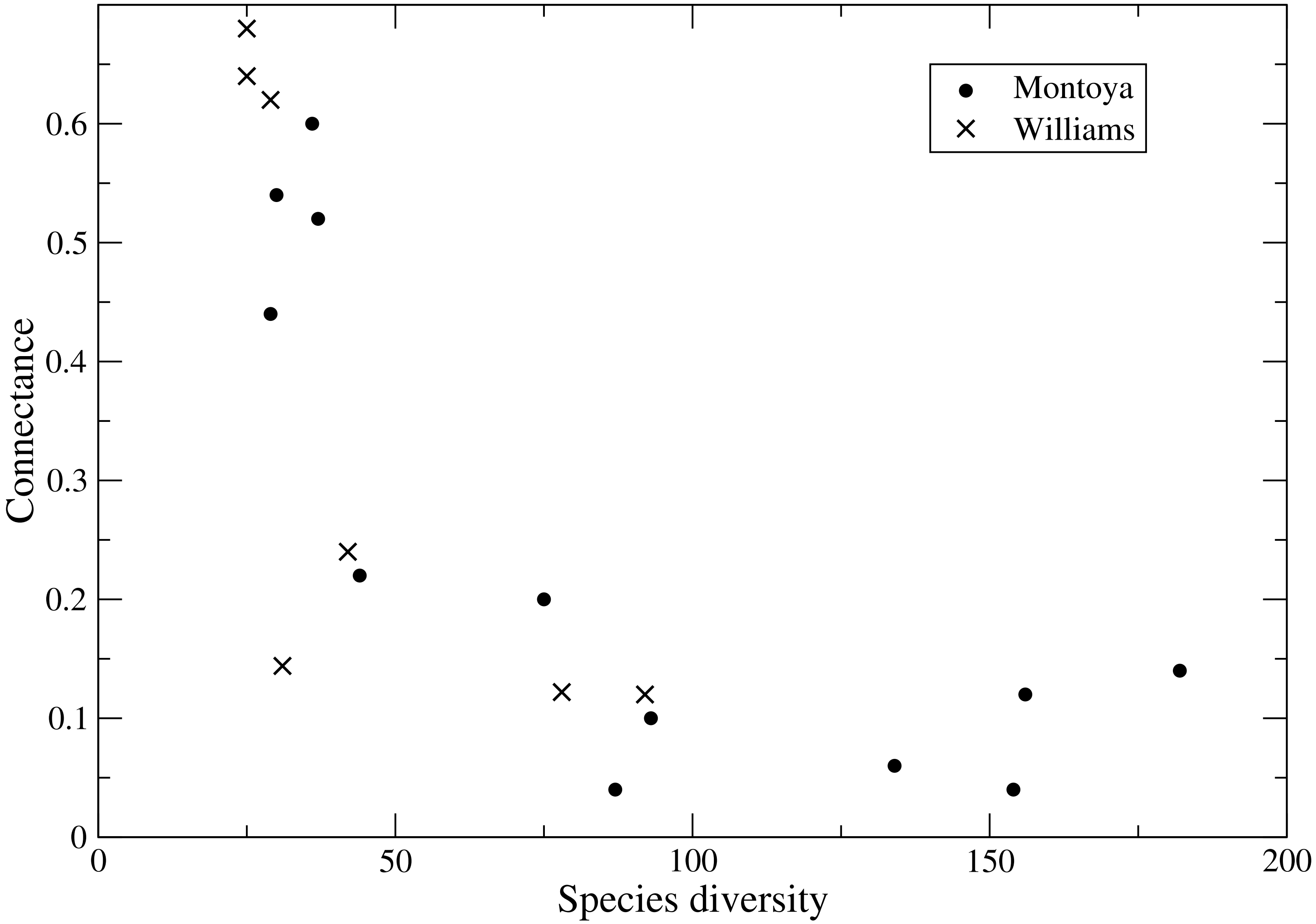

Montoya JM, Sole RV *Topological properties of food webs: from real data to community assembly models*, OIKOS **102**, 614-622 (2003)

Williams RJ, Berlow EL, Dunne JA, Barabasi AL, Martinez ND *Two degrees of separation in complex food webs*, PNAS **99**, 12913-12916 (2002)

Break ?

Degree Distribution

Tangled Nature IBM

- Reproducing individuals forming species in type space

Node model
Species level

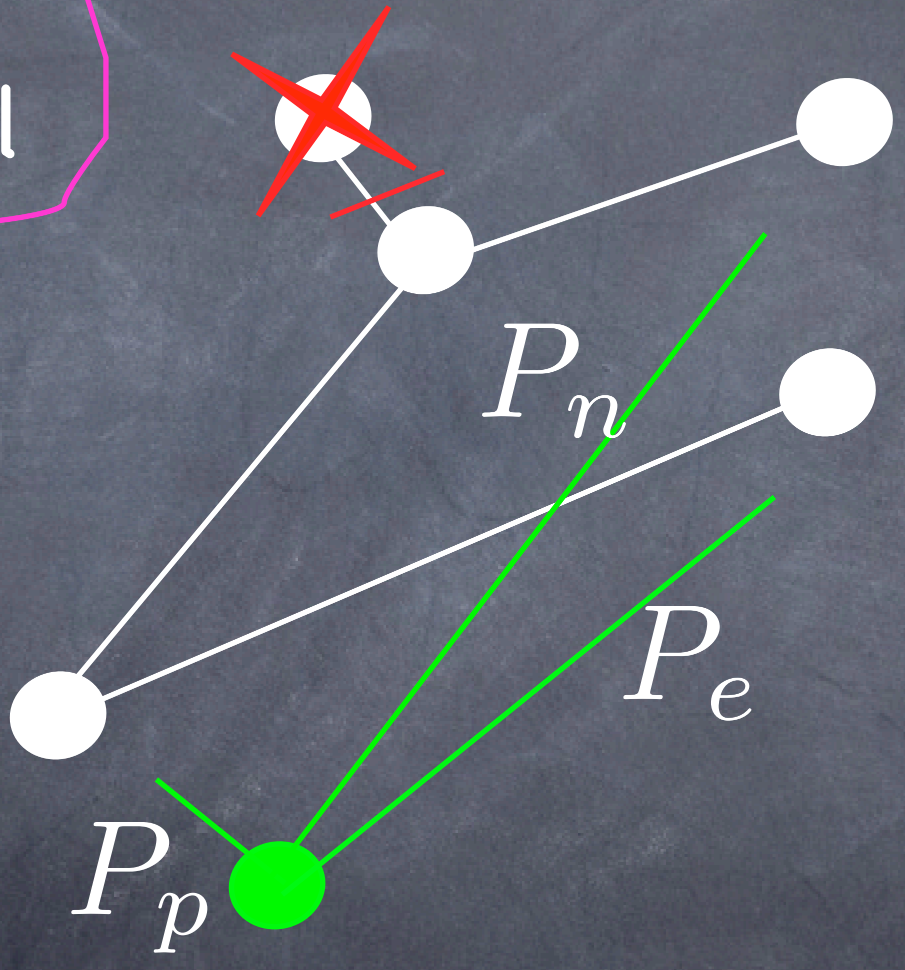

Remove node with all its edges

Copy with probabilities

Degree distribution: Exponential, except in limit where 1/k.

Self-consistent Mean Field Degree Dynamics

Resulting evolution equation for degree distribution

Removed node

$$\begin{aligned} n_k(t+1) &= n_k(t) - \frac{n_k(t)}{D} \\ &+ \langle k \rangle \frac{n_{k+1} - n_k}{D} \\ &+ [P_e \langle k \rangle + P_n(D - 1 - \langle k \rangle)] \frac{n_{k-1} - n_k}{D} \\ &+ P_p \frac{n_{k-1}}{D} + (1 - P_p) \frac{n_k}{D} \end{aligned}$$

Adjacent node looses an edge

Adjacent gains an edge

Daughter node

$$\begin{aligned} n_k(t+1) &= n_k(t) - \frac{n_k(t)}{D} \\ &+ \frac{P_p + (P_e - P_n)\langle k\rangle + p_n\langle n\rangle}{D}[n_{k-1}(t) - n_k(t)]. \end{aligned}$$

$$n(k) = n(0)\exp[-k/k_0]$$

$$k_0 \to \infty \text{ as } P_n \to 0$$

We can do better - full Fokker-Planck - see

H..J. Jensen, *Emergence of Network Structure in Models of Collective Evolution and Evolutionary Dynamics.* Royal Soc. Proc. A **464,** 2207-2217 (2008).

Connectance

Effect of adaptation on connectance

Underlying type space is a binomial net - place a sub-net of size D

Some regions of this space will, due to fluctuations, locally have an above average conenctance. It is beneficial for the evolved configurations to enter into these regions

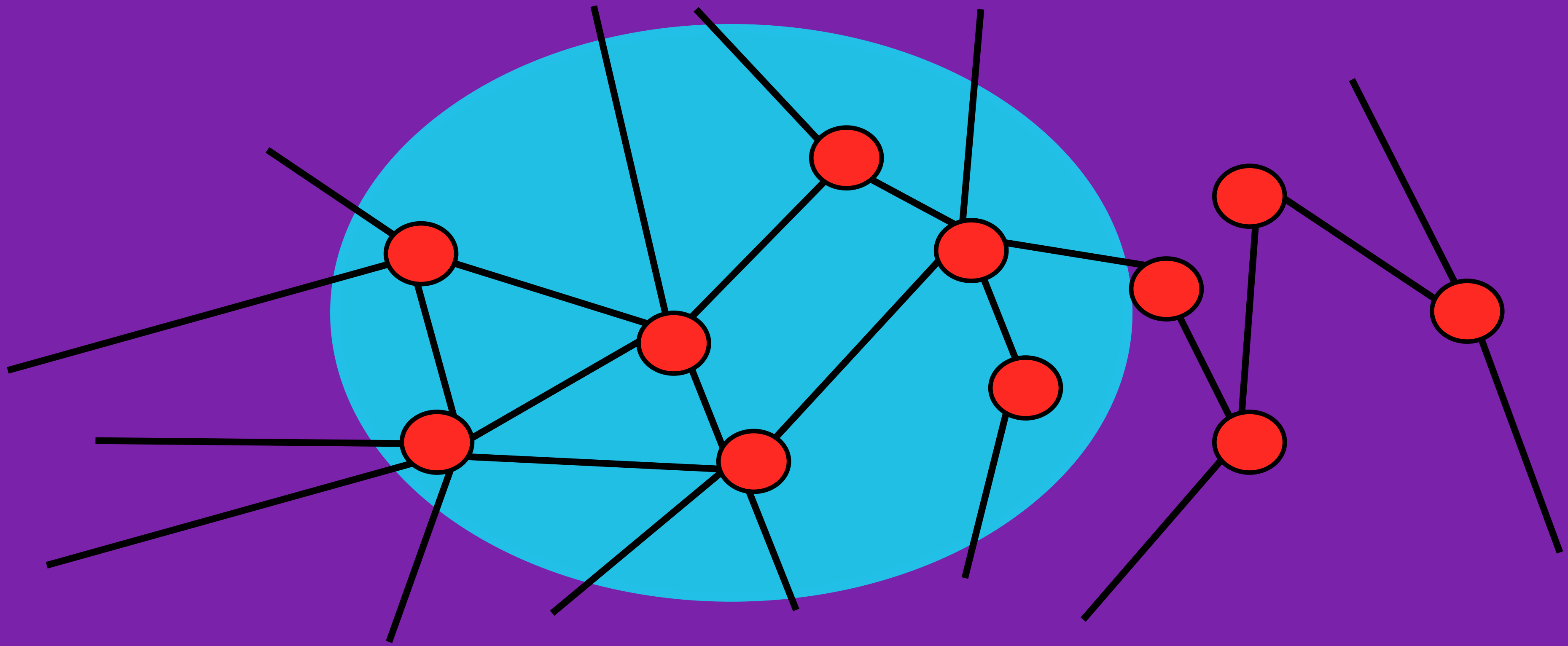

With increasing size, D, of the adapted sub-net; it becomes increasingly difficult to confine the sub-net to within the above average regions

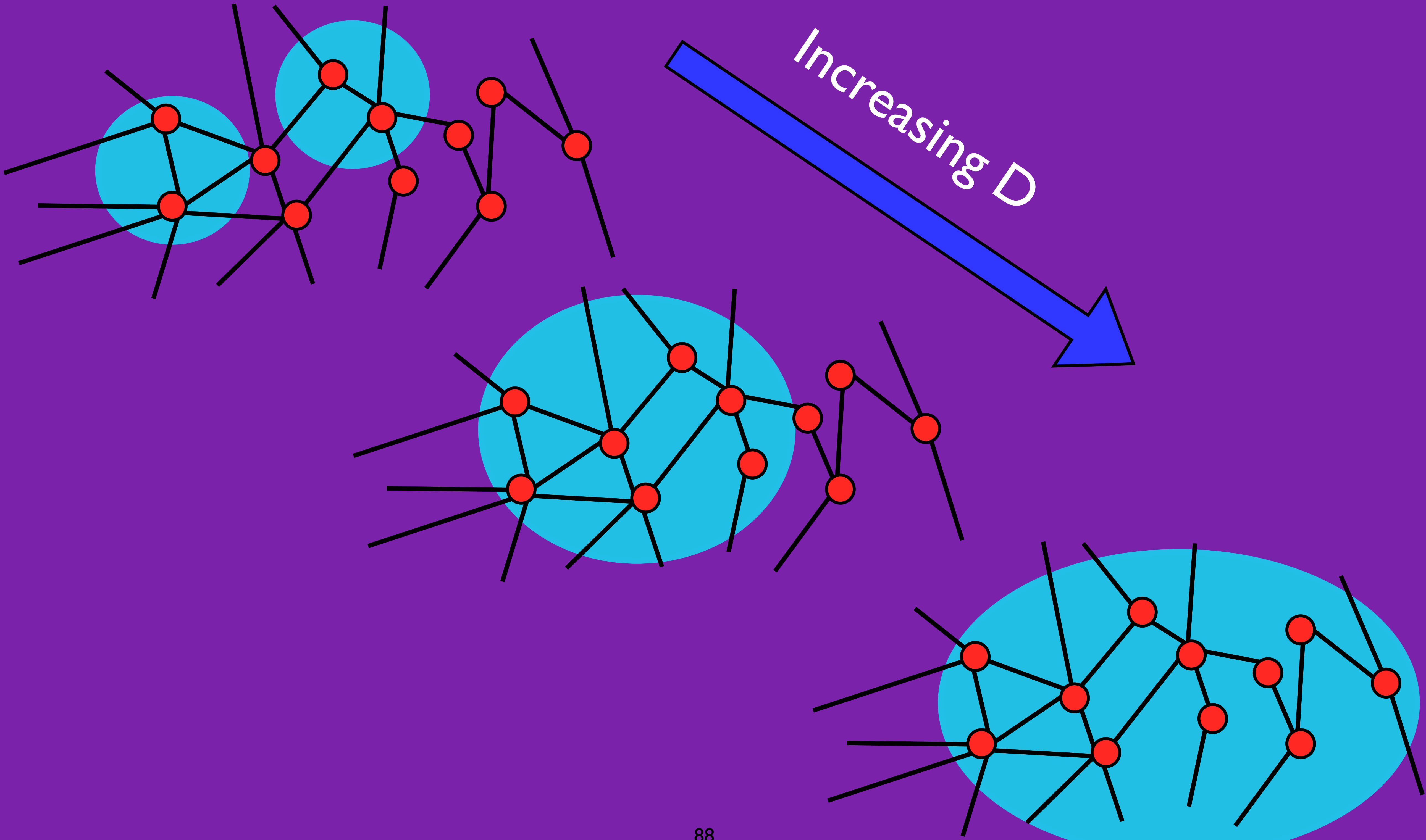

Effect of selection on connectance

Consider a binomial net of size D and connectance C (= edge probability).

Assume that adapted sub-net is located in a region of the master-network in which the total number of edges E is larger than the global average.

Estimate this increase as

Fraction

Fluctuations in E

$$\begin{aligned} E &= \langle E(D,C)\rangle + s\sigma(D,C) \\ &= E_m C + s[E_m C(1-C)]^{\frac{1}{2}} \end{aligned}$$

Max,i.e., Em=D(D-1)

Effect of selection on connectance

The resulting estimate for the connectance, E/Em, of the adapted sub-net

$$\begin{aligned} C_{Adap} &= C + s\left[\frac{C(1-C)}{E_m}\right]^{\frac{1}{2}} \\ &= C + s\left[\frac{2C(1-C)}{D(D-1)}\right]^{\frac{1}{2}}. \end{aligned}$$

Qualitative agreement with simulations of Tangled Nature model

The evolved connectance

Correlated Tangled Nature Simulations

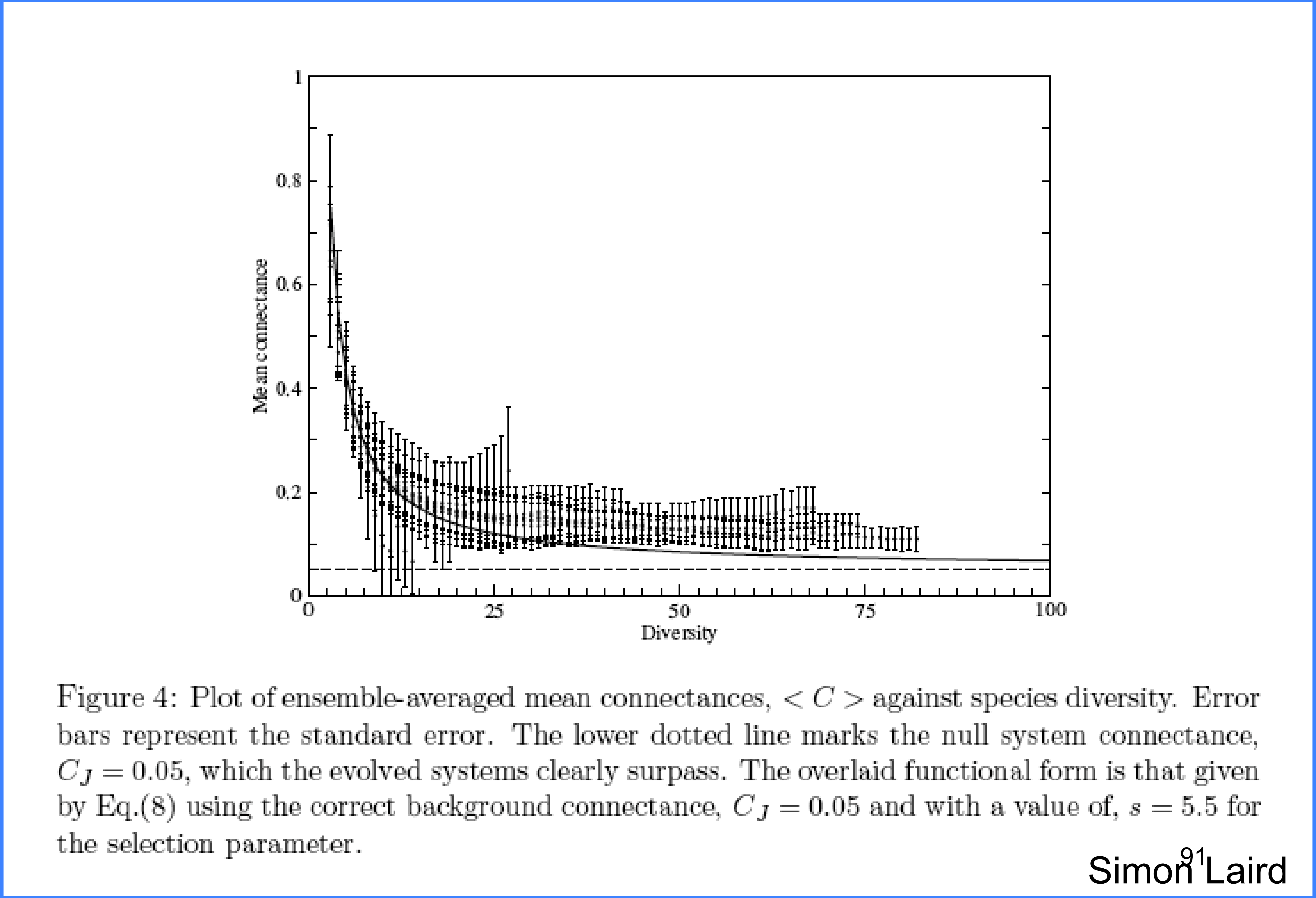

Figure 4: Plot of ensemble-averaged mean connectances, $< C >$ against species diversity. Error bars represent the standard error. The lower dotted line marks the null system connectance, $C_J = 0.05$, which the evolved systems clearly surpass. The overlaid functional form is that given by Eq.(8) using the correct background connectance, $C_J = 0.05$ and with a value of, $s = 5.5$ for the selection parameter.

Simon Laird

Species Area Relation

Species area relation: $\#S \propto A^z$

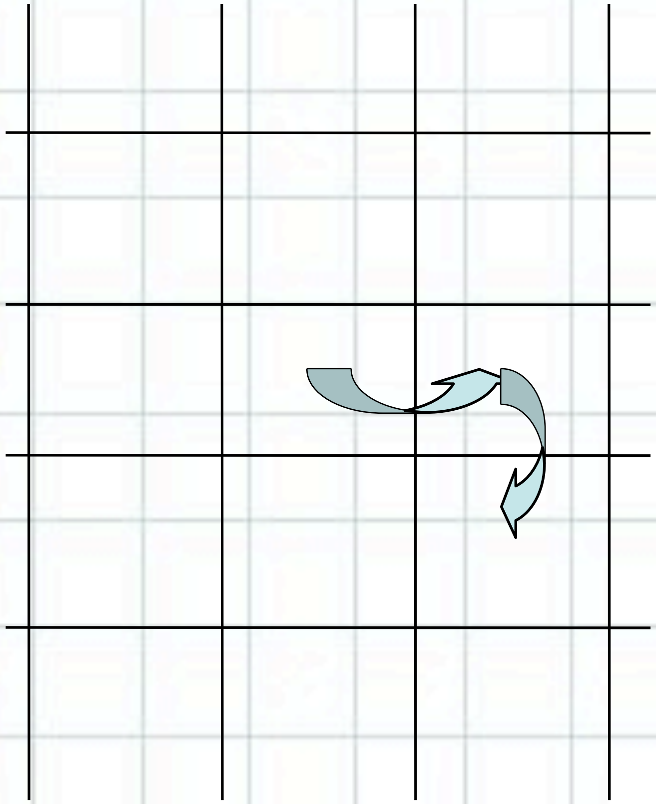

Dispersion by random walk

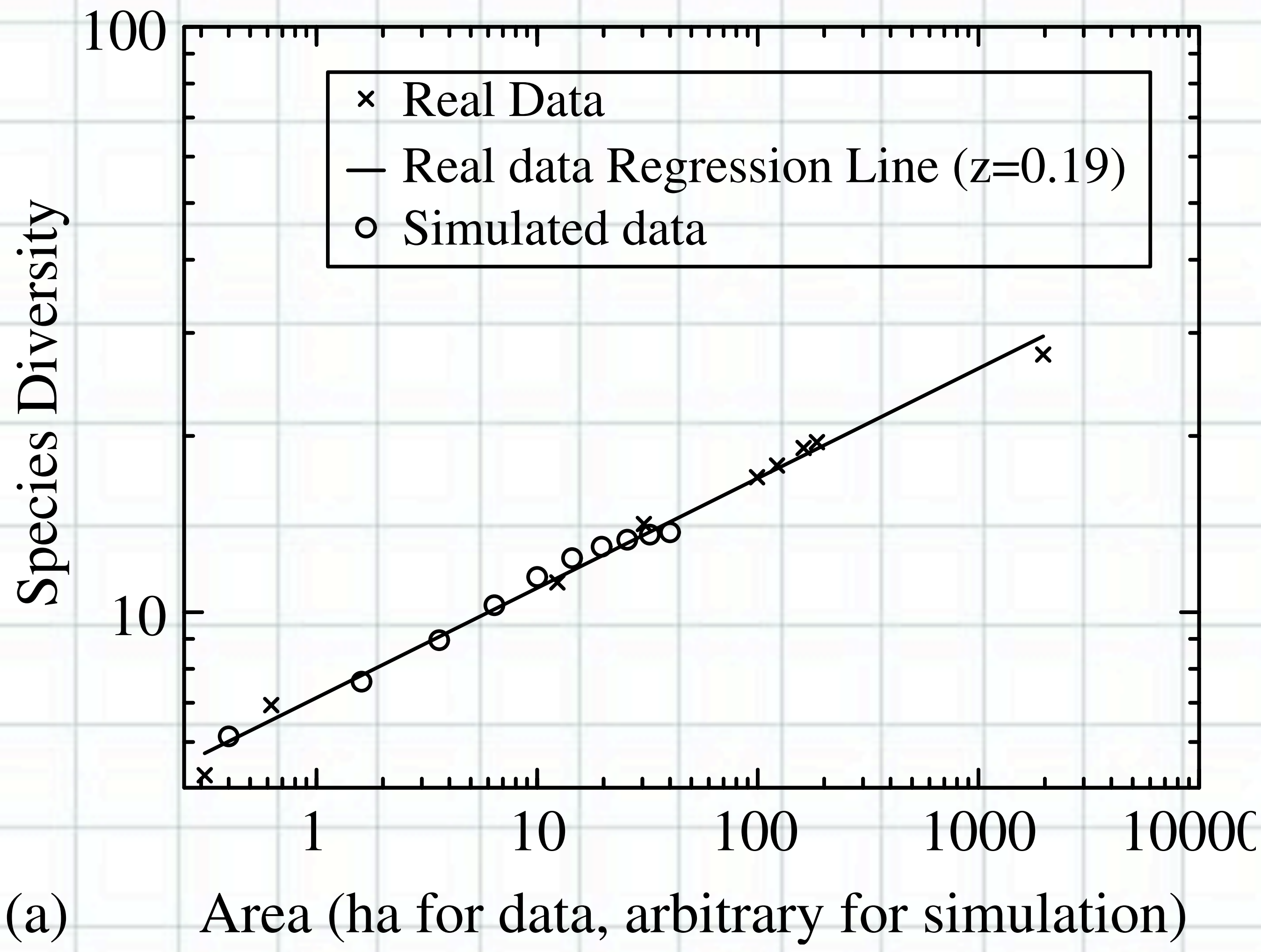

X plant data from Hertfordshire, see
ML Rosenzweig, Species Diversity in Space and Time,
Cambridge University Press, 1995

From Lawson & Jensen, J Theo. Biol. **241**, 590 (2006)

Diversity and Interaction

Diversity and interaction

Weight function $$H_0(\mathbf{S}^\alpha,t) = \frac{k}{N(t)}\sum_{\mathbf{S}} J(\mathbf{S}^\alpha,\mathbf{S})n(\mathbf{S},t) - \mu N(t)$$

$$H(S^\alpha) = H_0 + \begin{cases} \varepsilon\, E(S^\alpha)\dfrac{n(S^\alpha,t)}{N(t)} \\ \varepsilon\, E(S^\alpha) \end{cases}$$

Density dependent

Density independent
Fujiyama lanscape

with $E \in [0,1]$ and ε a scale parameter

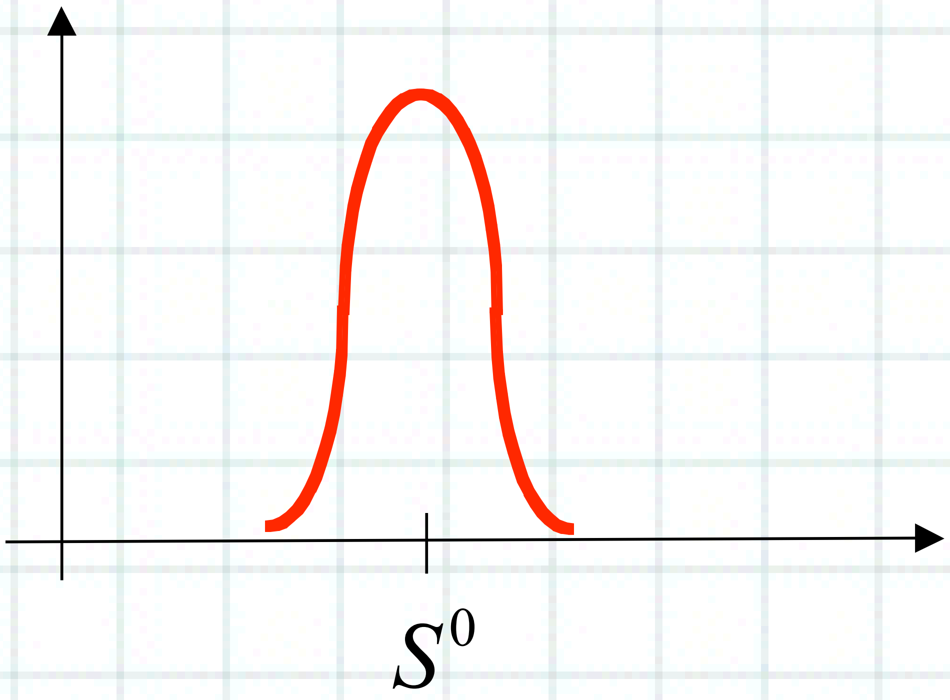

Diversity and interaction

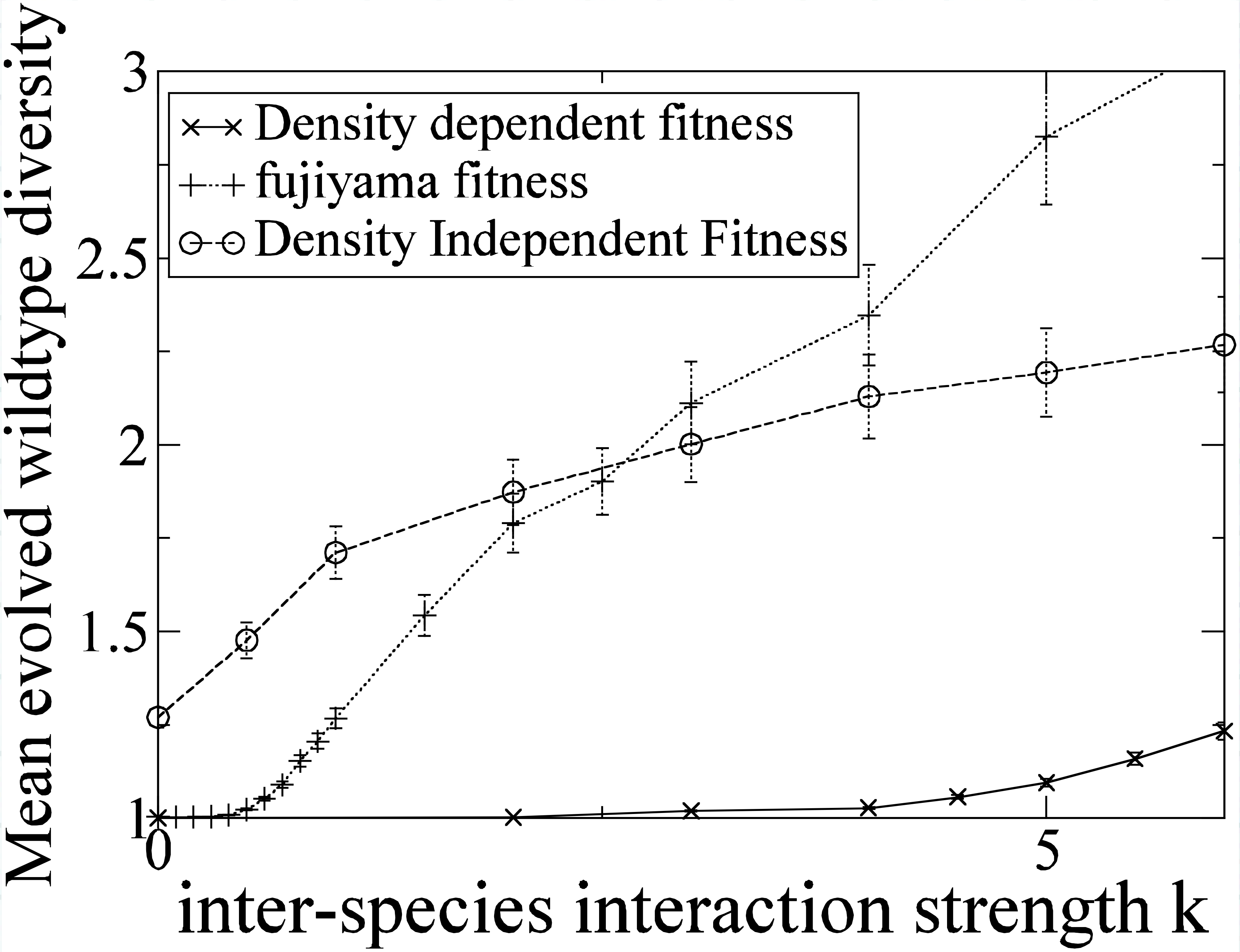

From Lawson, Jensen & Kaneko, J Theo. Biol. **243**, 299 (2006)

Origin of threshold in k:

A balance between inter-species and intra-species Interaction.

$$H = H_0 + \varepsilon\, E(S^\alpha,t)\frac{n(S^\alpha,t)}{N(t)},$$

where $E \in [0,1]$ and

$$\overline{H}(\mathbf{S}^\alpha,t) = \frac{k}{N(t)}\sum_{\mathbf{S}} J(\mathbf{S}^\alpha,\mathbf{S})n(\mathbf{S},t) - \mu\, N(t)$$

Mean field sketch

Weight function for $D = 1: \mathrm{H}_1 = \varepsilon E - \mu N_1$

Weight function for $D = 2: H_2 = \frac{k}{N_2}Jn_2 + \varepsilon E - \mu N_2$

Assume $n_2 = \frac{1}{2}N_2$ and $N_1 \approx N_2$ then

$$H_1 > H_2 \Rightarrow k > \frac{\varepsilon\, E}{J}$$

Variation in the environment

Variation in the external conditions

$$H(\mathbf{S}^{\alpha},t)=\frac{k}{N(t)}\sum_{\mathbf{S}}J(\mathbf{S}^{\alpha},\mathbf{S})n(\mathbf{S},t)-\mu N(t)$$

Manipulate μ

Variation in the external conditions

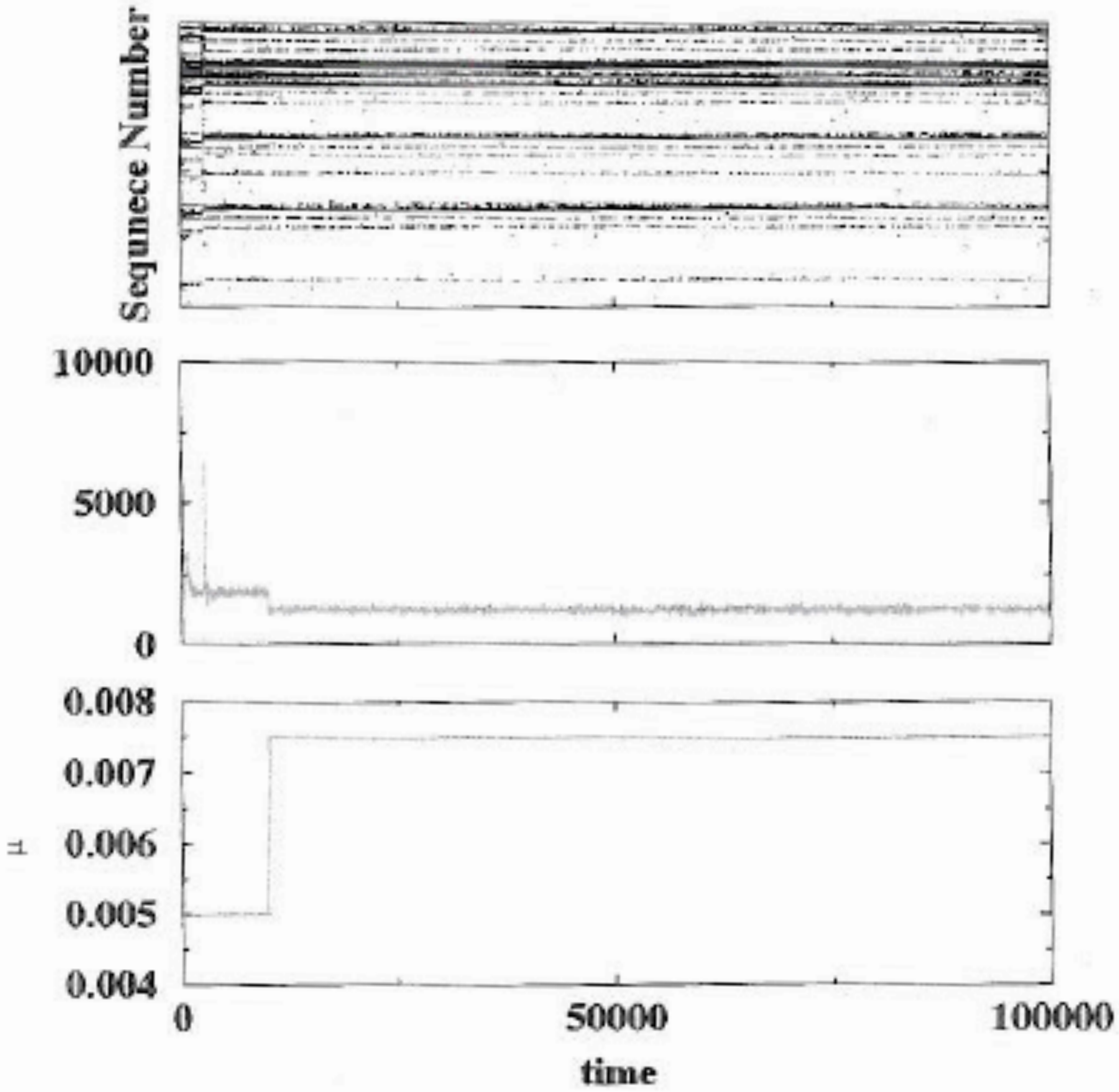

Figure 4.13: Step-like perturbation in the value of μ. Once again the q-ESS configuration is robust (*upper*), but here we observe a step-like change in population (*middle* coincident with the paramneter change (*lower*).

Graph courtesy to Matt Hall

Variation in mutation rate

Variation in the external conditions

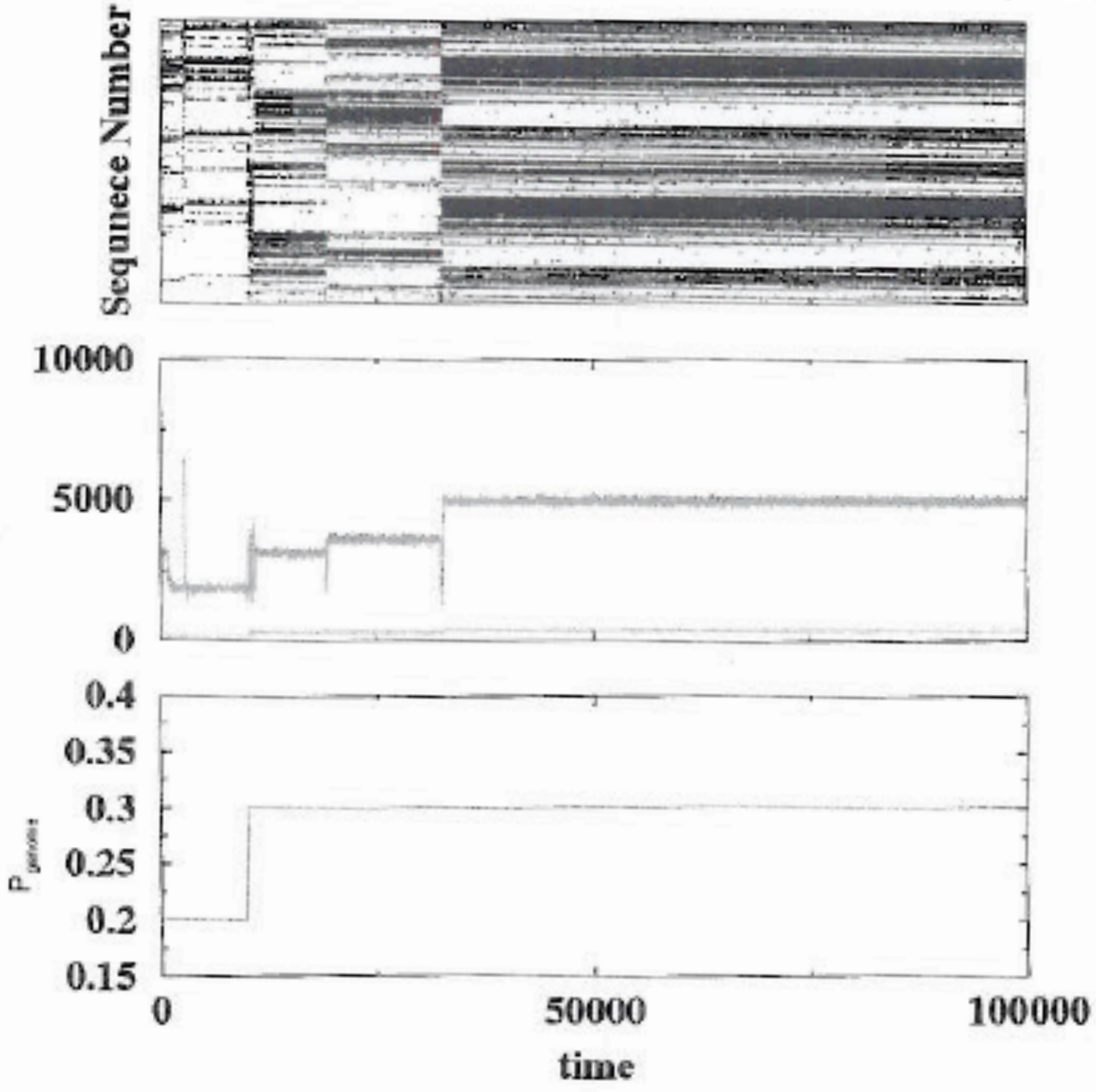

Graph
courtesy
to
Matt Hall

Figure 4.15: In constrast to previous pertubations, a step-like increase in *pgenome* has a considerable effect on the system. The occupation plot (*upper*) shows that the q-ESS state is interrupted by the perturbation, and the system evolves through a sequence of new configurations, each with different mean populations (*middle*). Transitions between these new q-ESS configurations are due only indirectly to the pertubation applied to the system, which is applied only once (*lower*).

Extinction of single types

Variation in the external conditions

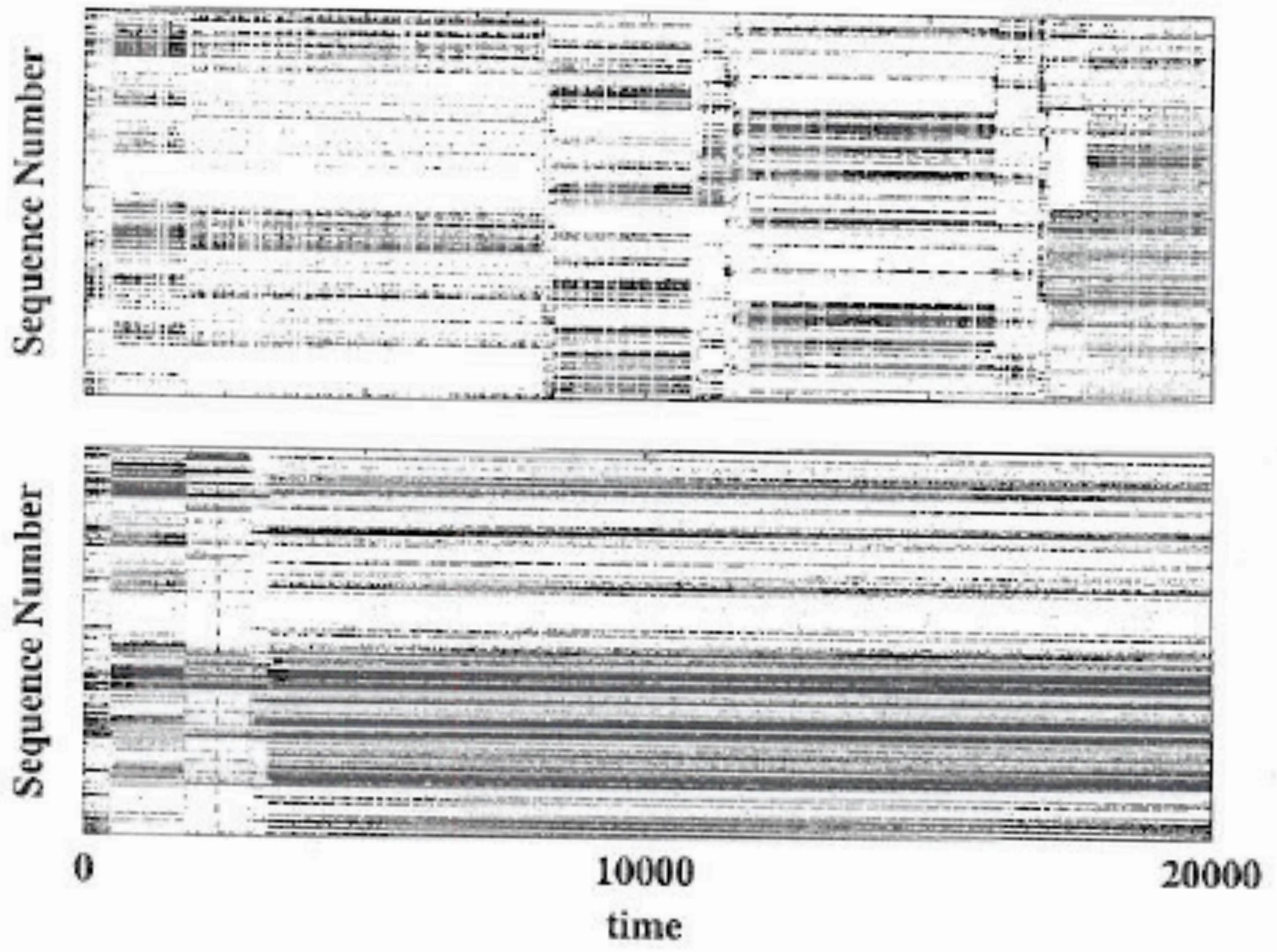

Graph
courtesy
to
Matt Hall

Figure 4.16: Comparison of occupation plots in a control simulation (*upper*) and one in which a randomly chosen sequence is removed from the system the point indicated by the dashed line (*lower*). See main text for discussion

Variation in the external conditions

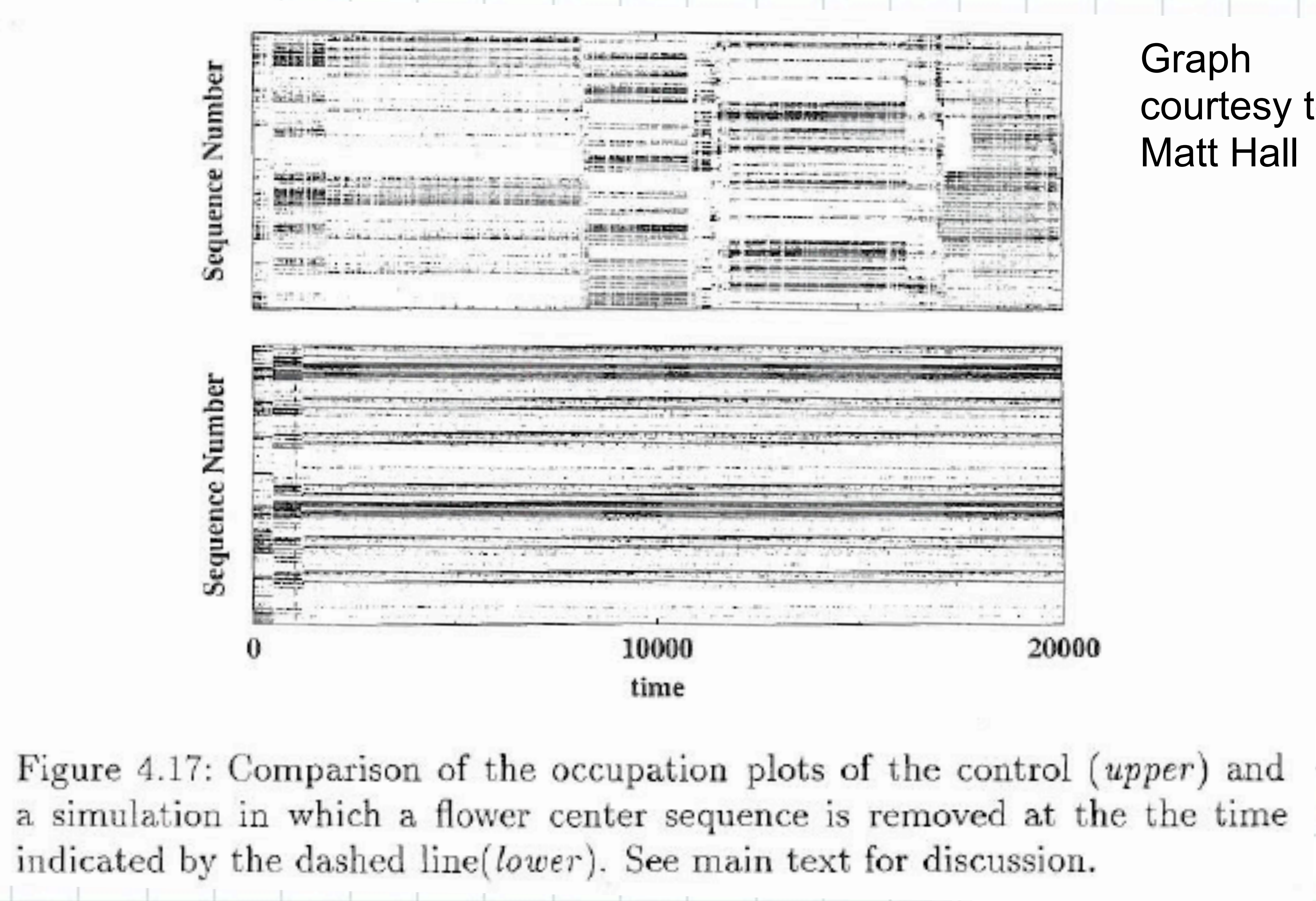

Figure 4.17: Comparison of the occupation plots of the control (*upper*) and a simulation in which a flower center sequence is removed at the the time indicated by the dashed line(*lower*). See main text for discussion.

Graph courtesy to Matt Hall

The individual in ever evolving surroundings:

- Collective system level adaptation towards mutualistic biased webs of interactions
- Macro-Evolution through intermittent transitions
- Type space properties -> network charateristics

Tangled Economy

Use correlated J(S₁,S₂)

Consider S to label economical entities, say companies of capital C(S,t)

Dynamics:

Define $$P_{gain}(S,t) = \frac{\exp[H(S,t)]}{1+\exp[H(S,t)]}$$

let

$$\mathrm{J}^{+}(\mathbf{S}) = \sum_{\mathbf{S}'} J(\mathbf{S},\mathbf{S}')\theta[\mathbf{J}(\mathbf{S},\mathbf{S}')]$$

$$\mathrm{J}^{-}(\mathbf{S}) = \sum_{\mathbf{S}'} J(\mathbf{S},\mathbf{S}')\theta[-\mathbf{J}(\mathbf{S},\mathbf{S}')]$$

With probability $P_{gain}(\mathbf{S},t)$: $$C(\mathbf{S},t+1) = C(\mathbf{S},t)(1+c_g\frac{J^{+}(\mathbf{S})}{J^{Tot}(\mathbf{S})})$$

With probability $1-P_{gain}(\mathbf{S},t)$: $$C(\mathbf{S},t+1) = C(\mathbf{S},t)(1+c_l\frac{J^{-}(\mathbf{S})}{J^{Tot}(\mathbf{S})})$$

Comparison between data and model:
Volume as GDP

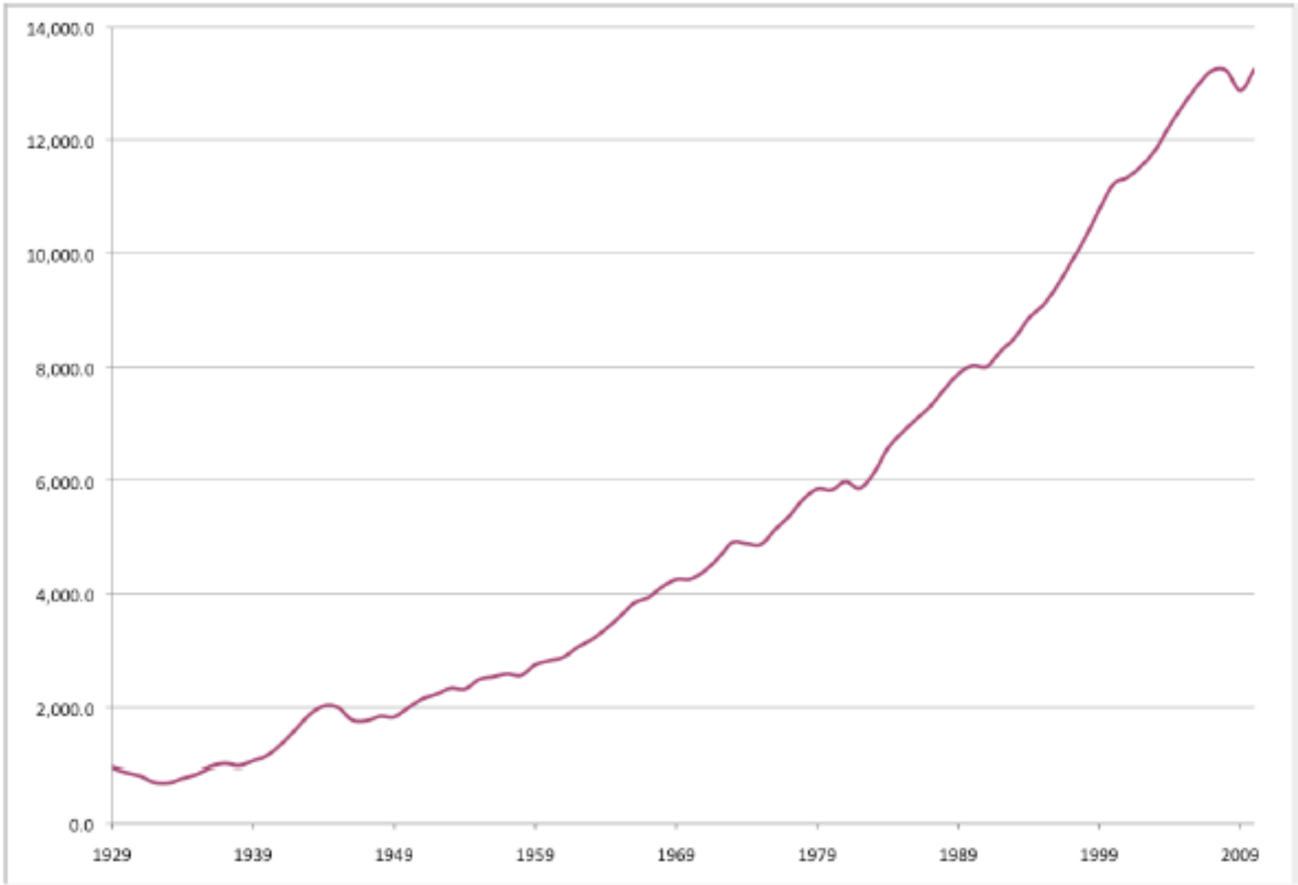

Figure 11: US GDP 1929-2010 corrected for inflation. (Source *Bureau of Economic Analysis*)

In model

$$\mathrm{GDP}(t) = \sum_{\mathbf{S}} C(\mathbf{S}, t)$$

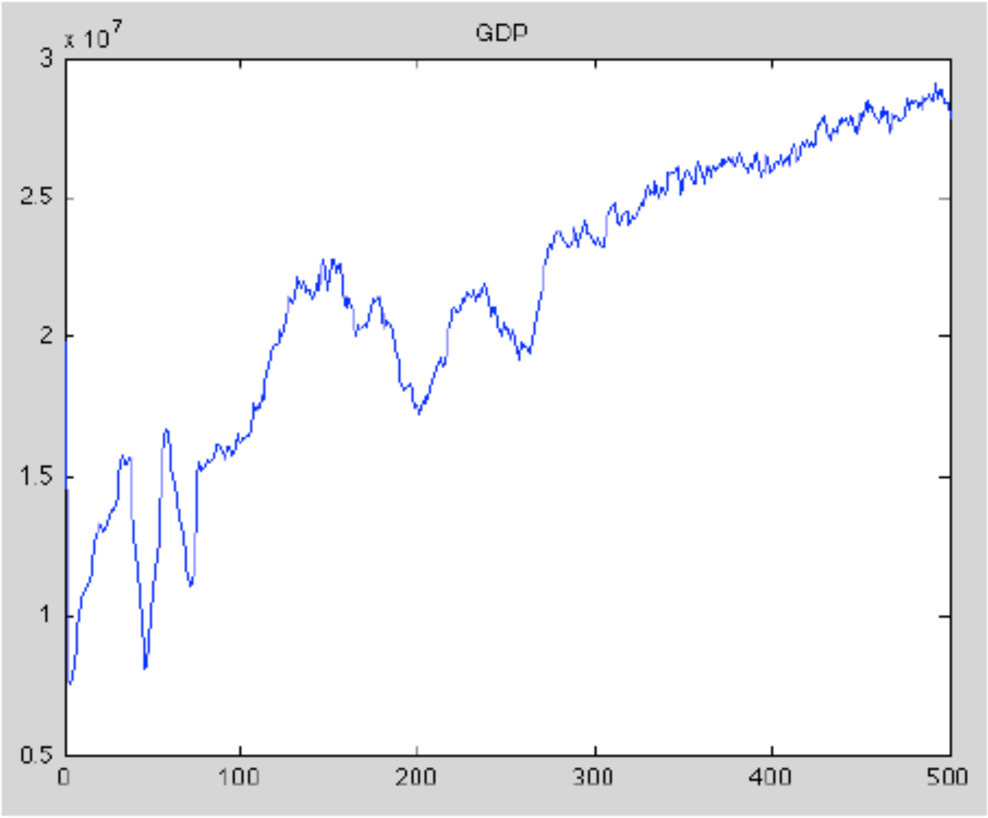

Figure 12: Model GDP (Iterations ×10).

David Robalino,
MSci Thesis

Comparison between data and model:

Growth rate

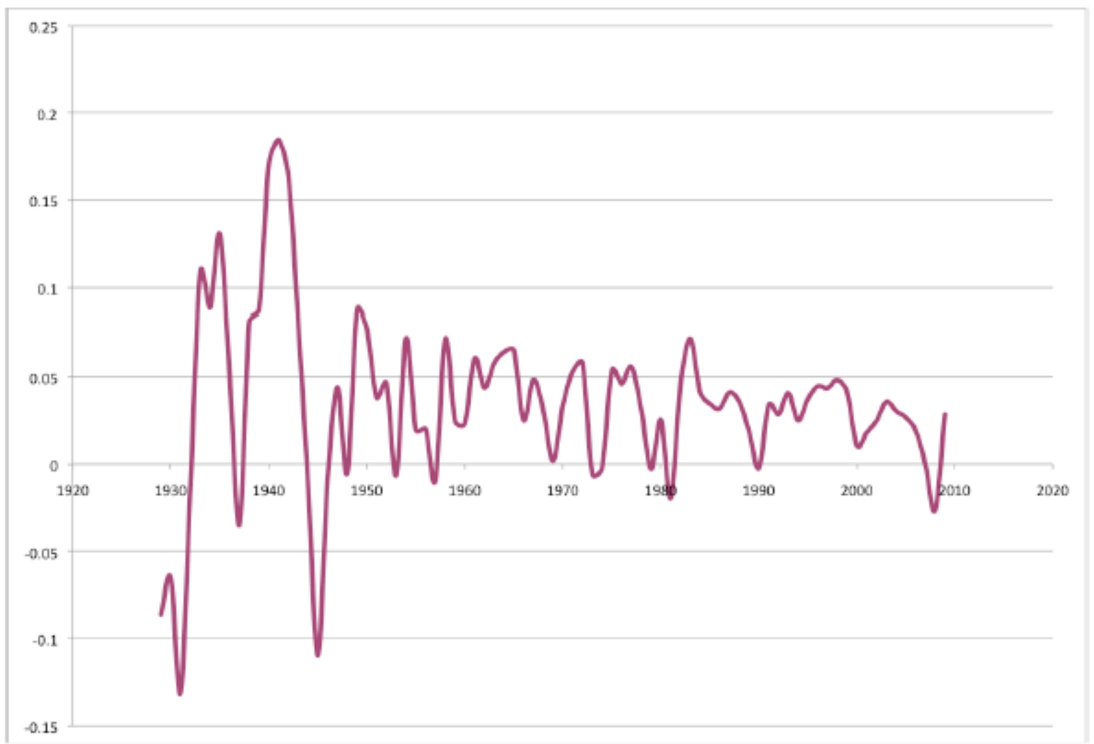

Figure 13: US GDP growth 1929-2010 corrected for infration (Source *Bureau of Economic Analysis*).

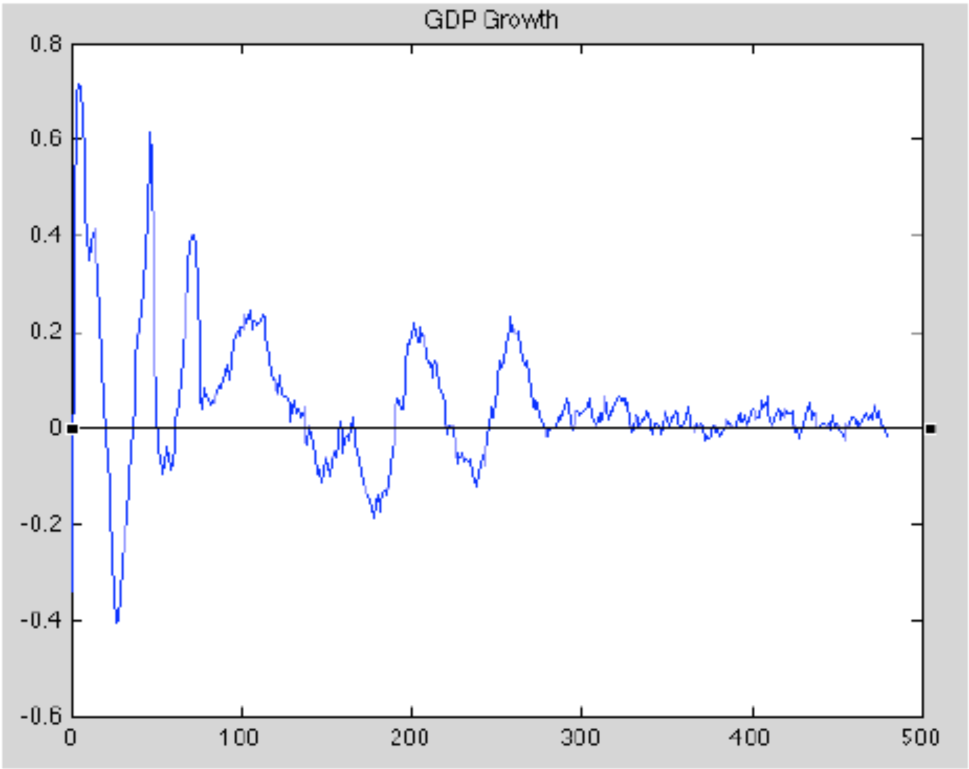

Figure 14: Model GDP growth (Iterations ×10).

David Robalino,
MSci Thesis

Comparison between data and model:
Size of companies

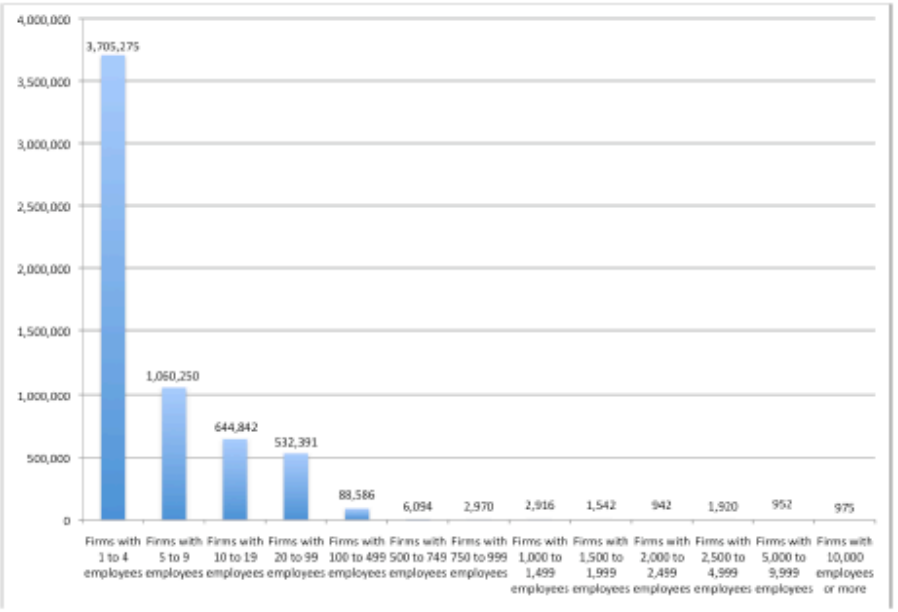

Figure 15: US firms by number of employees 2007 (Source *U.S. Census Bureau*).

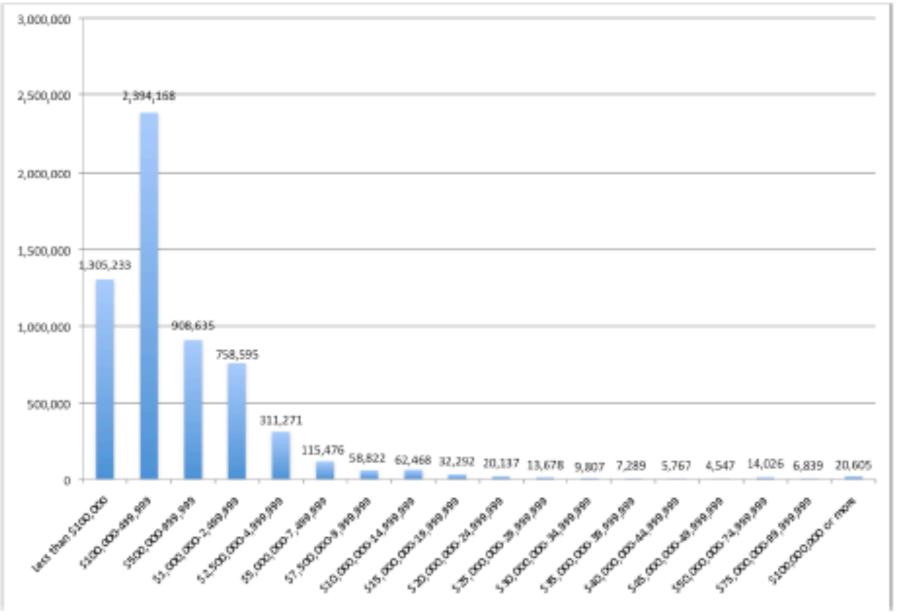

Figure 16: US firms by receipts size 2007 (Source *U.S. Census Bureau*).

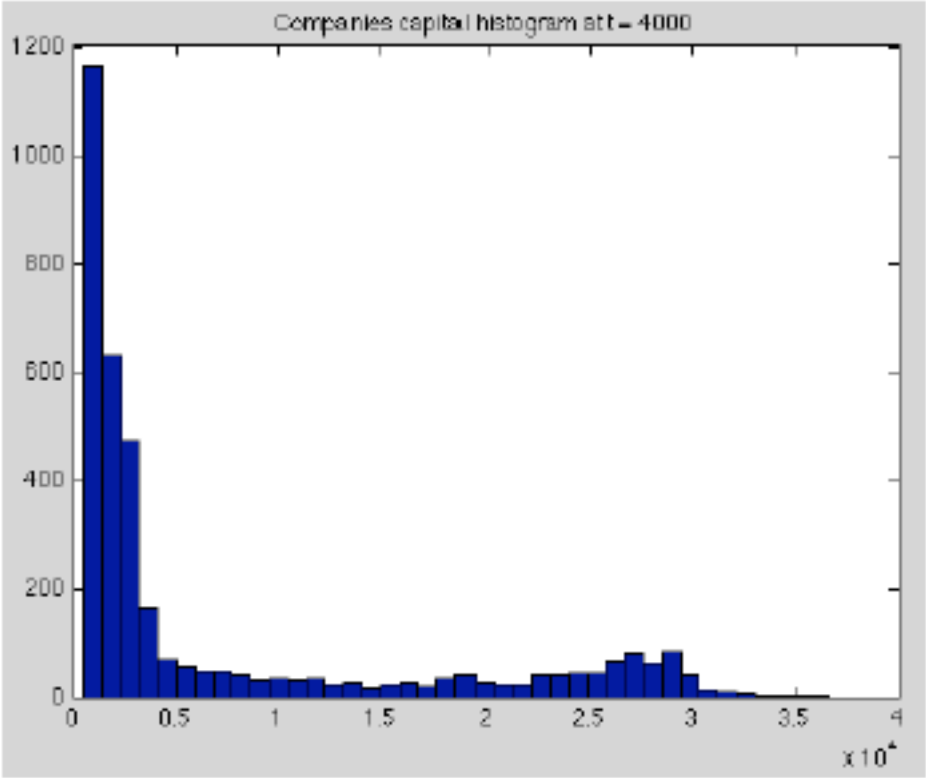

Figure 17: Model histogram of companies capital

David Robalino,
MSci Thesis

Comparison between data and model:

Company age

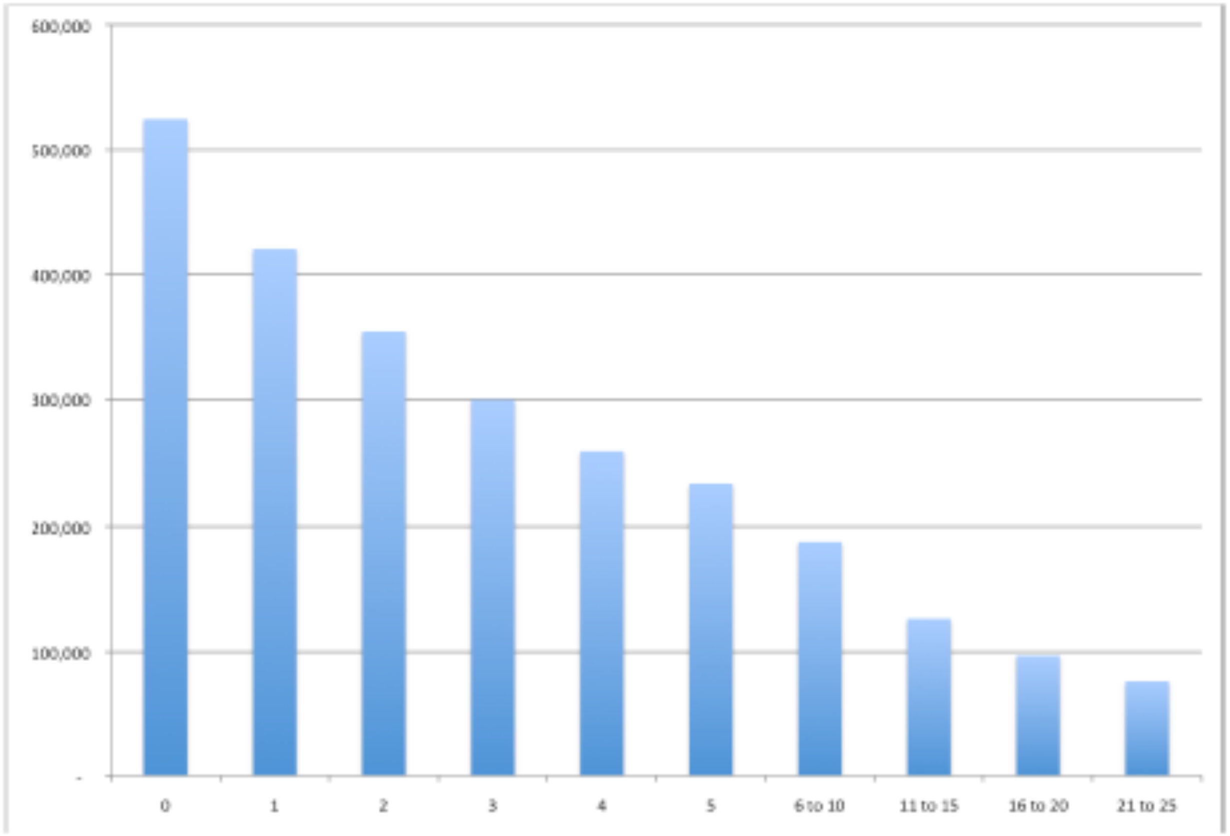

Figure 18: US firms by age in 2007 (Last 4 cols are averages; Source *U.S. Census Bureau*).

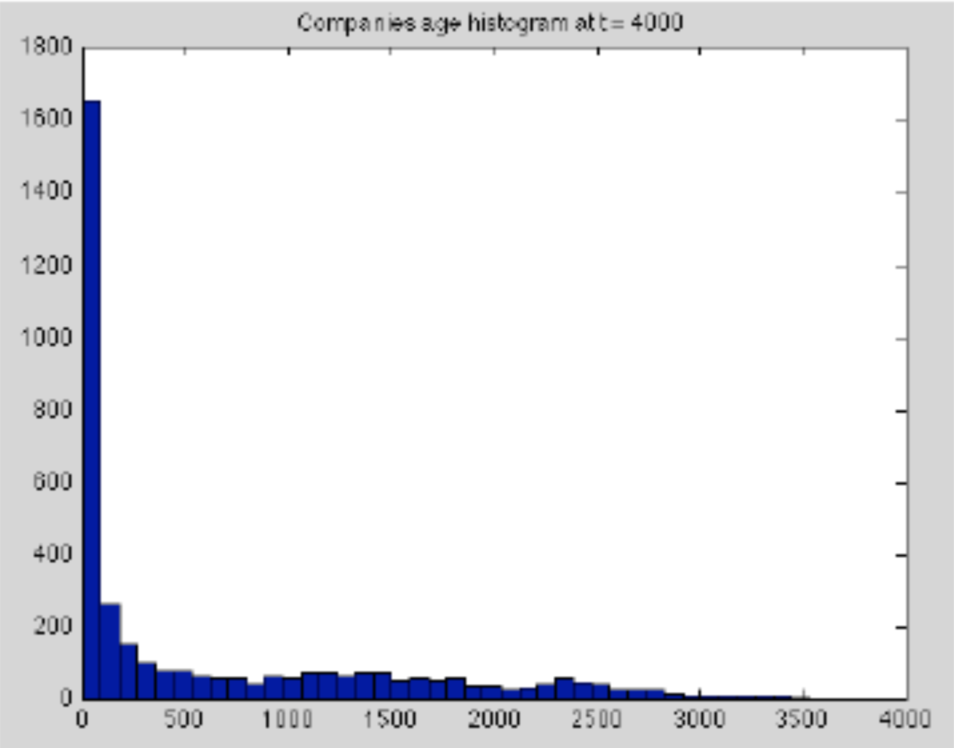

Figure 19: Model Companies by age at t=4000.

David Robalino,
MSci Thesis

Comparison between data and model:

Number of companies

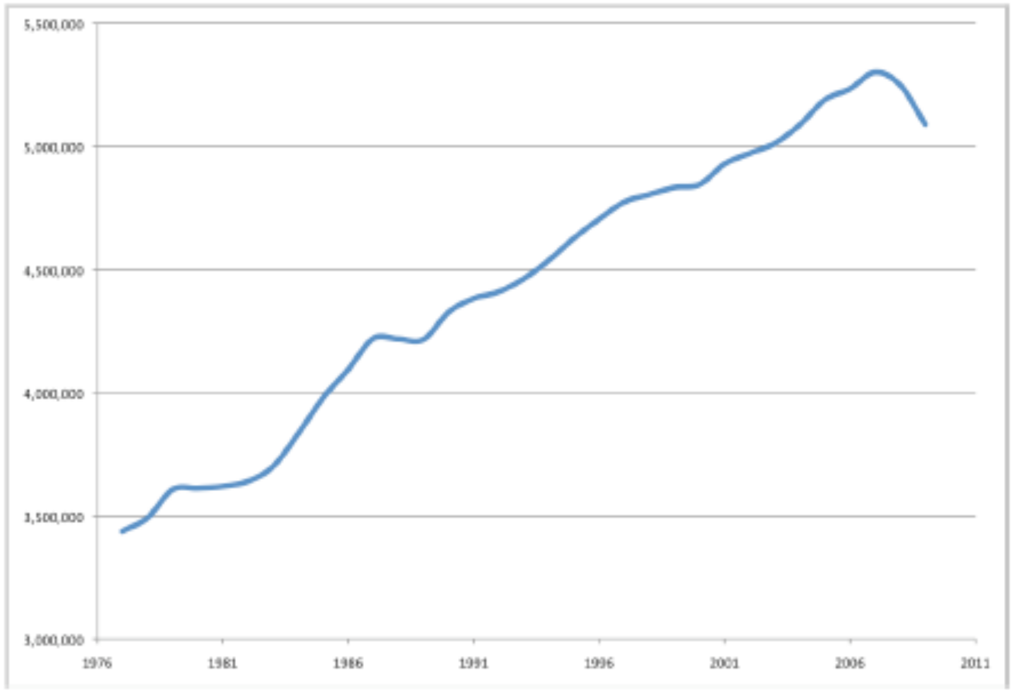

Figure 22: US Number of Firms (Source *U.S. Census Bureau*).

David Robalino,
MSci Thesis

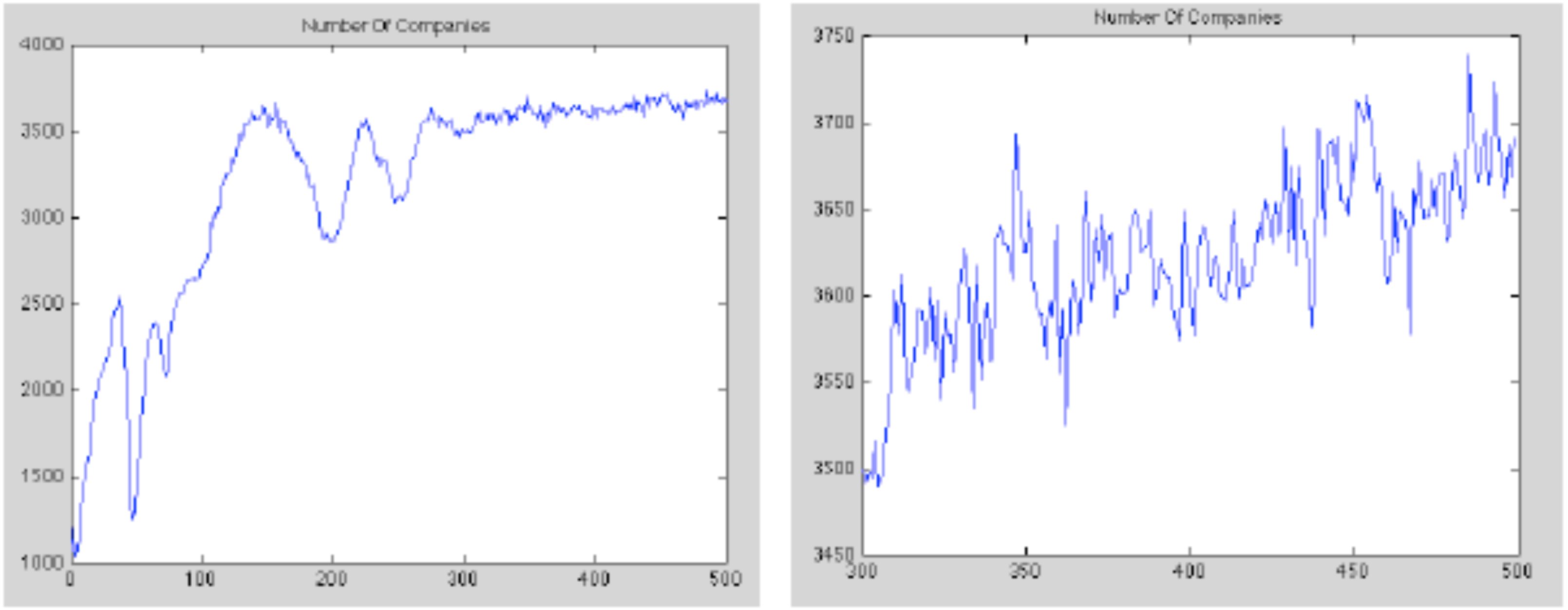

Figure 23: Model number of companies (Iterations ×10).

Ant colonies

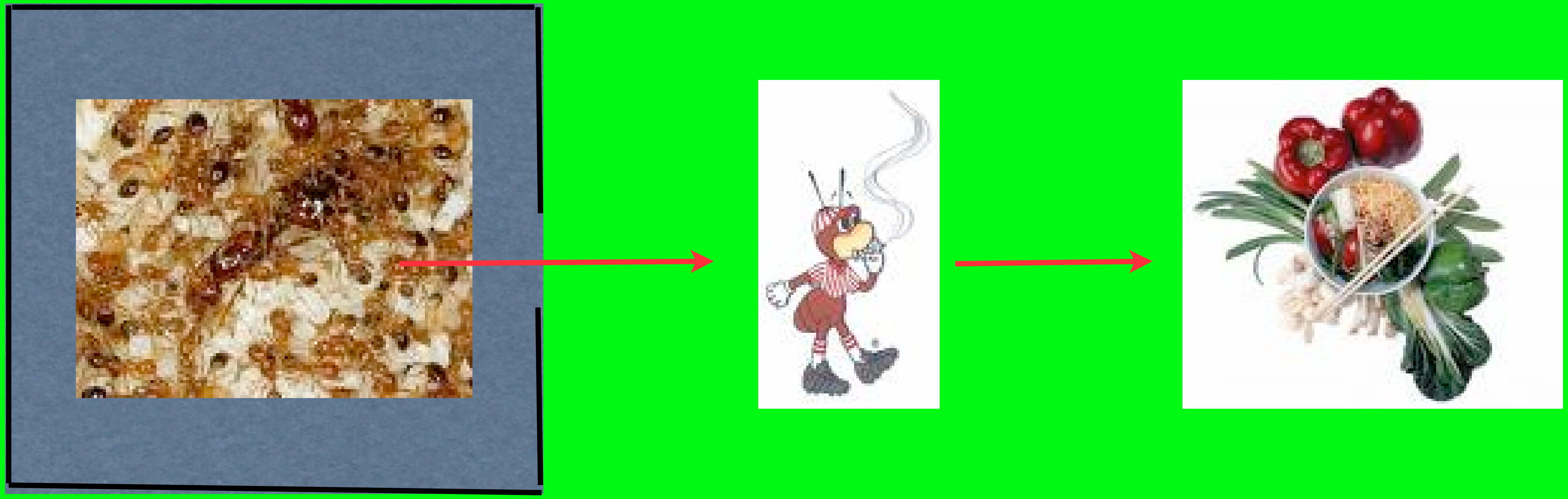

On ants: TO Richardson , EJH Robinson, AB Sendova-Franks,

NR Franks, E Arcaute, K Christensen

Ant colonies

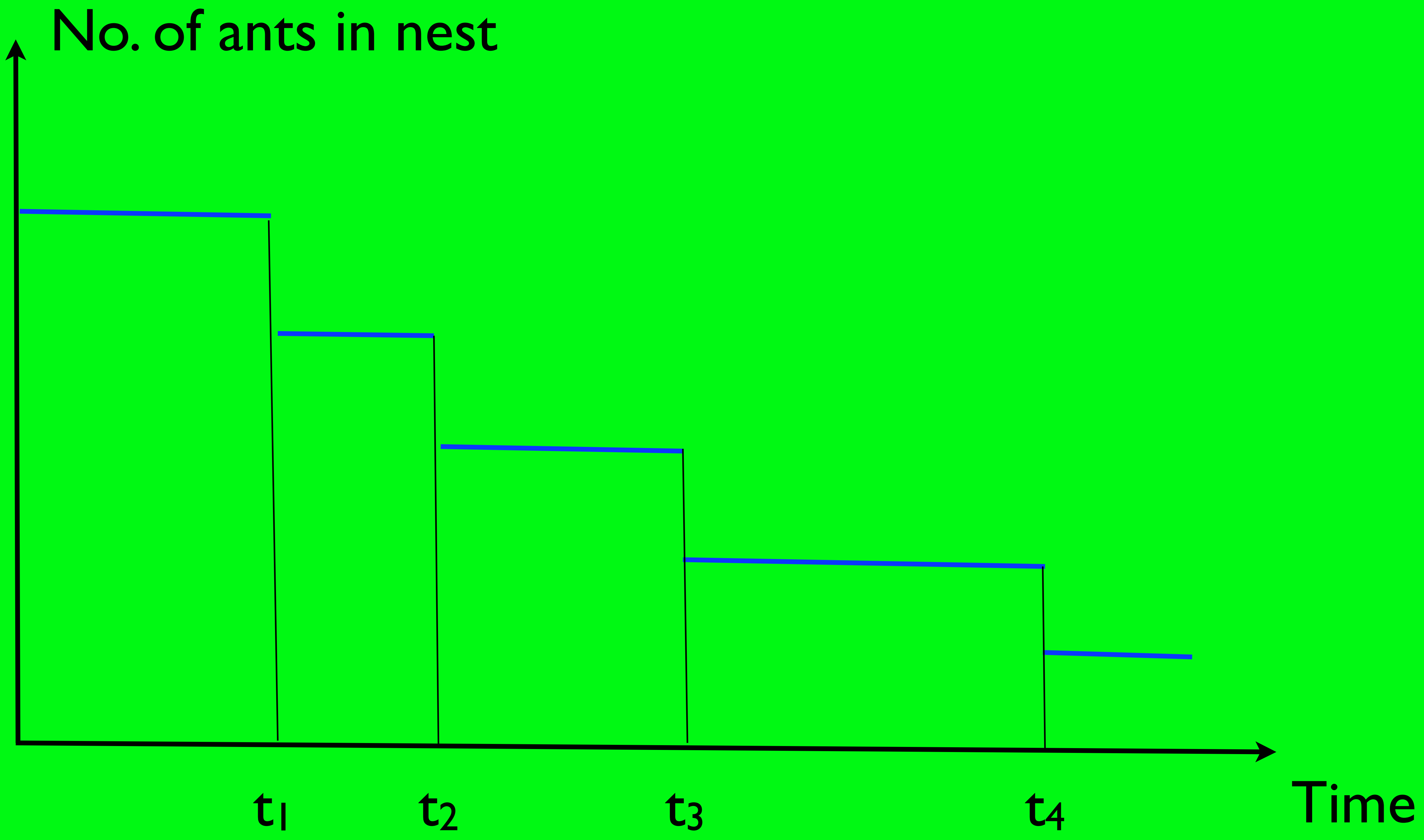

Ant colonies

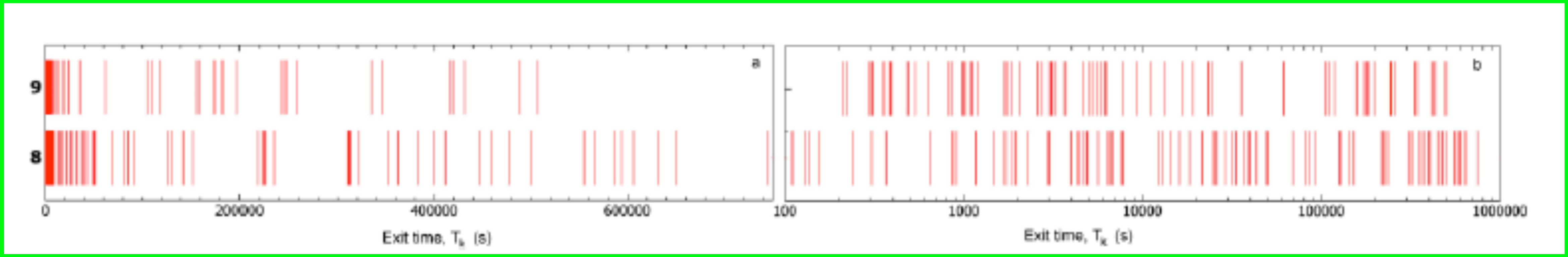

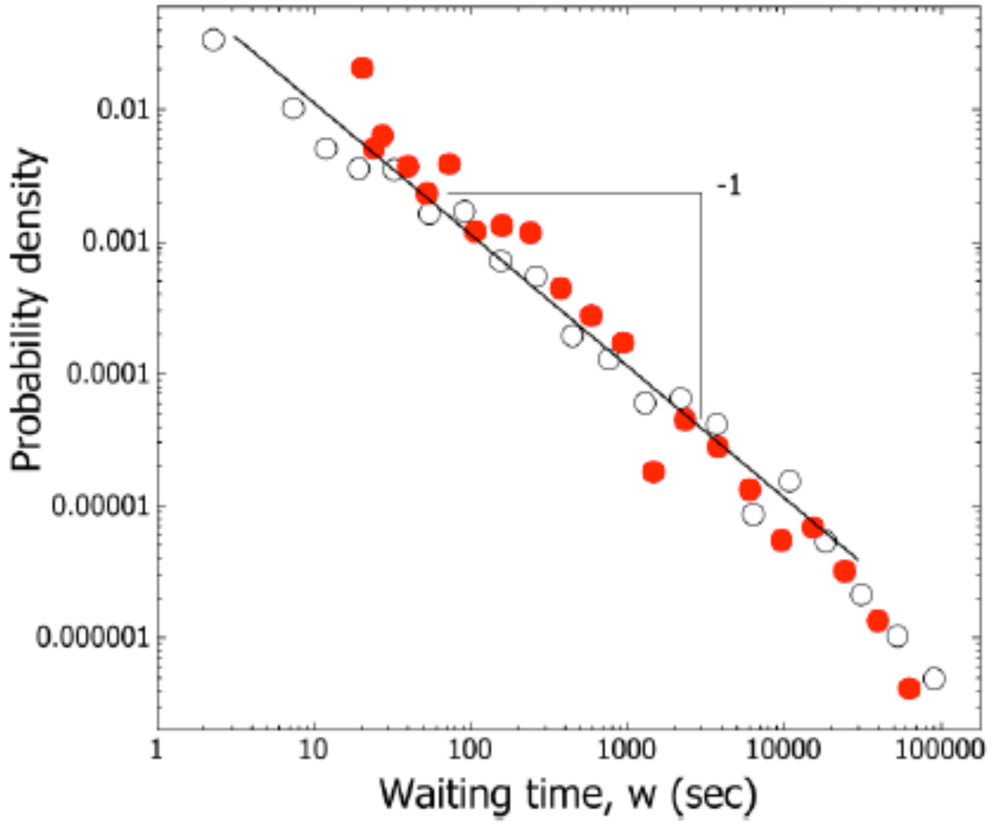

Figure 1. Waiting times between exits are not exponentially distributed.
In both removal (○) and non-removal (●) conditions for the five colonies which underwent both the waiting time probability densities between exits, $w = T_k - T_{k-1}$, follow a heavy-tailed distribution, that is closer to a power-law distribution, $P(w)=w^{-k}$, where k=1, than an exponential, $P(w)=e^{-\lambda x}$, which will not give a straight line on a log-log plot

T.O. Richardson, E.J.H. Robinson, K. Christensen, H.J. Jensen, N.R. Franks and A.B. Sendova-Franks, *Record Dynamics in Ants*, PloS One, **5**, e9621 (2010).

Ant colonies

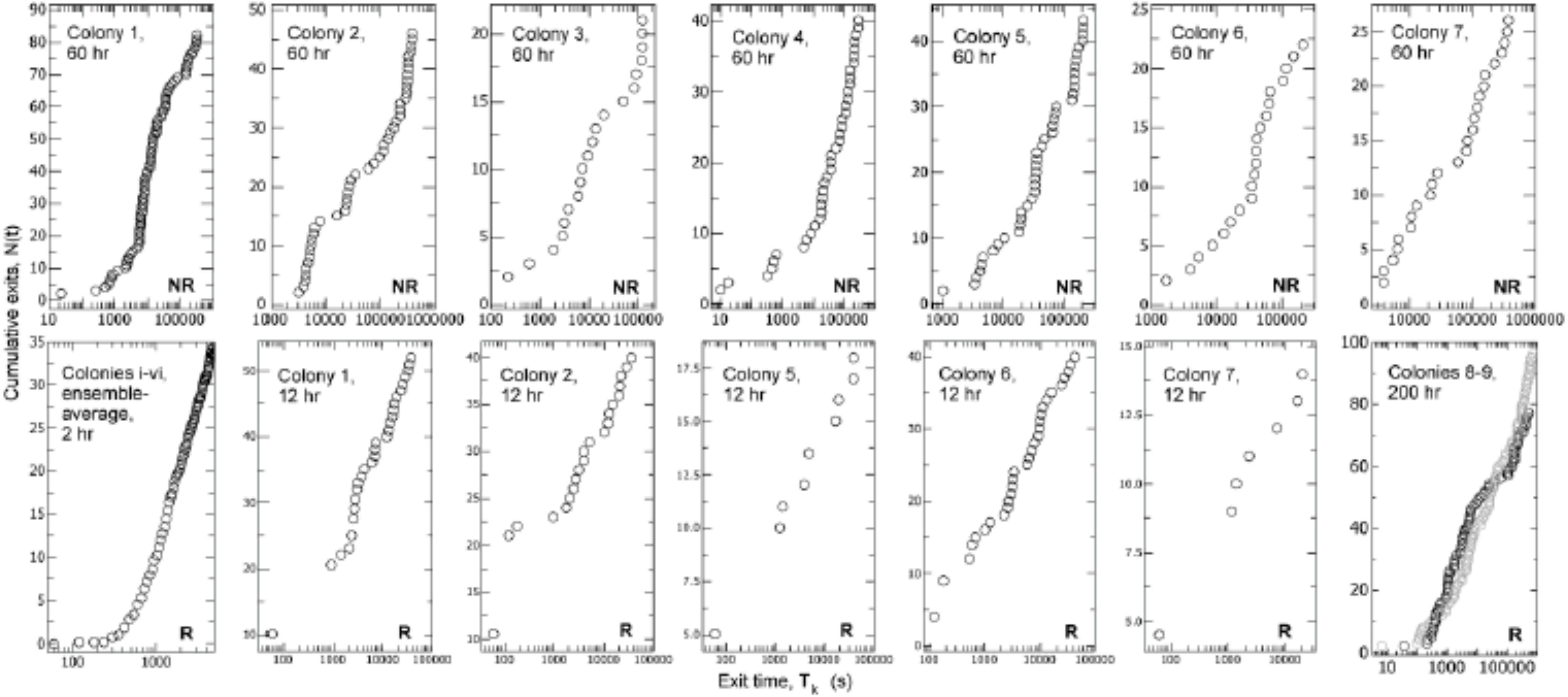

Figure 4. Events occur at random in logarithmic time. Accumulated number of ant exits over time, N(t) to exit time, T_k. The abscissa is logged to check for constant exit rates in logarithmic time when $T_k >> 1$. NR=non-removal control, R=removal treatment. Colum 1, row 2; Ensemble average, <N(t)> for six colonies (i-vi) undergoing 2 hours of external worker removal.

Earthquakes

The quakes are instantaneous on the time scale of the driving.

↓

after shocks relaxation under fixed boundary conditions

↓

Omori 1/t independent of ‘everything’

Earthquakes shocks - aftershocks

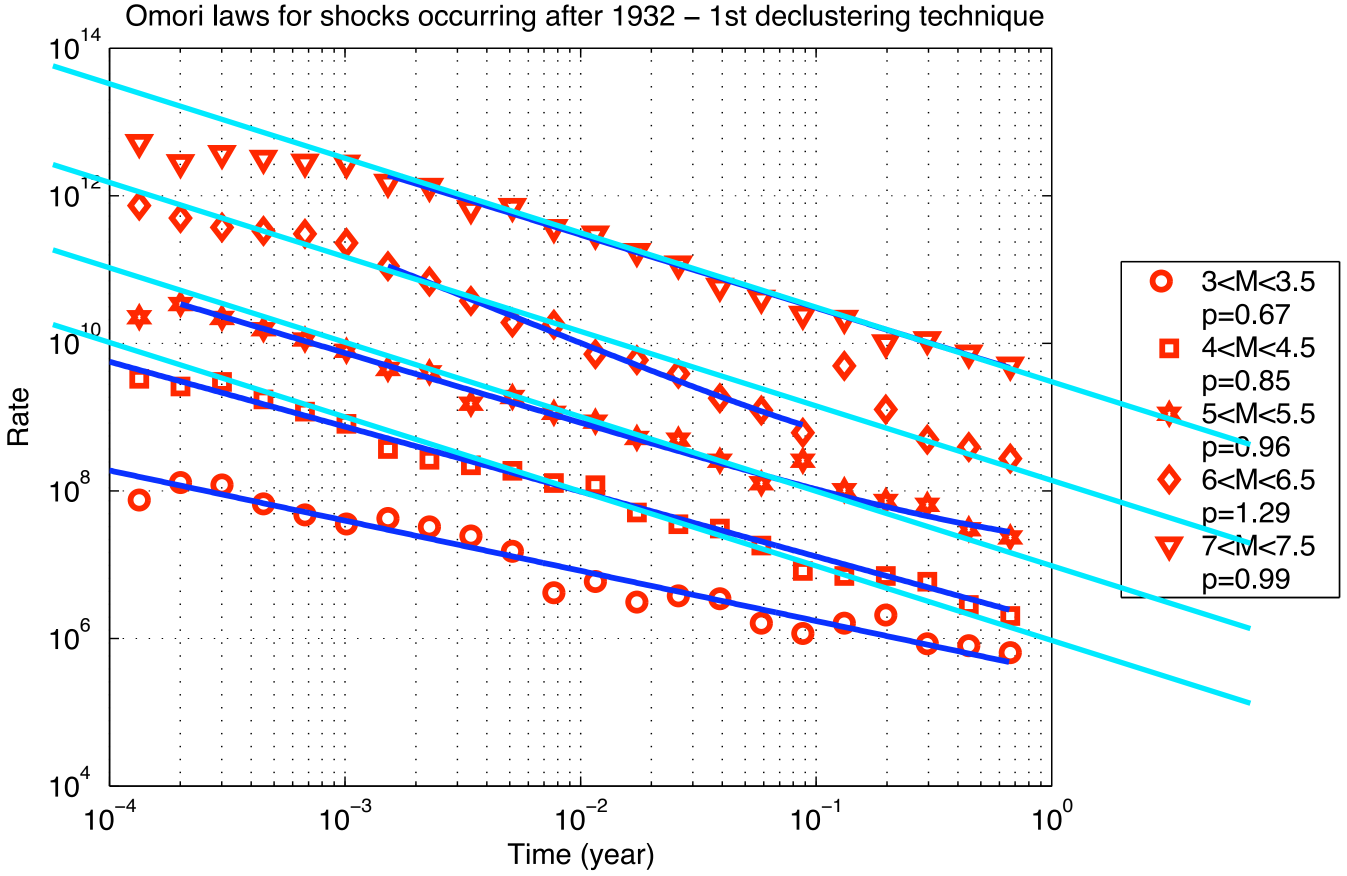

Figure 5. Seismic decay rates of stacked sequences for several magnitude intervals of the mainshocks, for the period from 1932 to 2003 when using the first declustering technique.

From Ouillon and Sornette
Magnitude-depended Omori law, J Geophys Res 111, B04306 (2005)

Record dynamics

The implicit nature of the relevant configuration/state space

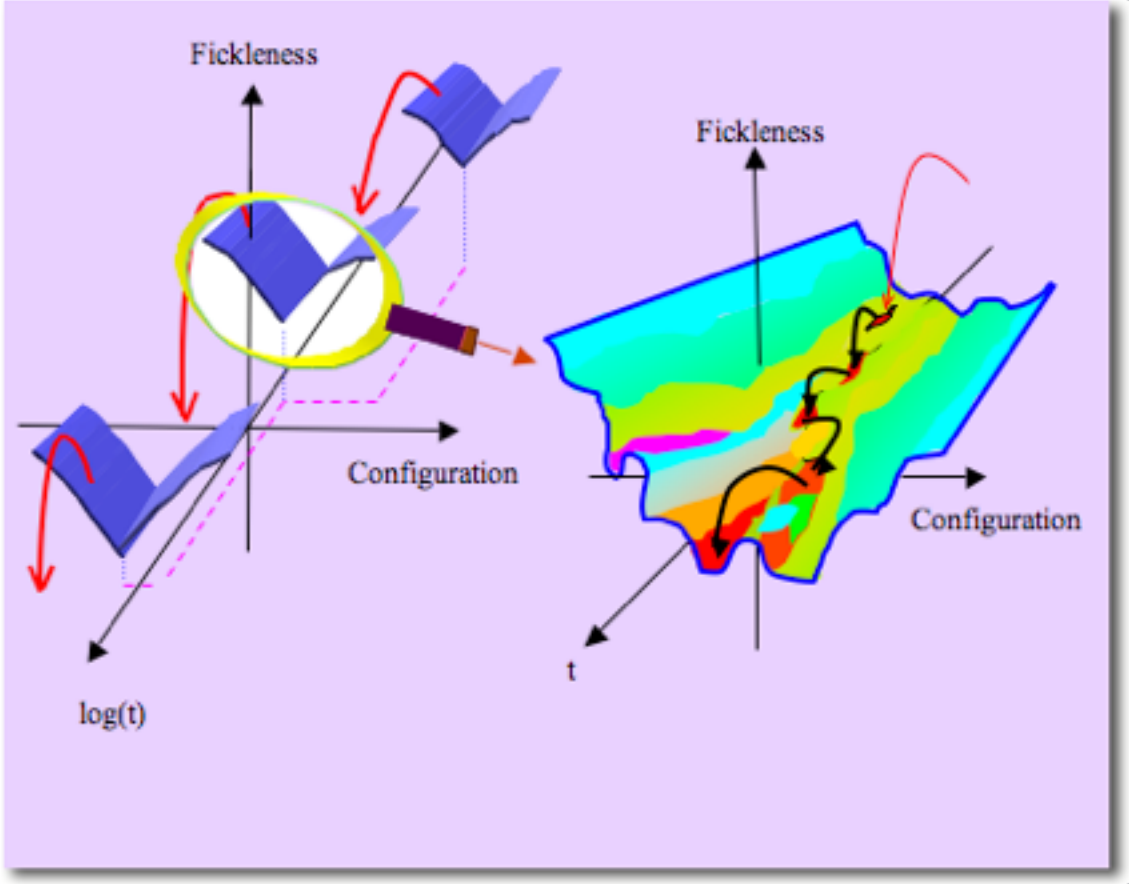

$$B_1 \lesssim B_2 \lesssim B_3$$

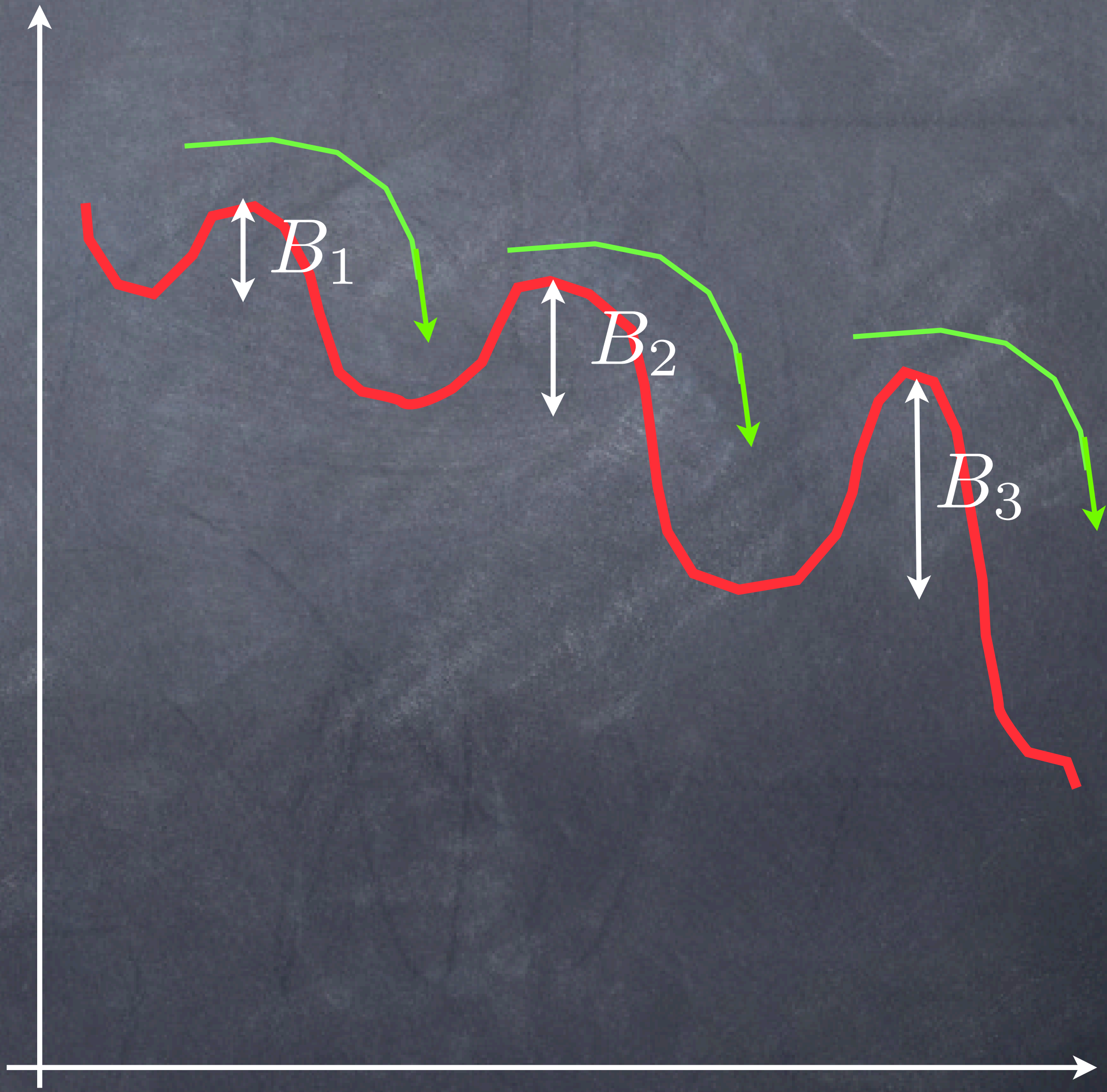

Record dynamics

Questions:

Which fluctuating quantity undergoes records?

or in other words: the events are related to which records?

Consequences of record dynamics.

Statistics of quake times independent of underlying “noise mechanism”.

- **Magnetic relaxation:** temperature independent creep rate
- **Spin glass:** exponential tails
- **Biology:** same intermittent dynamics in micro- as in macro-evolution - only different scales.

  Decreasing extinction rate.
- **Ants:** don’t really know yet!
- **Earthquakes:** Omori law ! ? !

Conclusion

Generic dynamics of complex systems is often:

- Non-stationary
- Intermittent record dynamics - "quakes"
- Rate of activity ~ *1/t*
- Stationary Poisson as function of log*(t)*

and some times it is:

- stationary
- Intermittent avalanches - SOC (?)

Thank you

Slides can be down loaded from

http://www2.imperial.ac.uk/~hjjens/

Henrik Jeldtoft Jensen
Department of Mathematics and Complexity and Networks Group
Imperial College London

Micro to macro time

Onset of synchronization

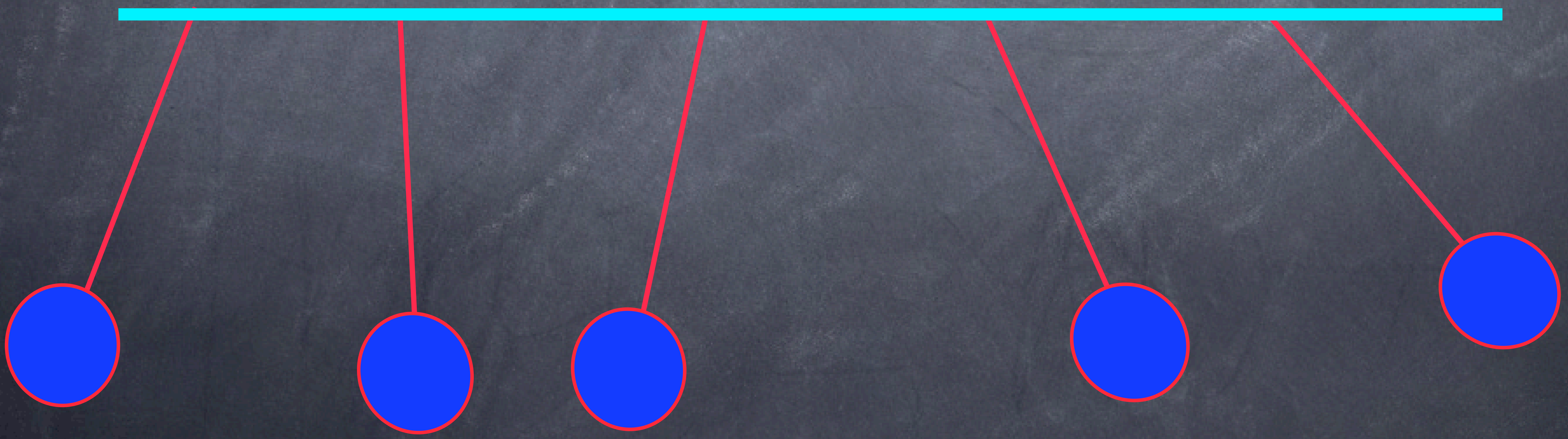

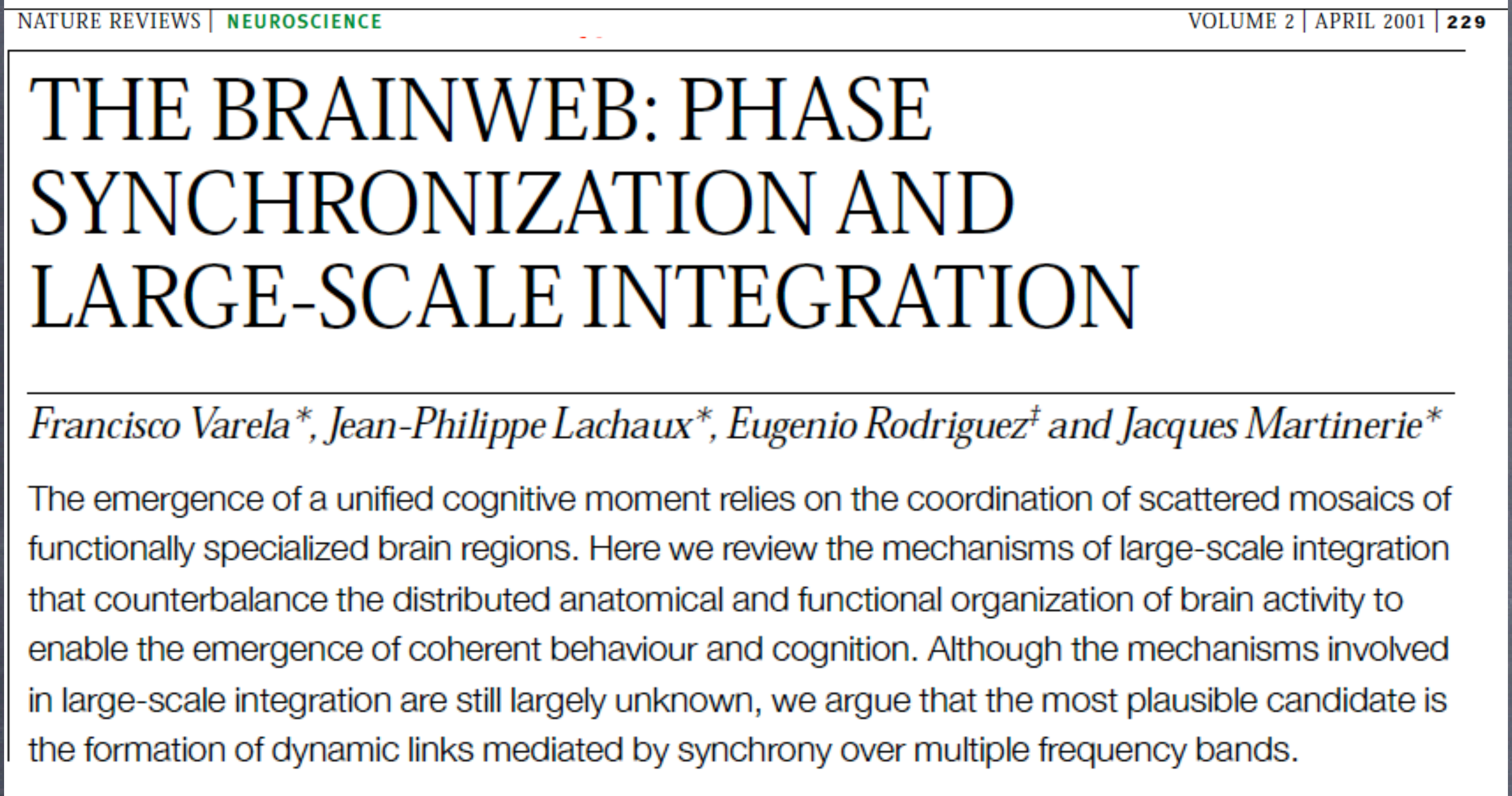

NATURE REVIEWS | NEUROSCIENCE VOLUME 2 | APRIL 2001 | 229

THE BRAINWEB: PHASE SYNCHRONIZATION AND LARGE-SCALE INTEGRATION

Francisco Varela, Jean-Philippe Lachaux*, Eugenio Rodriguez‡ and Jacques Martinerie**

The emergence of a unified cognitive moment relies on the coordination of scattered mosaics of functionally specialized brain regions. Here we review the mechanisms of large-scale integration that counterbalance the distributed anatomical and functional organization of brain activity to enable the emergence of coherent behaviour and cognition. Although the mechanisms involved in large-scale integration are still largely unknown, we argue that the most plausible candidate is the formation of dynamic links mediated by synchrony over multiple frequency bands.

Topics:

- > topology and synchronisation
  - > on static networks
  - > on evolving networks

Synchronization and the topology of networks

Kuramoto model

$$\frac{d\theta_i}{dt} = \omega + \sum_j K_{ij} \sin(\theta_i - \theta_j) \; i = 1, 2, ..., N$$

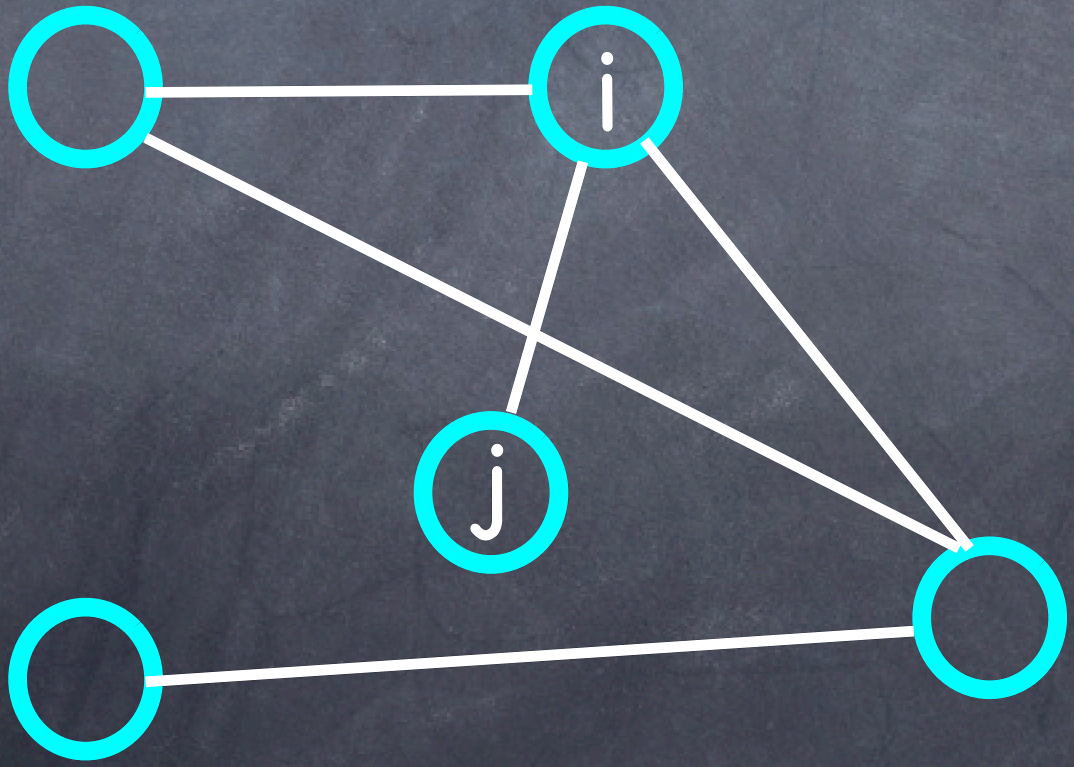

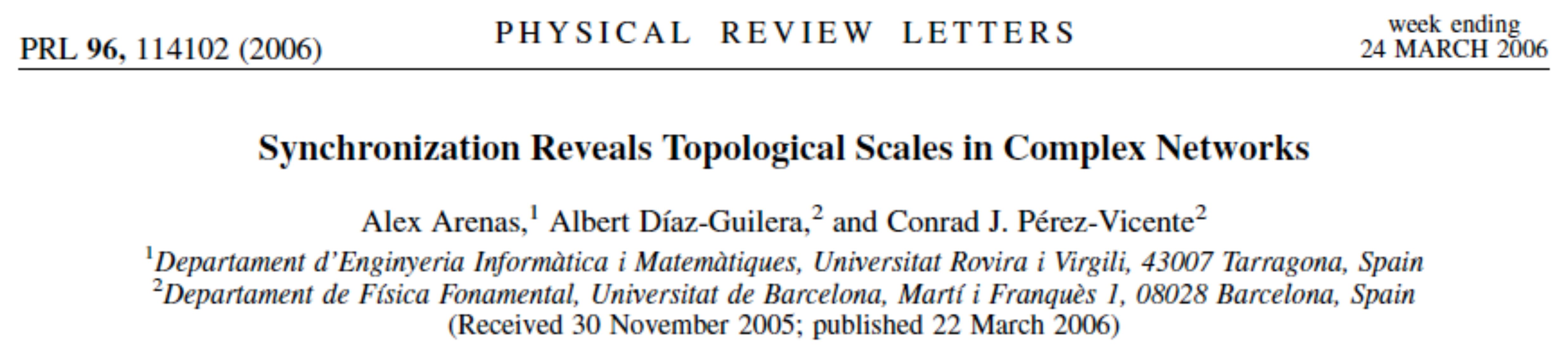

PRL **96,** 114102 (2006) PHYSICAL REVIEW LETTERS week ending 24 MARCH 2006

Synchronization Reveals Topological Scales in Complex Networks

Alex Arenas,[1] Albert Díaz-Guilera,[2] and Conrad J. Pérez-Vicente[2]
[1]*Departament d'Enginyeria Informàtica i Matemàtiques, Universitat Rovira i Virgili, 43007 Tarragona, Spain*
[2]*Departament de Física Fonamental, Universitat de Barcelona, Martí i Franquès 1, 08028 Barcelona, Spain*

(Received 30 November 2005; published 22 March 2006)

Arenas, Diaz-Guilera and Perez-Vicente Phys. Rev. Lett. **96**, 114102 (2006)

Synchronization and the topology of networks

$$\frac{d\theta_i}{dt} = \omega + \sum_j K_{ij}\sin(\theta_i - \theta_j) \; i = 1, 2, ..., N$$

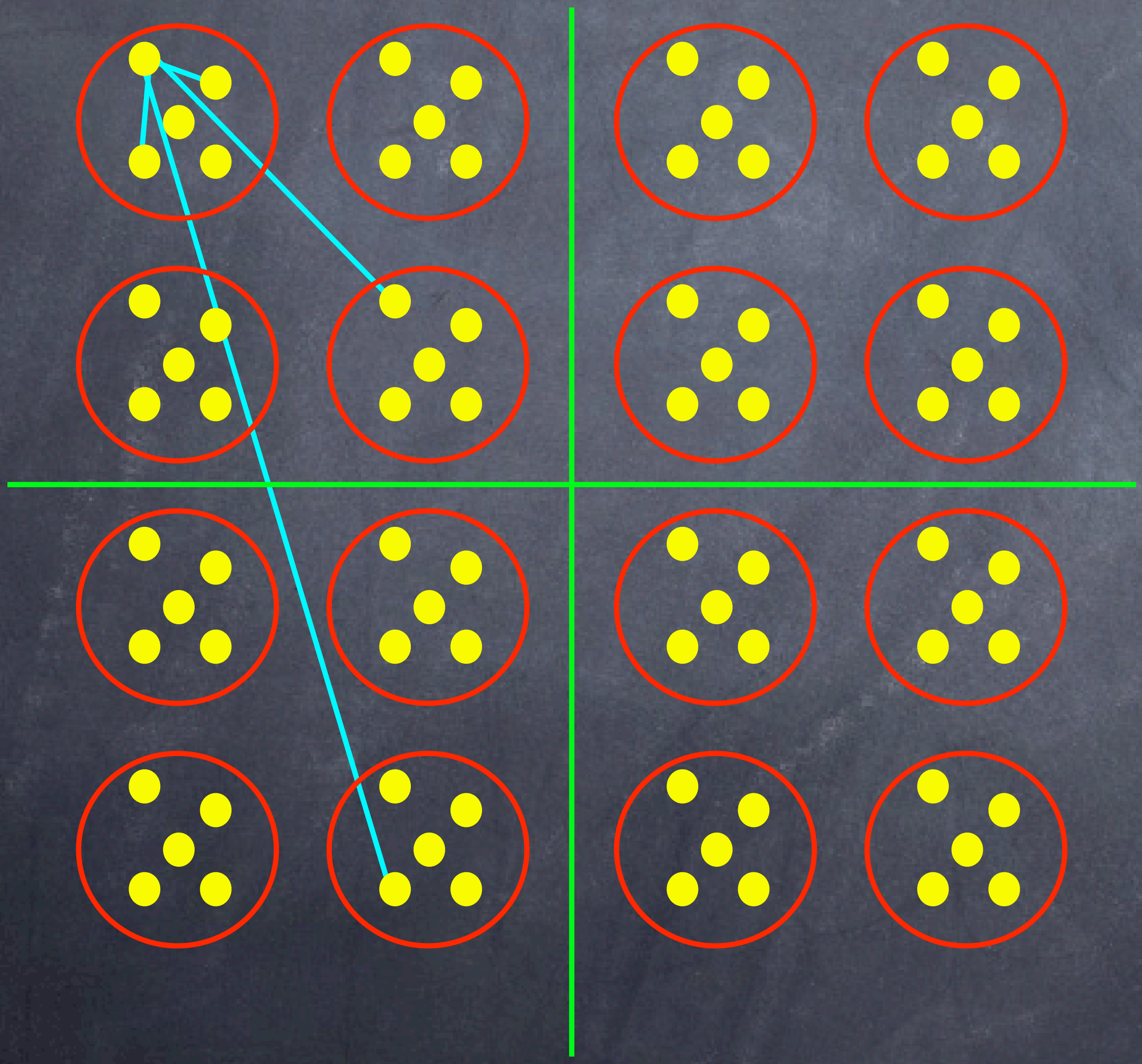

Rank the eigenvalues of the Laplacian Matrix

$$0 \leq \lambda_1 \leq \lambda_2 ... \leq \lambda_N$$

Linearised Kuramoto

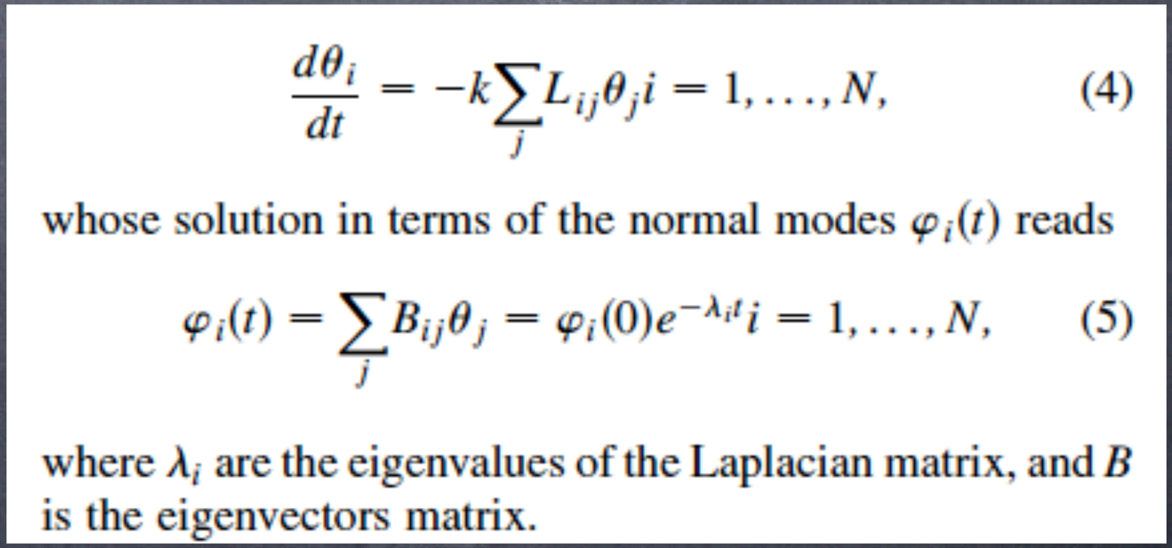

$$\frac{d\theta_i}{dt} = -k\sum_j L_{ij}\theta_j i = 1, \ldots, N, \tag{4}$$

whose solution in terms of the normal modes $\varphi_i(t)$ reads

$$\varphi_i(t) = \sum_j B_{ij}\theta_j = \varphi_i(0)e^{-\lambda_i t} i = 1, \ldots, N, \tag{5}$$

where λ_i are the eigenvalues of the Laplacian matrix, and B is the eigenvectors matrix.

$$z_1 + z_2 + z_3 = Z_{tot}$$

Synchronization and the topology of networks

$$\frac{d\theta_i}{dt} = \omega + \sum_j K_{ij} \sin(\theta_i - \theta_j) \; i = 1, 2, ..., N$$

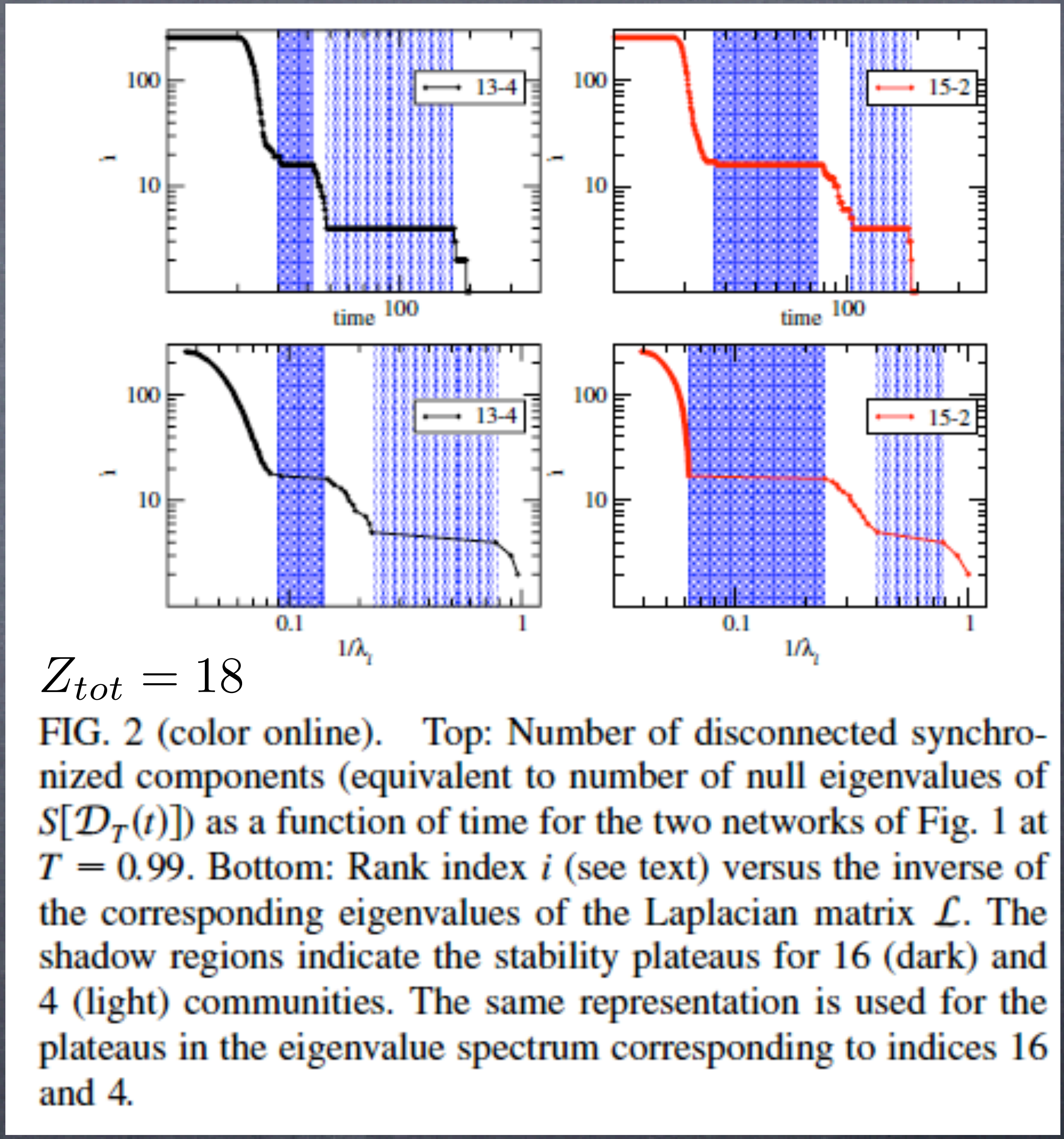

$Z_{tot} = 18$

FIG. 2 (color online). Top: Number of disconnected synchronized components (equivalent to number of null eigenvalues of $S[\mathcal{D}_T(t)]$) as a function of time for the two networks of Fig. 1 at $T = 0.99$. Bottom: Rank index i (see text) versus the inverse of the corresponding eigenvalues of the Laplacian matrix $\mathcal{L}$. The shadow regions indicate the stability plateaus for 16 (dark) and 4 (light) communities. The same representation is used for the plateaus in the eigenvalue spectrum corresponding to indices 16 and 4.

$$z_1 + z_2 + z_3 = Z_{tot}$$

Arenas, Diaz-Guilera and Perez-Vicente Phys. Rev. Lett. **96**, 114102 (2006)

Fireflies - The Movie

BBC - Trails of Life

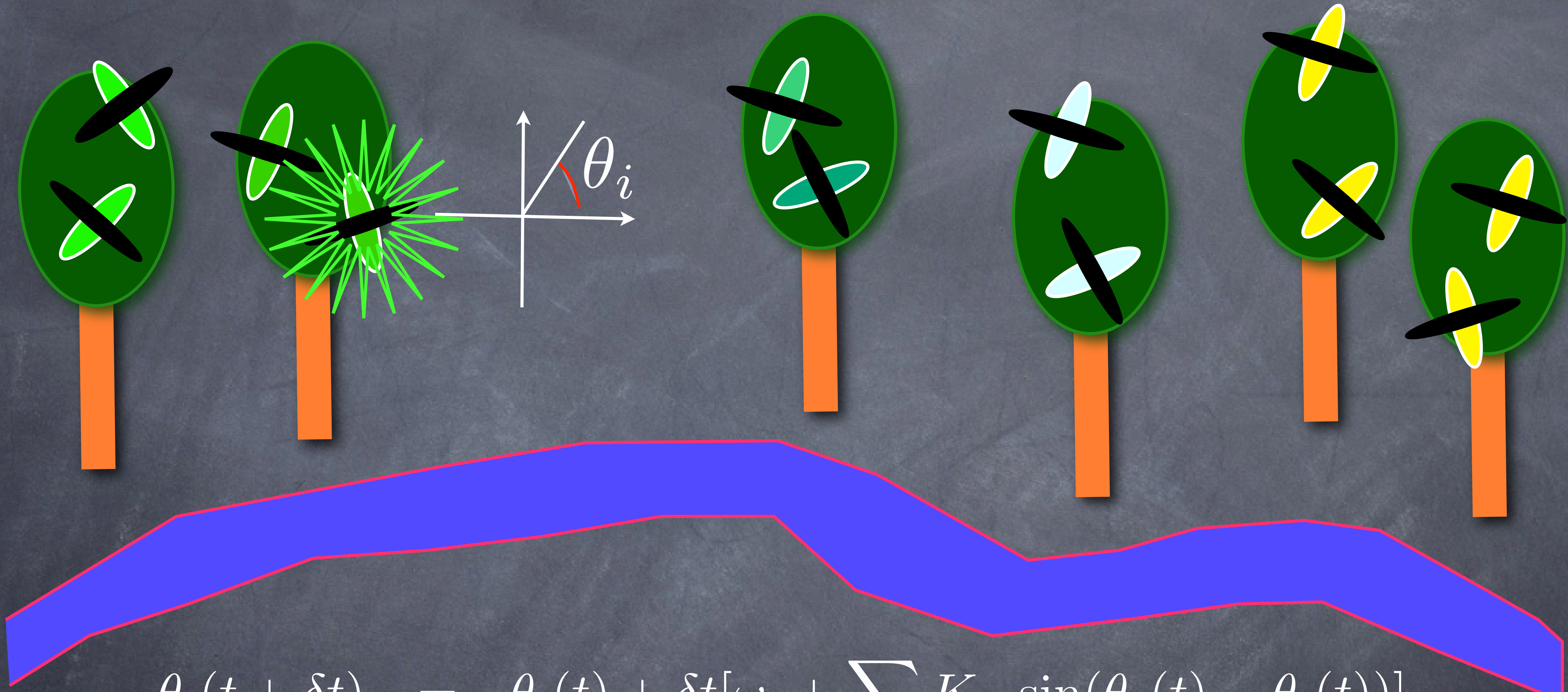

$$
\begin{aligned}
\theta_i(t+\delta t) &= \theta_i(t) + \delta t[\omega_i + \sum_j K_{ij} \sin(\theta_j(t) - \theta_i(t))] \\
K_{ij} &= \frac{L(j)}{r_{ij}^2} \\
L(j) &= \text{increasing with synch of cluster } j
\end{aligned}
$$

“Exponential” separation

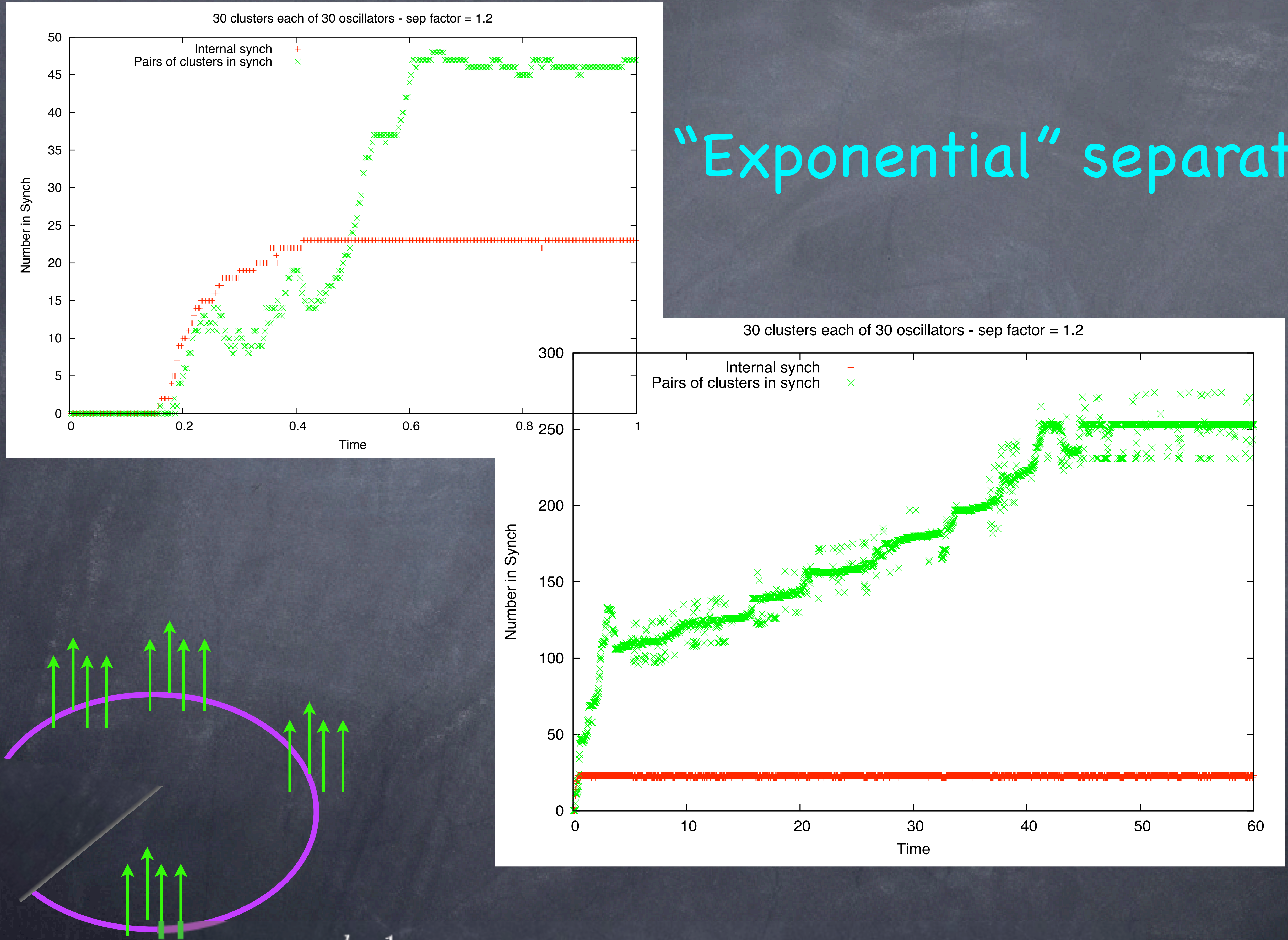

$$\mathbf{r}_i = \xi + \gamma^{k-1}, \quad \xi \in [-0.2, 0.2], \quad \gamma = 1.2, \quad k = \text{cluster } \#$$

Ito-Kaneko model

$$
\begin{aligned}
x^i_{t+1} &= (1-c)f(x^i_t) + c\sum_{j=1}^{N} w^{ij}_t f(x^j_t) \\
f(x) &= ax(1-x) \\
w^{ij}_{t+1} &= \frac{[1+\delta g(x^i_t, x^j_t)]w^{ij}_t}{\sum_{q=1}^{N}[1+\delta g(x^i_t, x^q_t)]w^{iq}_t} \\
g(x,y) &= 1-2|x-y|
\end{aligned}
$$

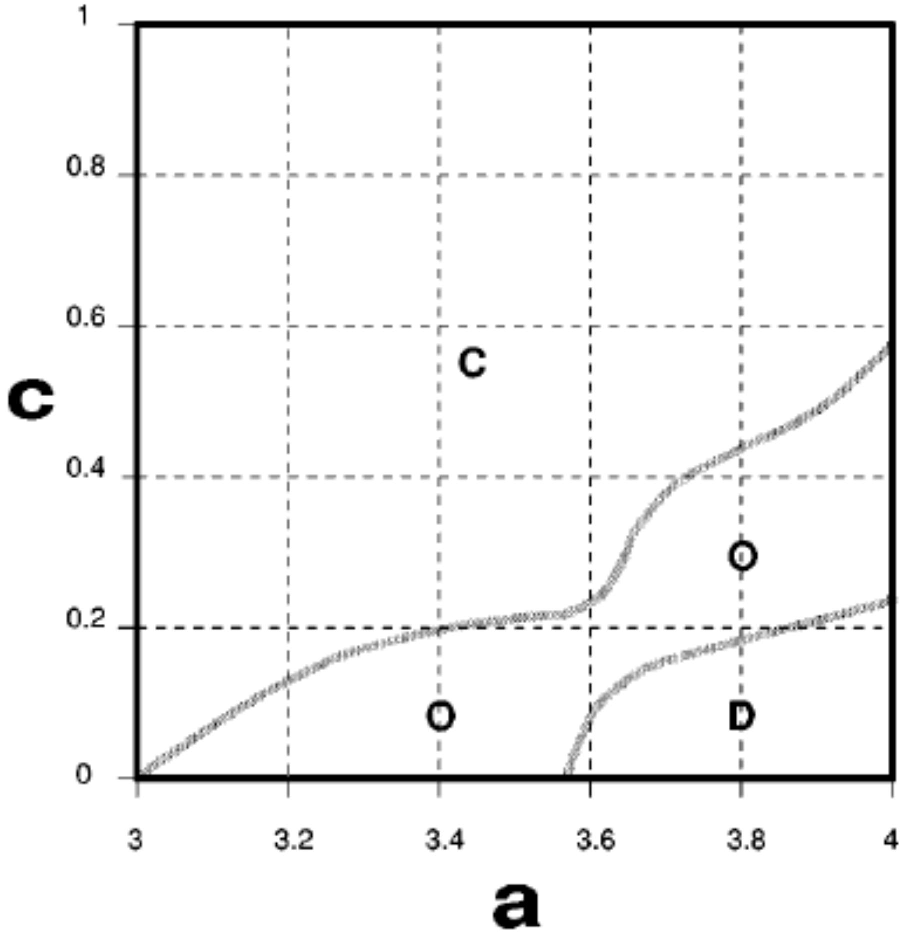

FIG. 1. Rough phase diagram of the model against the parameters a and c, obtained by computing the number of clusters. The simulation is carried out by changing both of the parameter values by 0.01. Letters in the figure represent the following: C, coherent phase; O, ordered phase; D, desynchronized phase.

Ito and Kaneko, PRL **88**, 028701, (2001) and PRE **67**, 046226 (2003)

Onset of synchronisation near the O/D border

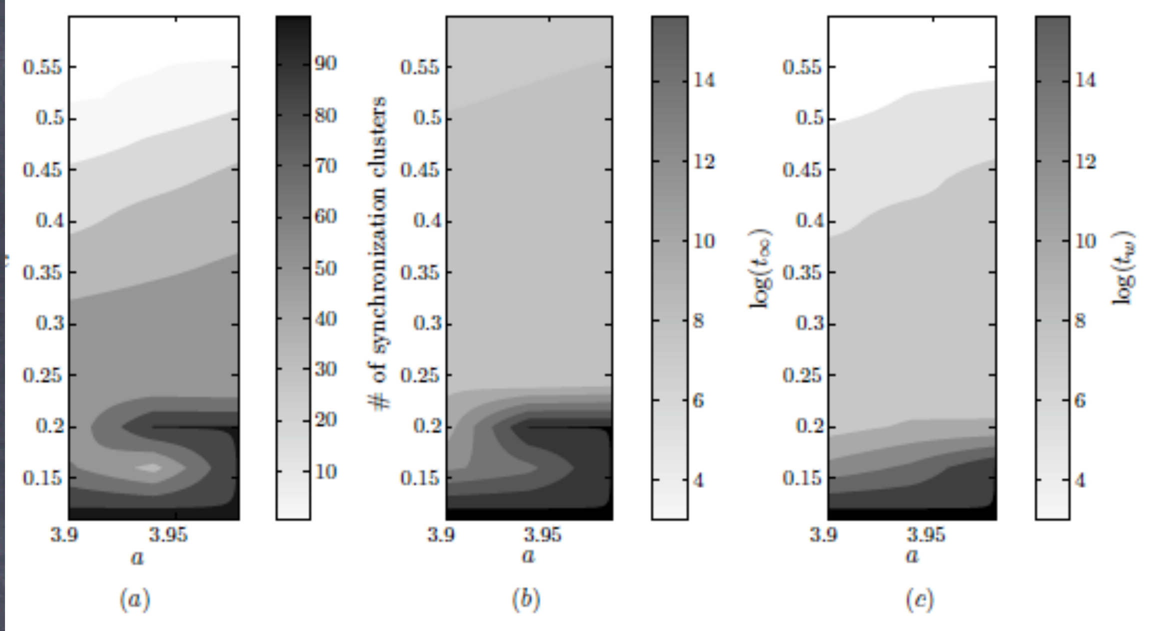

Figure 1. (*a*) Part of the phase diagram of the Ito–Kaneko model. (*b*) Length of the transient t_∞. (*c*) Time t_w until the variation of weights falls below 0.1% (all averaged over 25 realizations).

Simple description:
Synch events proportional to the rate with which two units "collide"

$$\frac{N_{synch}(t)}{dt} = k(N - N_{synch}(t))^2$$
$$\Downarrow$$
$$N_{synch}(t) = N - \frac{1}{1/N + kt}$$

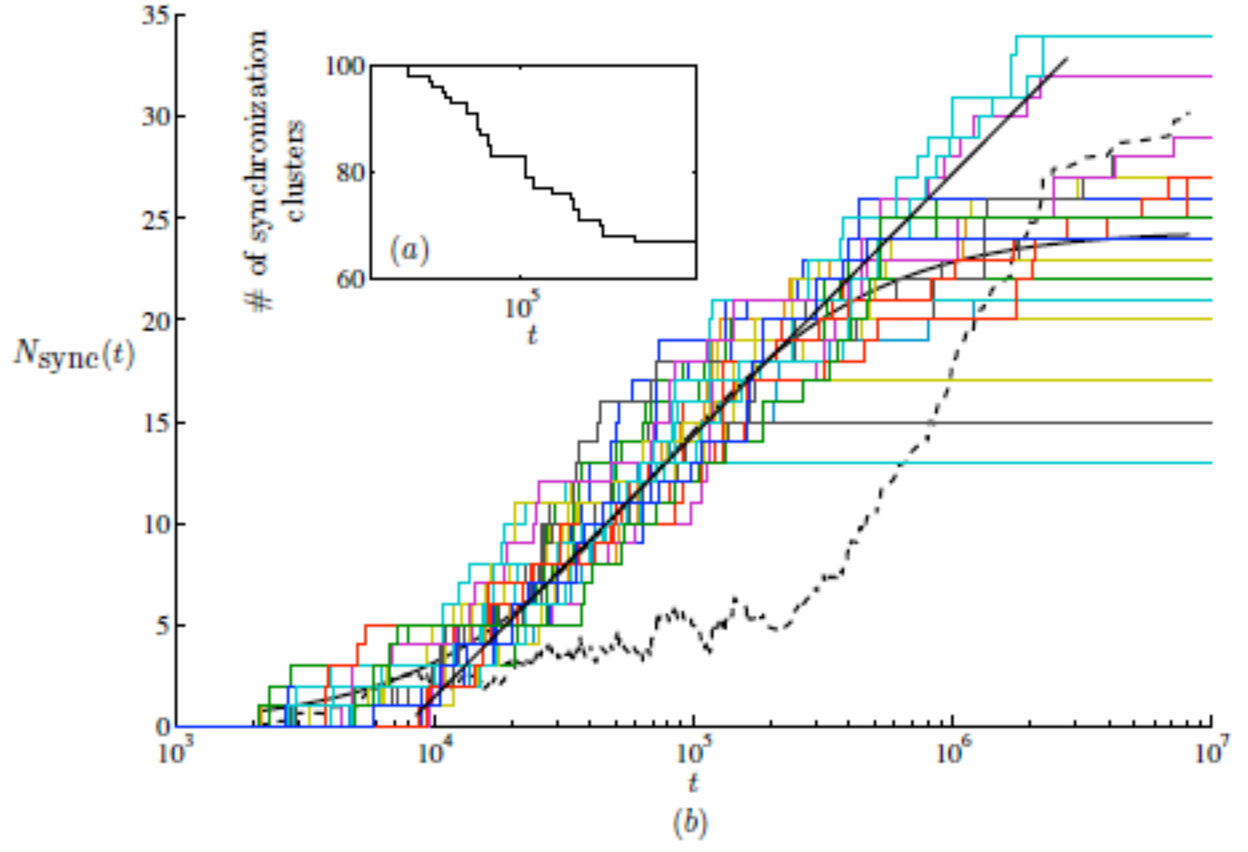

Figure 4. Synchronization transient near the border O/D, with $c = 0.158$. (a—inset) Time dependence of the number of synchronization clusters for a single simulation run. (*b*) Time dependence of the number of synchronization events for 25 simulation runs (thin lines) and corresponding variance (dashed), a linear fit and a fit of the simple model described by (5) (thick lines).

Benköe and Jensen, J Phys, A, **43** 165102 (2010)

Conclusion

Dynamics closely related to topological structure

> macroscopic temporal patterns reflect underlying (dynamical) spatial structure

Thank you

Slides can be down loaded from

http://www2.imperial.ac.uk/~hjjens/

Henrik Jeldtoft Jensen
Department of Mathematics and Complexity and Networks Group
Imperial College London